

5-13-2022

## Design, construction, and characterization of a test stand used to test filter media

Adam W. Parsons  
ICET, adam.parsons57@gmail.com

Follow this and additional works at: <https://scholarsjunction.msstate.edu/td>



Part of the [Other Mechanical Engineering Commons](#)

---

### Recommended Citation

Parsons, Adam W., "Design, construction, and characterization of a test stand used to test filter media" (2022). *Theses and Dissertations*. 5446.  
<https://scholarsjunction.msstate.edu/td/5446>

This Graduate Thesis - Open Access is brought to you for free and open access by the Theses and Dissertations at Scholars Junction. It has been accepted for inclusion in Theses and Dissertations by an authorized administrator of Scholars Junction. For more information, please contact [scholcomm@msstate.libanswers.com](mailto:scholcomm@msstate.libanswers.com).

Design, construction, and characterization of a test stand used to test filter media

By

Adam W. Parsons

Approved by:

Heejin Cho (Major Professor)

Alta Knizley

Prashant Singh

Tonya W. Stone (Graduate Coordinator)

Jason M. Keith (Dean, Bagley College of Engineering)

A Thesis

Submitted to the Faculty of

Mississippi State University

in Partial Fulfillment of the Requirements

for the Degree of Master of Science

in Mechanical Engineering

in the Bagley College of Engineering

Mississippi State, Mississippi

May 2022

Copyright by  
Adam W. Parsons  
2022

Name: Adam W. Parsons

Date of Degree: May 13, 2022

Institution: Mississippi State University

Major Field: Mechanical Engineering

Major Professor: Heejin Cho

Title of Study: Design, construction, and characterization of a test stand used to test filter media

Pages in Study: 1411

Candidate for Degree of Master of Science

Air filters are routinely used to remove various aerosols ranging from radioactive particles to airborne viruses. The overall performance of a filter may be simplified to consider only two main performance characteristics: 1) the efficiency at which particles are removed by the filter, and 2) the filter's resistance to air flow. Per the DOE Nuclear Air Cleaning Handbook, HEPA filters require a minimum filter efficiency of 99.97% for particles 0.3 micrometers in diameter. Understanding how filters will perform with respect to time and mass loading is essential towards building more robust filters that operate more efficiently and safely. Analyzing the mechanics of the filter media will provide better direction towards design improvement by exploring the relationship between the pressure drop and loaded particle mass. This work summarizes the design, construction, and characterization of a testing apparatus intended to perform penetration and loading testing on various test medias with selected aerosols.



## DEDICATION

This thesis is dedicated to my biggest fan and supporter, my wife, Kallie Smith Parsons. I would not be where I am today without my wife motivating me to strive to be the best person I can be. To my wife's and I's parents and families, I hope this work represents the support that you have given us to this day.

## ACKNOWLEDGEMENTS

I would like to offer my deep appreciation and gratitude to Dr. Heejin Cho. Dr. Cho provided me an incredible opportunity to continue my education at a time when I was not sure what direction I wanted to go with my career. He has provided me incredible guidance and support from the time that I met him. I would also like to acknowledge Gentry Berry for his willingness to answer any questions I had and his thoroughness in the design of the test stand. A huge appreciation belongs to Matthew Morgan and Titus Rogers for their work on developing the LabVIEW control program for the test stand. Without them, the test stand would not work nearly as well. Thank you to Jaime Rickertt, Jay McCown, John Wilson, Spencer Philips, Zach Phillips, Bill Trainor, Tucker Malone, and everyone else at ICET for their willingness to help, train, and provide past experiences. Finally, a special thanks to Tony Wofford, Devin Starkey, Kris Gonzalez, and Mike Sullivan for using their talents to construct the test stand.

## TABLE OF CONTENTS

DEDICATION.....	ii
ACKNOWLEDGEMENTS.....	iii
LIST OF TABLES.....	vi
LIST OF FIGURES.....	vii
CHAPTER	
I. INTRODUCTION.....	1
1.1 Project Overview.....	1
1.2 Statement of Need.....	2
1.3 Objectives.....	2
II. OVERVIEW OF HIGH EFFICIENCY FILTRATION AND AEROSOL MEASUREMENT.....	3
2.1 Background of HEPA Filtration.....	3
2.2 Sampling Method.....	10
2.3 Sampling Instrumentation.....	14
III. TEST STAND DESIGN AND CONSTRUCTION.....	23
3.1 Test Stand Criteria.....	23
3.2 Design Calculations.....	24
3.3 Test Stand Components.....	36
IV. RESULTS AND DISCUSSION.....	56
4.1 Air Flow Condition Capabilities.....	56
4.2 Diluter Characterization.....	60
4.3 Sampling Efficiency Verification.....	65
4.4 Well Mixing of Aerosols Verification.....	68
4.5 Filter Efficiency Results.....	72
4.6 Filter Loading Results.....	80
V. CONCLUSIONS.....	89

REFERENCES .....92

APPENDIX

A. PRELIMINARY DESIGN OF THE SMALL-SCALE FILTRATION TEST STAND .93

B. SMALL-SCALE TEST STAND FILTER EFFICIENCY TEST PROCEDURE.....128

C. SMALL-SCALE TEST STAND LOADING TEST PROCEDURE .....135

## LIST OF TABLES

Table 3.1	SSTS Performance Criteria .....	23
Table 3.2	Probe Diameters for 5 L/min Sampling.....	31
Table 3.3	SSTS Instrumentation.....	54
Table 4.1	5 ft/min Filter Efficiency Test Results .....	74
Table 4.2	15 ft/min Filter Efficiency Test Results .....	76
Table 4.3	31.7 ft/min Filter Efficiency Test Results .....	78
Table 4.4	45 ft/min Filter Efficiency Test Results .....	80

## LIST OF FIGURES

Figure 2.1	HEPA Filter Diagram .....	4
Figure 2.2	Stages of Particle Loading: (a) clean filter, (b) depth loading, (c) transition from depth loading to surface loading, (d) surface loading.....	5
Figure 2.3	Pre-Filter Loading Test.....	6
Figure 2.4	Post-Filter Loading Test .....	7
Figure 2.5	General Loading Curve for Flat Sheet Media .....	9
Figure 2.6	Example of an Isokinetic Sampling Probe .....	11
Figure 2.7	Examples of anisokinetic sampling probes .....	12
Figure 2.8	Electrostatic Classifier Schematic .....	15
Figure 2.9	Schematic of the DMA.....	16
Figure 2.10	Schematic of the CPC.....	17
Figure 2.11	SMPS Configuration .....	18
Figure 2.12	Schematic of the LAS.....	19
Figure 2.13	LAS for SSTS.....	20
Figure 2.14	Set of Diluters for the SSTS .....	21
Figure 2.15	Schematic of a TSI Inc. Diluter.....	22
Figure 3.1	Layout of Lab 282 at ICET. ....	24
Figure 3.2	Instrumentation Diagram of the SSTS .....	25
Figure 3.3	$Re$ for the Desired Flow Rates in a 4-inch Duct. ....	26
Figure 3.4	2-kilowatt Heater Coil.....	27
Figure 3.5	Heater Relay Controller.....	28

Figure 3.6	Estimated Head Loss through the SSTS.....	29
Figure 3.7	1.5 hp Blower and VFD.....	30
Figure 3.8	Stk Calculation for Al(OH) <sub>3</sub> .....	32
Figure 3.9	Stk Calculation for PAO.....	32
Figure 3.10	Concentration Ratios for Al(OH) <sub>3</sub> .....	33
Figure 3.11	Concentration Ratios for PAO.....	34
Figure 3.12	Injection Manifold Assembly.....	35
Figure 3.13	Pre-and-Post-Filter .....	36
Figure 3.14	Pre-Filter Housing .....	37
Figure 3.15	Post-Filter Housing.....	37
Figure 3.16	Coupon Holder Assembly. ....	38
Figure 3.17	NI CompactDAQ.....	39
Figure 3.18	Control Loop for the VFD.....	40
Figure 3.19	Control Loop for the Heater Relay.....	40
Figure 3.20	CFM to ACFM .....	41
Figure 3.21	LabVIEW Control Panel. ....	42
Figure 3.22	Sampling Train .....	43
Figure 3.23	Upstream and Downstream Flow Conservation.....	44
Figure 3.24	Sampling Vacuum Pump and Mass Flow Controller .....	45
Figure 3.25	Flow Splitter .....	46
Figure 3.26	Schematic of the SSTS Sampling System.....	46
Figure 3.27	Powder Feeder for Al(OH) <sub>3</sub> and ARD.....	47
Figure 3.28	Atomizer schematic from TSI. ....	48
Figure 3.29	Atomizer for PAO. ....	49
Figure 3.30	Upstream Temperature and RH Probe and Static Pressure Transducer. ....	50

Figure 3.31 dP Sensor for Test Filter.....	51
Figure 3.32 Downstream Temperature and Humidity Probe and Mass Flow Meter.....	52
Figure 3.33 Make-up Air Valve and Actuator .....	53
Figure 3.34 Completed SSTS Labeled.....	53
Figure 4.1 0.5 cfm Flow Measurement.....	57
Figure 4.2 17 cfm Flow Measurement.....	57
Figure 4.3 17 cfm Temperature Measurement.....	59
Figure 4.4 New vs Baked Filter Coupon .....	60
Figure 4.5 Diluter Characterization Baseline Test.....	61
Figure 4.6 100:1 Dilution Particle Distribution .....	62
Figure 4.7 20:1 Dilution Particle Distribution .....	63
Figure 4.8 Scaled 2000:1 Particle Distribution.....	64
Figure 4.9 Diluter Characterization Distributions .....	65
Figure 4.10 0.27-inch ID Sampling Probe .....	66
Figure 4.11 0.67-inch ID Sampling Probe .....	66
Figure 4.12 Anisokinetic Sampling Condition Test .....	68
Figure 4.13 Diagram of Traverse Measurement in the Duct .....	69
Figure 4.14 Traverse Sample Probe.....	70
Figure 4.15 0.5 cfm SMPS Traverse Sample Measurements .....	71
Figure 4.16 6 cfm SMPS Traverse Sample Measurements .....	71
Figure 4.17 5 ft/min Up and Downstream Particle Distributions per LAS and SMPS .....	73
Figure 4.18 LAS and SMPS Penetration Distribution for 5 ft/min .....	73
Figure 4.19 15 ft/min Up and Downstream Particle Distributions per LAS and SMPS .....	75
Figure 4.20 LAS and SMPS Penetration Distribution for 15 ft/min .....	75
Figure 4.21 31.7 ft/min Up and Downstream Particle Distributions per LAS and SMPS .....	77



Figure 4.22 LAS and SMPS Penetration Distribution for 31.7 ft/min.....	77
Figure 4.23 45 ft/min Up and Downstream Particle Distributions per LAS and SMPS .....	79
Figure 4.24 LAS and SMPS Penetration Distribution for 45 ft/min .....	79
Figure 4.25 Al(OH) <sub>3</sub> Particle Size Distributions for 5 ft/min Loading Test.....	81
Figure 4.26 dP and Mass Loaded for 5 ft/min .....	82
Figure 4.27 Mass Loading Curve for 5 ft/min .....	82
Figure 4.28 Al(OH) <sub>3</sub> Particle Size Distributions for 10 ft/min Loading Test.....	83
Figure 4.29 dP and Mass Loaded for 10 ft/min .....	84
Figure 4.30 Mass Loading Curve for 10 ft/min .....	84
Figure 4.31 Al(OH) <sub>3</sub> Particle Size Distributions for 30 ft/min Loading Test.....	85
Figure 4.32 dP and Mass Loaded for 30 ft/min .....	86
Figure 4.33 Mass Loading Curve for 30 ft/min .....	86
Figure 4.34 Al(OH) <sub>3</sub> Particle Size Distribution for 45 ft/min Loading Test .....	87
Figure 4.35 dP for 45 ft/min Loading Test .....	88

# CHAPTER I

## INTRODUCTION

### 1.1 Project Overview

The process of filtration can be described as removing particles suspended in a gas or liquid by utilizing a porous medium. Although the definition of filtration is broad, it is typically subdivided into liquid and gas filtration. Gas filtration is commonly used in everyday applications ranging from residential Heating, Ventilation, and Air Conditioning (HVAC) air filters to pleated High Efficiency Particulate Air (HEPA) filters to remove radioactive particles and airborne viruses. Ensuring that these filters perform as well as they physically can is essential to protect workers and their environments. Therefore, improving the understanding of how these filters work, specifically how particles load onto the filter during its service life, is essential. In order to simplify the testing methods and analysis of filtration, flat sheet HEPA media is used in place of the full-sized pleated filter specifically for this characterization. Focusing squarely on the media itself provides an isolated baseline of understanding that can be built upon to further improve filter designs. Therefore, we have designed, constructed, and characterized the Small Scale Test Stand (SSTS) that is capable of performing penetration and loading tests on various forms of flat sheet filter media with a range of particle types to study the filter's efficiency and the relationship between the differential pressure (dP) drop and the total mass of the deposited particles.

## **1.2 Statement of Need**

The Institute for Clean Energy Technology (ICET) has been collaborating with the Department of Energy (DOE) to continue research of HEPA filtration. The SSTS was developed with the hope of contributing to our understanding of the mechanics of aerosols and filter loading. The concept of exploring the need for a small scale filter loading test stand originates from what ICET's large scale testing stands cannot offer: flat sheet filter media testing. ICET's two large scale test stands, the Axial Large Scale Test Stand (ALSTS) and the Radial Large Scale Test Stand (RLSTS), perform tests using full-sized pleated axial (or box) and radial pleated HEPA filters, respectively. The SSTS is funded by the DOE under contract DE-EM0003163.

## **1.3 Objectives**

The objective of the development of the SSTS was to produce high-quality, research-grade data that could determine a filter media's efficiency and evaluate the particle loading of various filter medias. The prescribed requirements to achieve this objective include:

- Generating a constant flow rate of up to 20 actual cubic feet per minute (ACFM) with a maximum temperature of 250°F
- Inject particles, such as Aluminum Trihydroxide ( $\text{Al}(\text{OH})_3$ ), Arizona Road Dust (ARD), and Polyalphaolefin (PAO)
- Ensure that the aerosols become well-mixed with a uniform flow distribution prior to reaching the test filter face
- Efficiently sample the air stream to capture accurate data of the particle counts and particle size distribution

## CHAPTER II

### OVERVIEW OF HIGH EFFICIENCY FILTRATION AND AEROSOL MEASUREMENT

#### **2.1 Background of HEPA Filtration**

Understanding the development of HEPA filters and the testing that has been done is crucial in being able to move forward to produce quality results. HEPA filters were developed due to a series of events stemming from World War II. The British forces acquired German gas masks containing filter paper that greatly outperformed the resin-wool filters typically used at the time. The German filter was sent to the United States Army Chemical Warfare Service Laboratories where they performed testing in order to be able to reproduce the superior media. The filter media was found to be made of asbestos mixed with esparto grass. This combination provided improved air flow while still having a high particle capturing ability. Obtaining the new type of filter media was the jump start of aerosol filtration research which had previously been a basis of water filtration knowledge [1]. The next step taken was to develop a larger scale filter that used the same high efficiency properties to protect workers in a facility from chemicals in the air. This eventually led to the development of modern HEPA filters, such as the filter illustrated in Figure 2.1 [1].

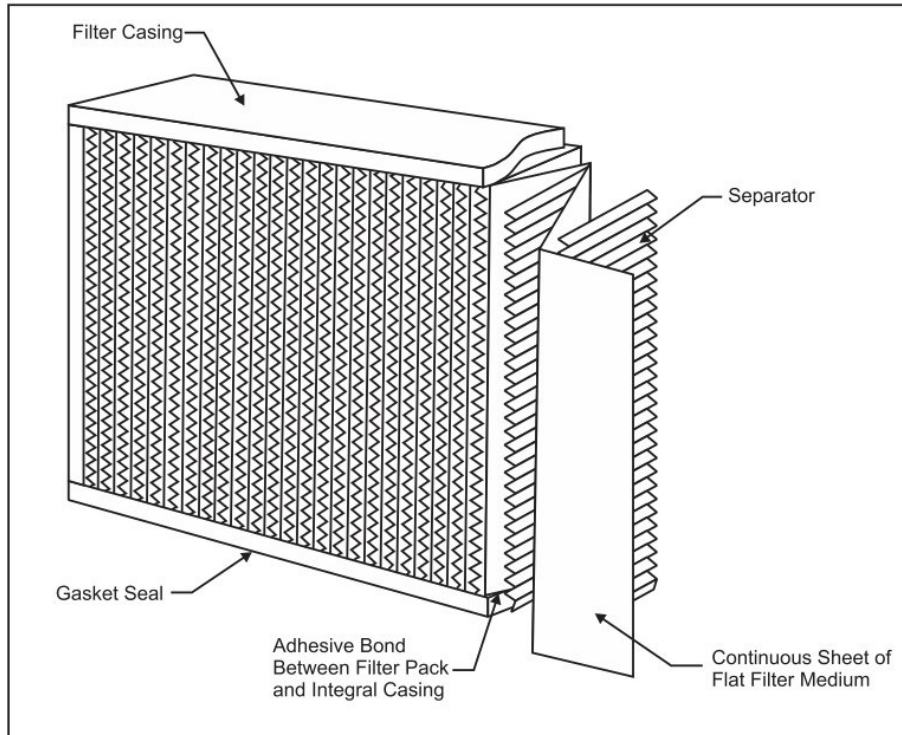


Figure 2.1 HEPA Filter Diagram

This filter uses pleated filter media, usually comprised of fiberglass fibers, in order to maximize the area of the media, therefore increasing the efficiency. The American Society of Mechanical Engineers (ASME) AG-1 Code on Nuclear Air and Gas Treatment standard set the performance and construction criteria for HEPA filters used in many DOE facilities. In short summary: (1) a 99.97% particle removal efficiency for particles of 0.3 micrometers; (2) a maximum pressure drop of 1 inch of water column (inWC) when the filtration media is clean; (3) a ridge frame or casing that covers the entire depth of the filter. These casings are typically made of wood or metal. HEPA filters are used in multiple industries today, especially in medical or industry settings where radioactive particles are a potential threat [1–3].

With these standards, high-efficiency filters are now commonly produced and used in various applications. The efficiency of the HEPA filters leads to a more rapid particle cake formation compared to less efficient filter media. The filter cake eventually performs as the primary filtration of the air. The stages of particle loading are shown in Figure 2.2 [2].

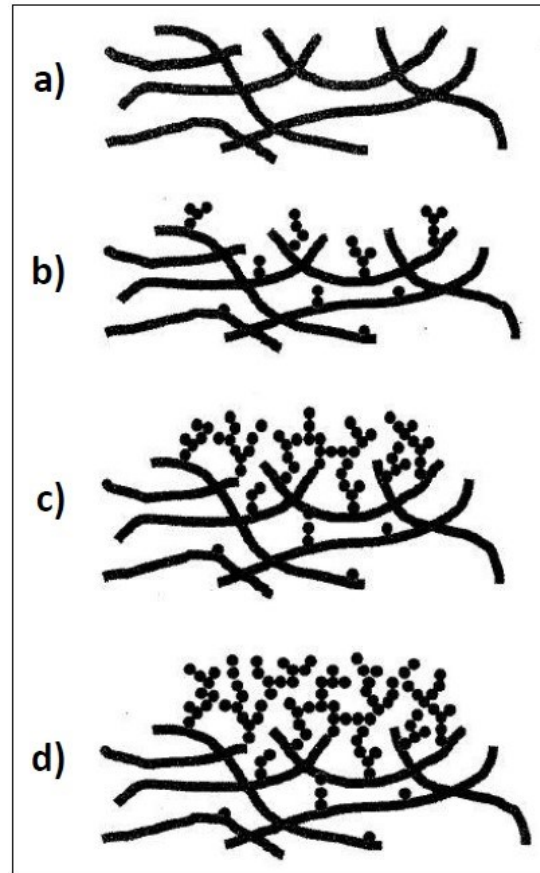


Figure 2.2 Stages of Particle Loading: (a) clean filter, (b) depth loading, (c) transition from depth loading to surface loading, (d) surface loading

Initially, the HEPA filter experiences normal particle deposition inside the depth of the filtration media. As the particles load into the filter, the loading regime as the particle deposits merge together, transitioning from depth loading to surface loading where the deposited particles

themselves constitute the main filtration component. Figures 2.3 and 2.4 show the before and after results, respectively, of a full-sized HEPA filter loading test performed at ICET.



Figure 2.3 Pre-Filter Loading Test





Figure 2.4 Post-Filter Loading Test

Flat sheet media is commonly selected in filtration loading research, as the filtration area remains constant. In contrast, the filtration area of a pleated filter will change over time as the creases in-between the pleats become clogged. The importance of having a constant surface area can be shown using Bergman's analytical model for HEPA filter loading, shown in Equation 2.1 [2].

$$(\Delta P_m - \Delta P_{m0}) * \frac{\rho_{pD} D_p^n}{V_m} = k_i * \frac{M}{A} \quad (2.1)$$

Where  $\Delta P_m$  is the pressure drop for particle loaded filter,  $\Delta P_{m0}$  is the initial pressure drop of the clean filter,  $\rho_{pD}$  is the density of the particles deposited,  $D_p$  is the particle diameter,  $V_m$  is the velocity at the filter face,  $n$  is either 1 for depth loading or 2 for surface loading,  $M$  is the



mass of the particles deposited, and  $k_i$  is a constant depending on the previously mentioned type of loading. For depth loading, Equation 2.2 may be used.

$$k_1 = \frac{64\sqrt{\alpha_f}}{D_f} \quad (2.2)$$

Where  $\alpha_f$  is the porosity of the filter and  $D_f$  is the fiber diameter. When the filter transitions to surface loading, Equation 2.3 is used.

$$k_2 = \frac{180\alpha_p}{(1 - D_p)^3} \quad (2.3)$$

Where  $\alpha_p$  is the porosity of the particle cake. Unfortunately, both of these porosities are difficult to calculate or measure. However, an experimental correlation from Novick et al may be used to circumvent the need for knowing the porosity, shown below in Equation 2.4 [4].

$$k_3 = \left( \frac{0.963}{D_p} - 1.64 * 10^5 \right) * \rho_{pD} * D_p^n \quad (2.4)$$

These equations can be used to generate a theoretical pressure drop evolution as particle mass is loaded onto the flat sheet media. Three distinct regions are expected as the particle loading goes through the stages shown in Figure 2.5.

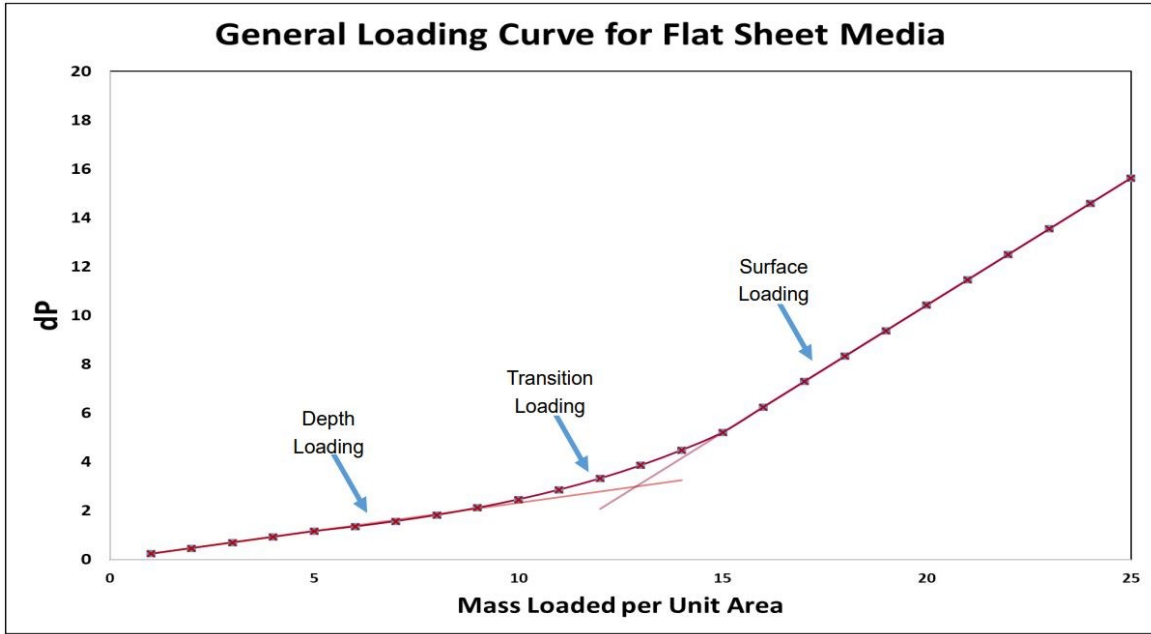


Figure 2.5 General Loading Curve for Flat Sheet Media

The shown loading curve is what is expected for the SSTS to produce when performing a loading test. The differential pressure across the test filter is directly measured during testing, but the mass loaded onto the test filter must be calculated. In order to determine the mass loaded onto the filter over a period of time, Equation 2.5 can be used [5].

$$M = N * D_p^3 * \rho_p * \frac{\pi}{6} \tag{2.5}$$

Where N is the number concentration. It is important to note that this equation only accounts for the mass the particles for a single diameter, although it is common to have an aerosol with a distribution of particle diameters. Equation 2.5 may be easily modified to sum the masses of the particle diameters to accurately represent the total mass.

## 2.2 Sampling Method

In order to calculate the loaded particle mass, the concentration of the particles in the air before and after the filter must be determined. This is accomplished using the aerosol sampling system, and constitutes one of the most important components of the SSTS. The aerosol sampling system consists of the sampling probes, tubing, sampling train, and the previously mentioned sampling instrumentation. The sampling must be as accurate as possible in order to provide meaningful data. The main concern when sampling is whether or not the samplers are isokinetic. By definition, isokinetic sampling requires that the air velocity in the sampling tube is equal to the velocity of the duct. Thus, the kinetic energy of the particles remains the same, and inertial effects of large particle or the effects from external forces on smaller particles are ideally avoided. The relationship of the flow rates and diameters of the sampling probe and duct is shown in Equation 2.6 [5].

$$\frac{Q_s}{Q_o} = \left(\frac{D_s}{D_o}\right)^2 \quad (2.6)$$

Where  $Q_s$  is the sampling flow rate,  $Q_o$  is the duct flow rate,  $D_s$  is the probe diameter, and  $D_o$  is the duct diameter. An example of an isokinetic sampling probe is shown in Figure 2.6 [5]. Having the air velocities to be equivalent is one of the best ways to ensure that the sample flow concentration is the same as the duct flow.

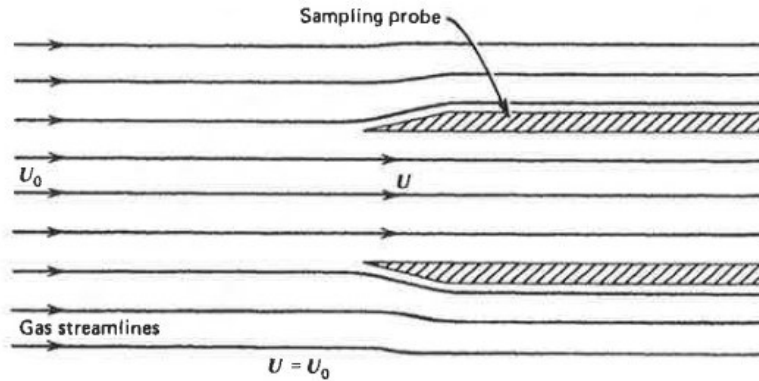


Figure 2.6 Example of an Isokinetic Sampling Probe

The opposite of isokinetic sampling is anisokinetic sampling. There are three examples of anisokinetic sampling shown in Figure 2.7 [5]. The first is a misaligned probe. A misaligned probe will not sample accurately as the particles may be unable to make the turn into the probe. The next anisokinetic sampling type is super-isokinetic. This occurs when the sample line is sampling more than the duct. Super-isokinetic sampling causes particles with a large amount of inertia to cannot make the sharp turn into the sampling probe leading to the sampled concentration to be lower than the actual. Finally, if the sample line is sub-isokinetic, the sample probe will not capture enough of the particles.

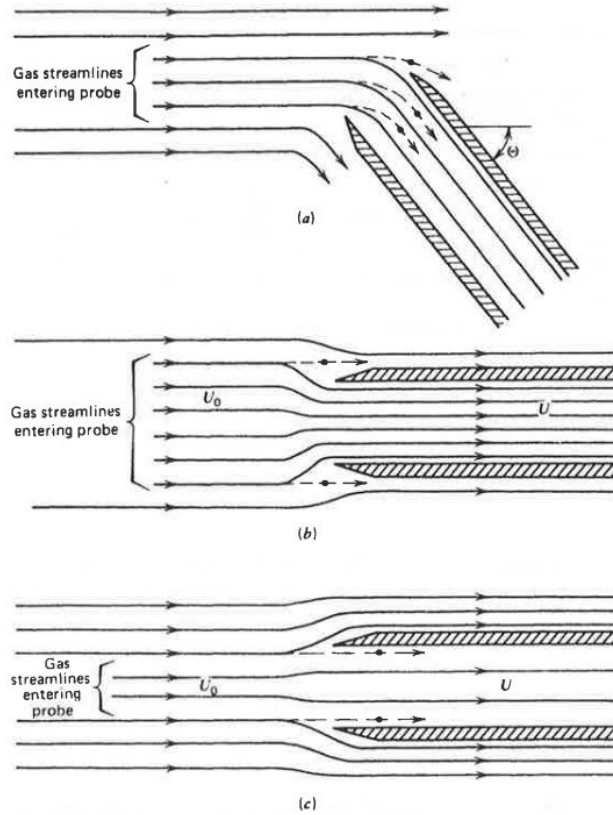


Figure 2.7 Examples of anisokinetic sampling probes

(a) Misaligned probe. (b). Super isokinetic sampling. (c) Sub isokinetic sampling

If unable to satisfy the isokinetic conditions, an analysis of the particle motion can be conducted to determine the impact of having anisokinetic conditions. An important part of this analysis focuses on a dimensionless number called the Stokes number ( $Stk$ ). The  $Stk$  can be determined by the equation 2.7.

$$Stk = \frac{\tau * U_0}{D_s} \quad (2.7)$$

Where  $\tau$  is the “relaxation time” of the particle,  $U_0$  is the undisturbed air velocity, and  $D_s$  is the diameter of the sampling probe.  $\tau$  is referred to as the relaxation time it represents

the time required for a particle to transition from one velocity to another.  $\tau$  can be found using equation 2.8.

$$\tau = m * B \quad (2.8)$$

Where  $m$  is the mass of the particle and  $B$  is the mechanical mobility of the particle. The mass of the particle can be found using equation 2.9.

$$m = \frac{\pi}{6} * \rho_p * d_p^3 \quad (2.9)$$

Where  $\rho_p$  is the density of the particle and  $d_p$  is the diameter of the particle. The mechanical mobility of the particle can be determined using equation 2.10

$$B = \frac{C_c}{3\pi\eta d_p} \quad (2.10)$$

Where  $C_c$  is the Cunningham correction factor, and  $\eta$  is the viscosity of the air. The Cunningham correction factor is needed due to smaller particles (<1.0  $\mu\text{m}$ ) settling faster. This is a result of the smaller particles are more influenced by the gas velocity. Whichever Cunningham correction factor equation that is used is dependent on the size of the particle. For diameters greater less 0.1 $\mu\text{m}$  equation 2.11 is used. For diameters 0.1-1 $\mu\text{m}$ , equation 2.12 is used. For diameters greater than 1 $\mu\text{m}$ , no correction is needed.

$$C_c = 1 + \frac{\lambda}{d_p} (2.34 + 1.05 \exp(-0.39 \frac{d}{\lambda})) \quad (2.11)$$

$$C_c = 1 + \frac{2.52\lambda}{d_p} \quad (2.62)$$

Where  $\lambda$  is the mean free path for air. The mean free path takes into account a particle's interaction with the molecules of the gas the particle is traveling through. This value is represented as the number of collisions between the particle and gas molecules during a one second time period divided by the distance covered in that time. After deriving the Stk number from the previous equations, if the resulting value is less than 0.01, the particles inertia can be neglected, and the sampling can be considered efficient [5]. In order to further assure that the sampling efficiency is adequate, the concentration ratio of the aerosols in the duct compared to the aerosol concentration in the sampling probe can be determined. This equation is given in equation 2.13.

$$\frac{C}{C_o} = 1 + \left( \frac{U_o}{U} - 1 \right) * \left( 1 - \frac{1}{1 + (2 + 0.62 * \frac{U}{U_o}) Stk} \right) \quad (2.73)$$

Where  $C_o$  is the concentration in the duct,  $C$  is the concentration in the sampling probe, and  $U$  is the velocity of the gas in the duct. If the resulting ratio is close to 1, it can be assumed that the anisokinetic conditions have a negligible effect on the concentration output of the measurement instruments.

### 2.3 Sampling Instrumentation

Assuming that either the sampling probes are isokinetic or the concentration ratio evaluation is satisfactory, the next step is running the sampled air through particle counting instruments. In general, there are two methods of sampling instrumentation: direct and indirect [5]. Direct measurement of mass concentration is done by detecting the particle's inertia or mass, while an indirect measurement is typically done by light scattering. The simplest form of direct aerosol measurement would be to perform a gravimetric analysis by measuring the weight of the

filter before and after a particle loading test. However, there can be errors associated with ensuring the particles remain on the filter when moving to measure. Another disadvantage of gravimetric analysis is that the concentration during the test is unknown. Therefore, a common alternative to obtain real time, direct particle measurements is to use an electrical mobility analyzer [5,6]. A diagram of a TSI Inc. Electrostatic Classifier (EC) can be seen in Figure 2.8 [7].

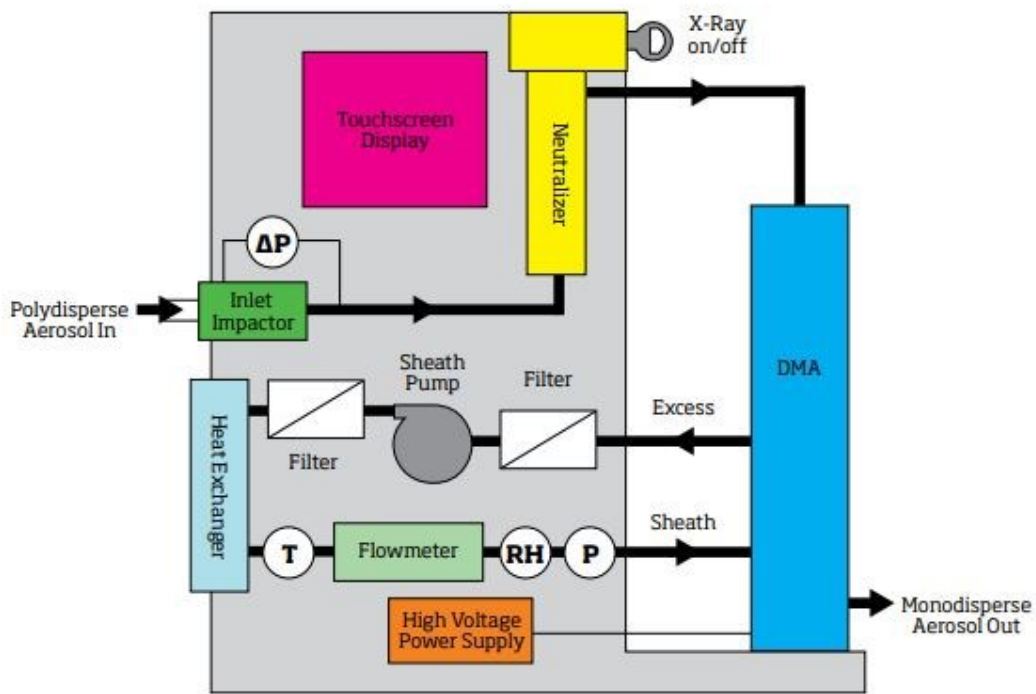


Figure 2.8 Electrostatic Classifier Schematic

This instrument takes sampled aerosol and sorts it by their diameters by utilizing their electrical mobility. This is done by the use of a Differential Mobility Analyzer (DMA). The DMA generates a varying electric field in order to sort the different particle diameters based



upon their electrical mobility. The relationship between a particles diameter and their electrical mobility can be seen in equation 2.14 [6].

$$Z_p = \frac{\text{Particle Velocity}}{\text{Electric Field Strength}} = \frac{v}{E} = \frac{n_p * e * C}{3 * \pi * \mu * D_p} \quad (2.14)$$

where  $Z_p$  is the electrical mobility,  $n_p$  is the number of charges per particle,  $e$  is the elementary unit of charge, and  $\mu$  is the viscosity of the gas. As the field intensity changes by increasing or decreasing the input voltage, the particles electrical mobility change. The aerosol is sorted based upon the concept illustrated below in Figure 2.9 [7].

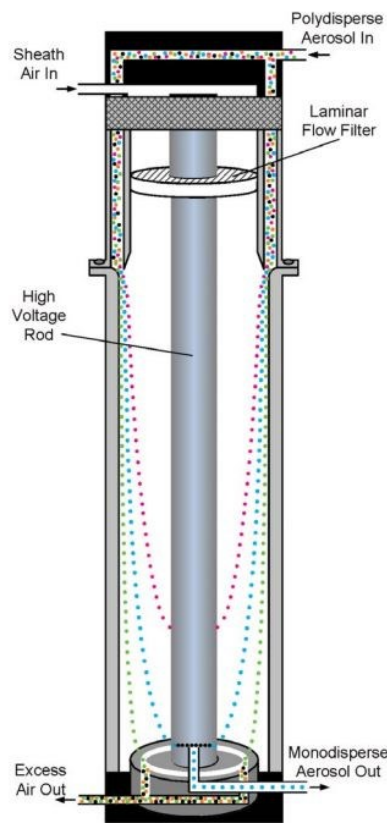


Figure 2.9 Schematic of the DMA

As these particles are sorted, they are sent to a Condensation Particle Counter (CPC) to be counted. The CPC condensates a fluid, such as butanol, to the sorted particles in order to make them larger to be more easily detected [7]. The CPC lines up the particles and counts them as they pass through a laser photodetector. The counting process can be seen in Figure 2.10 [8].

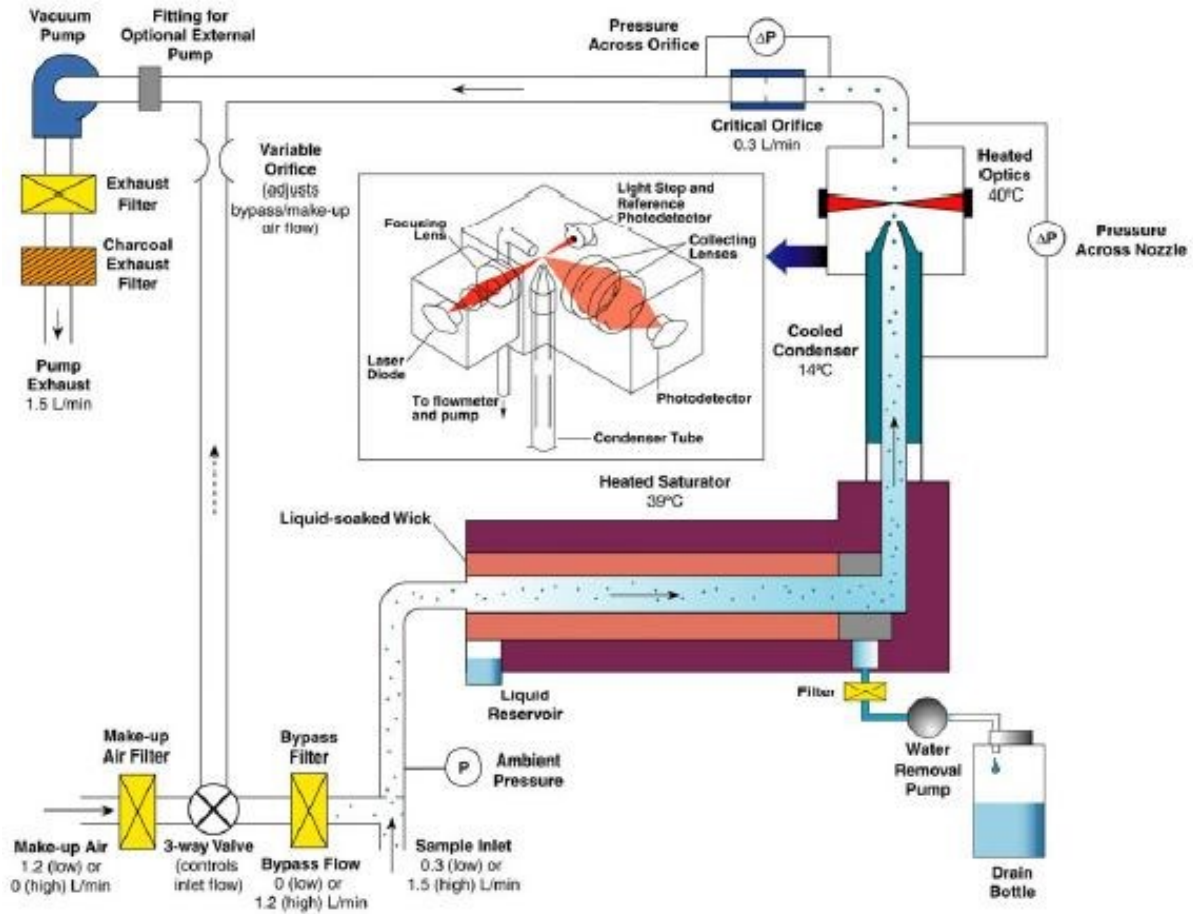


Figure 2.10 Schematic of the CPC

The combination of the EC, DMA, and the CPC is known as the Scanning Mobility Particle Sizer (SMPS), manufactured by TSI Inc. During the sampling period, by knowing the DMA voltage and flow rates through the EC and CPC, the instruments can determine the total

concentration per volume. This instrument is capable of handling concentrations up to  $10^7$  particles per cubic centimeter (ccm). However, the particle size range can be limited depending on the aerosol to be measured, namely its size if it's comprised of large particles. The SMPS can measure diameters of 0.24nm – 1 $\mu$ m. Therefore, a combination of two different types of sampling instruments can be used in tandem. The SMPS set up is shown in Figure 2.11.



Figure 2.11 SMPS Configuration

A common indirect measurement instrument is TSI Inc.'s Laser Aerosol Spectrometer (LAS). Similar to the counting method of the CPC, the LAS uses the optical method of light scattering to measure the particle size. The LAS schematic can be seen in Figure 2.12 [9].

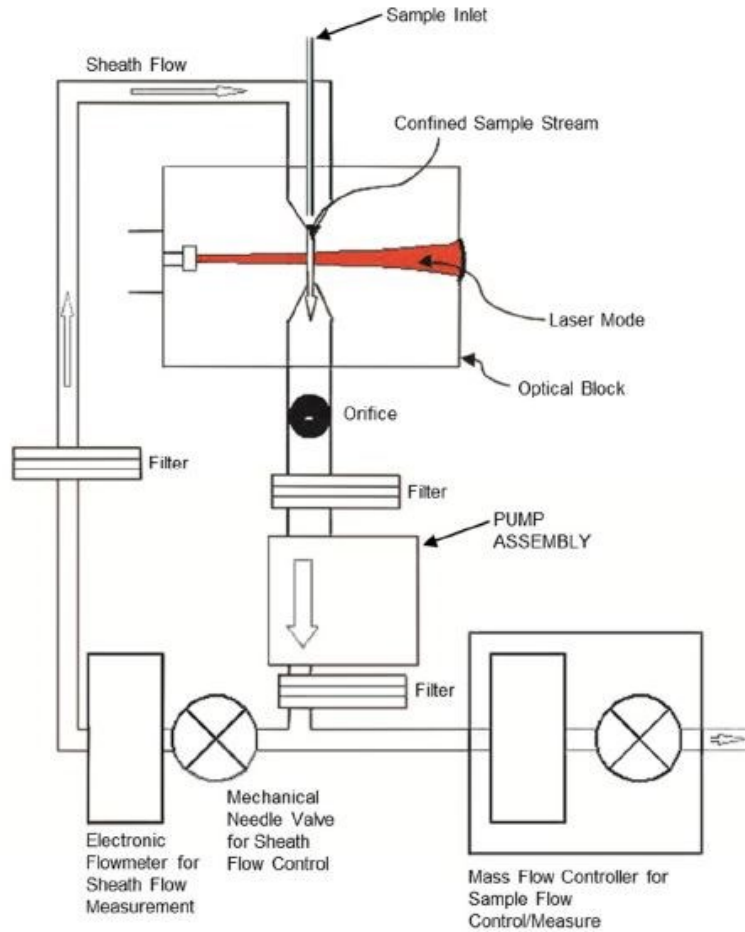


Figure 2.12 Schematic of the LAS

The LAS can provide a larger particle size range compared to the SMPS with the capability of detecting a size range of 0.09 $\mu\text{m}$  – 7.5 $\mu\text{m}$ . A LAS is pictured in Figure 2.13. Using the SMPS and LAS at the same time provides a greater range of particle sizes to be measured, as well as validate each other since there is an overlap of the diameter ranges. The given uncertainties for the LAS and SMPS are provided later in Chapter 3 within Table 3.3.



Figure 2.13 LAS for SSTS

However, the drawback of the LAS is that maximum readable concentration is 3,600 particles/ccm. Any higher of a concentration would lead to the laser to be overwhelmed. Therefore, when using the LAS, the sample must be diluted before entering the instrument. Diluters use isokinetic capillaries in order to reduce the concentration by a factor of either 20 or 100. A set of 20:1 and 100:1 diluters are shown in Figure 2.14.



Figure 2.14 Set of Diluters for the SSTS

In order to function correctly, the diluters are sized to subsample a flow of 5 L/min. The dilution method of subsampling is more of an artificial dilution. Instead of a typical dilution method of adding clean air to a sampled concentration, subsampling decreases the concentration by the rated factor. The dilution factor ( $DF$ ) is a ratio of the subsample flow rate ( $Q_s$ ) and the dilution flow rate ( $Q_{dilute}$ ). This ratio is shown in Equation 2.8.

$$DF = \frac{Q_{dilute}}{Q_{sample}} \quad (2.8)$$

The flow rate through the capillary is adjusted by a dP adjustment valve to the calibrated aerosol and total dP values. These diluters can be used in series in order to reduce the concentration low enough for the LAS to be used. A schematic of a typical diluter is provided in Figure 2.15 [10].



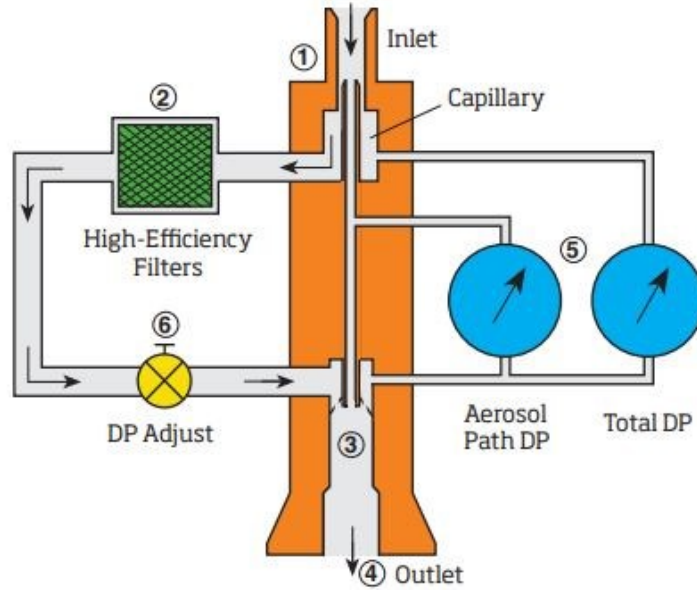


Figure 2.15 Schematic of a TSI Inc. Diluter

Since the HEPA filter media is so efficient, in order to be able to sample downstream, very high concentrations must be used upstream. Therefore, this requires the use of the diluters when sampling upstream.

CHAPTER III  
TEST STAND DESIGN AND CONSTRUCTION

**3.1 Test Stand Criteria**

With an understanding of particle loading, sampling, and particle counting instrumentation, the design and construction of the SSTS can be reviewed. As previously mentioned, the design criteria of the SSTS is as shown in Table 3.1.

Table 3.1 SSTS Performance Criteria

Flow	Generate a constant flow of near zero to 20 ACFM
Particle Measurement	Accurate sampling and measurement of particle concentration and size distributions
Condition Measurement	Accurate measurements of differential pressure across test article, static pressure, temperature, relative humidity, and flow rate
High Temperature	Range of lab temperature (~70°F) to 250°F

Another design constraint given was the assigned lab to hold the SSTS. Lab 282 at ICET was provided to be used to house the SSTS. The dimensions of Lab 282 in inches can be seen in Figure 3.1. In order to minimize the footprint of the SSTS, a duct diameter of 4 inches was assigned for the testing section. Since the SSTS would be operating at atmospheric pressure, schedule-10 stainless steel piping was selected.



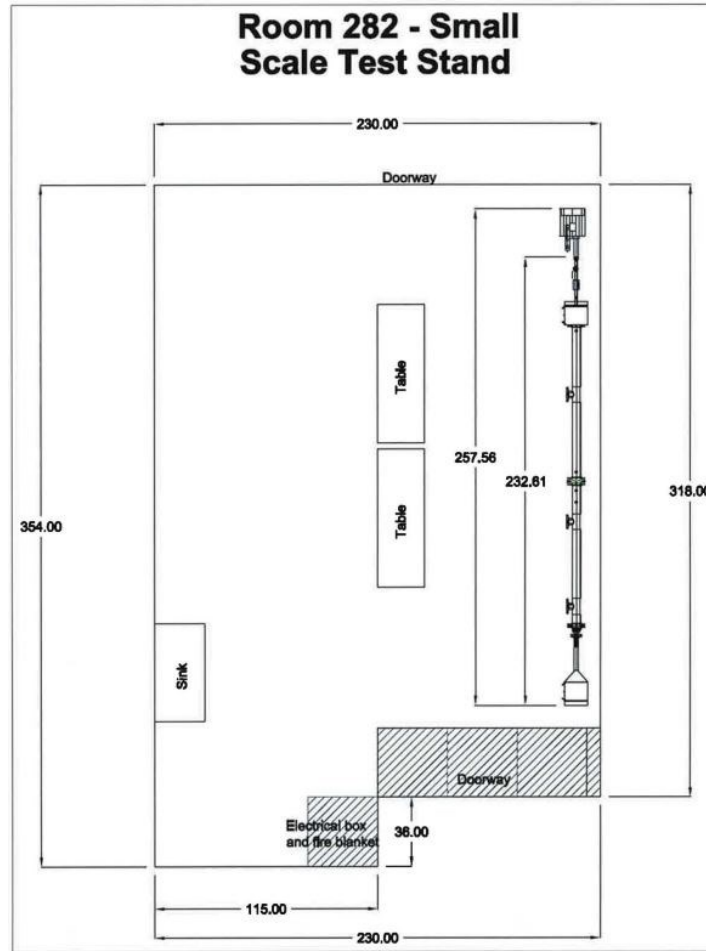


Figure 3.1 Layout of Lab 282 at ICET.

With the given design criteria and constraints known, the calculations of the individual components could be performed.

### 3.2 Design Calculations

In order to satisfy these design criteria, the instrumentation diagram shown in Figure 3.2 was developed as a preliminary concept.

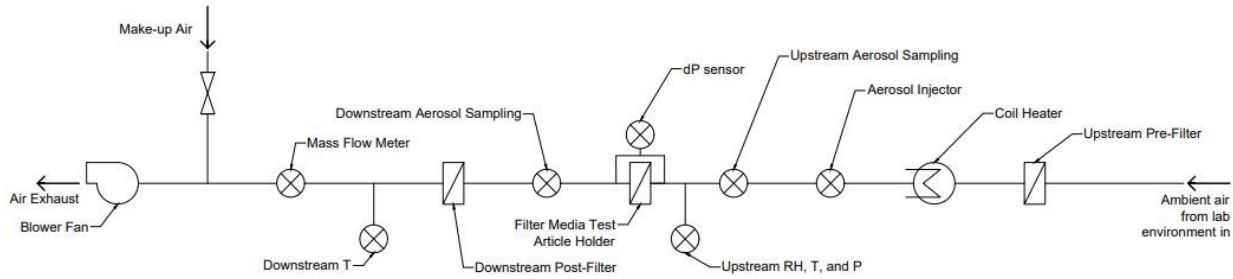


Figure 3.2 Instrumentation Diagram of the SSTS

*Piping.* To ensure that the aerosols injected into the duct would fully develop by the time they reach the upstream sampling probe, the 10 duct diameters “rule of thumb” was applied when determining the pipe length [5]. This “rule of thumb” also calls for 5 duct diameters of length downstream of the sampling probe. Since the duct diameter is 4 inches, 40 inches of obstruction free piping was allotted upstream of the probe and 20 inches downstream of the probes. While 10 duct diameters rule is adequate for flow development, the Reynolds number ( $Re$ ) for each of the flow rates must be determined. The  $Re$  is a dimensionless value and is used to characterize the air flow by determining if the flow is laminar or turbulent [6]. Equation 3.1 provides the  $Re$  formula.

$$Re = \frac{\rho V d}{\eta} \quad (3.1)$$

Where  $\rho$  is the air density,  $V$  is the air velocity,  $d$  is the nominal duct diameter, and  $\eta$  is the air viscosity. If the  $Re$  is less than 2000, the flow is considered laminar. Turbulent flow within a pipe is considered to be when  $Re$  is greater than 4000. Any  $Re$  value between these two phases is considered to be transitional flow. Standard conditions for air are considered to be 68°F and 14.7 pounds per square inch (psi). At these conditions, air density and viscosity are 0.075

lb/ft<sup>3</sup> and 1.216e-5 lb/ft\*s, respectively. Using these values and considering a 4-inch duct, the  $Re$  for flows between 0 and 20 cfm can be found. The  $Re$  for each flow can be found using the plot in Figure 3.3.

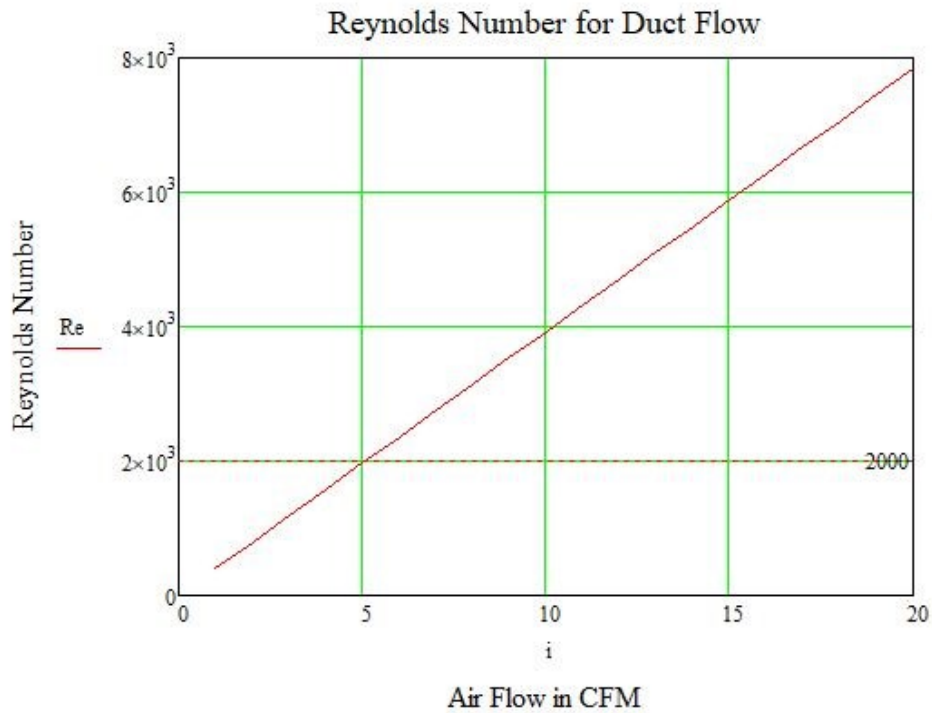


Figure 3.3  $Re$  for the Desired Flow Rates in a 4-inch Duct.

It can be observed that air flows between 0 and 5 cfm may be considered laminar, flows between 5 and 10 cfm are transitional, and flows greater than 10 cfm are turbulent. This is important to note for sampling particles in elevated flow rates that they may not be evenly distributed, possibly resulting in random fluctuations in the concentration or size distribution in the sampled flow. Tests later performed mostly took place in the laminar zone of flow rates to ensure repeatability when characterizing the SSTS.

*Coil Heater.* In order to achieve the desired air flow temperature of 250°F, a detailed heat transfer analysis was performed. These calculations for the different expected air flow rates can be found in Appendix A. These calculations resulted in needing a minimum of a 1.053-kilowatt (kW) heater coil to obtain the maximum temperature. As a result, a 2 inch, 2 kW heat coil was procured. This coil is pictured in Figure 3.4.

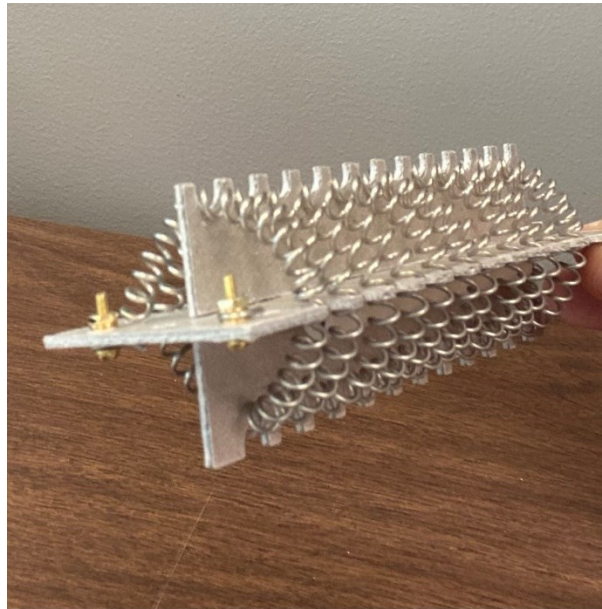


Figure 3.4 2-kilowatt Heater Coil

These calculations considered cool air from the aerosol injection as well. A relay is used to regulate the current provided to the heater coil. The relay is controlled by a constant control loop in order to hold the temperature at near steady-state. The selected relay is pictured in Figure 3.5.



Figure 3.5 Heater Relay Controller.

*Blower.* To ensure that the selected blower was adequately sized to pull the desired flow rate, an expected head loss estimate was performed. This estimate can also be found in Appendix A. This estimate considered pulling air through the pre- and post-filters, test filter at max loading, heater coil, instrumentation, piping, and transitional piping. Figure 3.6 provides the anticipated head loss with respect to the selected flow rate.

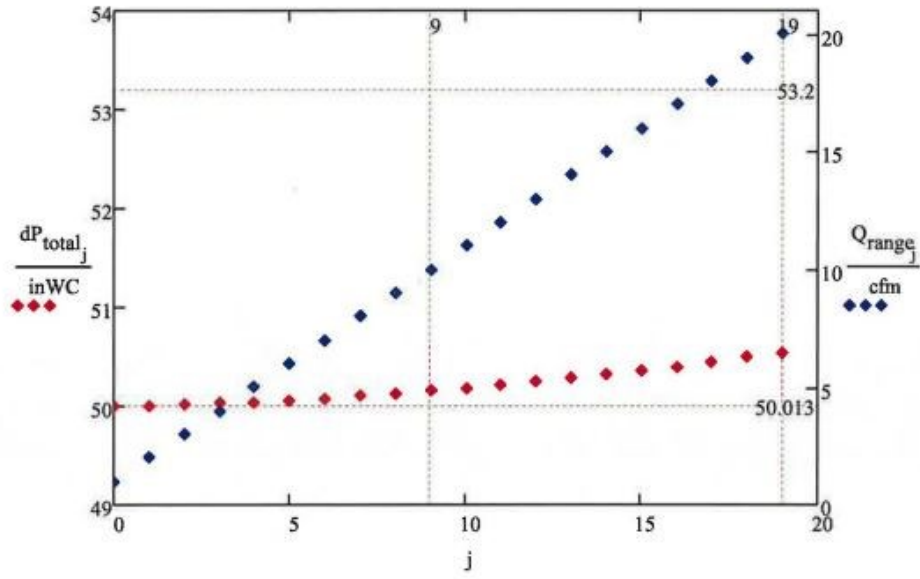


Figure 3.6 Estimated Head Loss through the SSTs.

Using the maximum expected head loss, a 1.5 horse power (hp) blower was selected to pull the air flow through the test stand. In order to control the flow, a Variable Frequency Drive (VFD) is used. This is done by simply scaling the frequency to the set flow rate. The blower and the VFD can be seen in Figure 3.7.



Figure 3.7 1.5 hp Blower and VFD.

*Sampling System.* As discussed in section 2.2, when possible, having isokinetic sampling probes is the best way to ensure that the duct samples accurately represent the aerosol concentration within in the duct. The diluters that are used at ICET also use the concept of isokinetic sampling by sizing the capillaries, shown in Figure 2.15, to sample either a twentieth or hundredth of the sampled flow rate. As previously mentioned, these diluters are specified to be used at a flow rate of 5 L/min to be functioning as characterized. Therefore, the flow rate going through the sampling probes will also be 5 L/min. Using Equation 2.6, the size of the

sampling probes can be determined for isokinetic sampling. The needed probe diameter and the percentage of the duct it would occupy for a range of low flow values is provided in Table 3.2.

Table 3.2 Probe Diameters for 5 L/min Sampling

Duct Flow Rate (cfm)	Isokinetic Probe Diameter (inches)	Percent of Duct (%)
0.5	2.377	59.4
1.0	1.681	42
1.5	1.372	34.3
2.0	1.189	29.7
2.5	1.063	26.6

There is no considered maximum amount of space that a probe is allowed to take up; however, it can be assumed that taking nearly 60% of the aerosols out of the test stand would have negative impacts on the test. In order to get around this issue, the Stk for the particles was calculated using Equations 2.7 through 2.12. Figures 3.8 and 3.9 provide plots of the Stk for  $\text{Al}(\text{OH})_3$  and PAO, respectively, for particle diameters between 0.025 and 5.025  $\mu\text{m}$ .



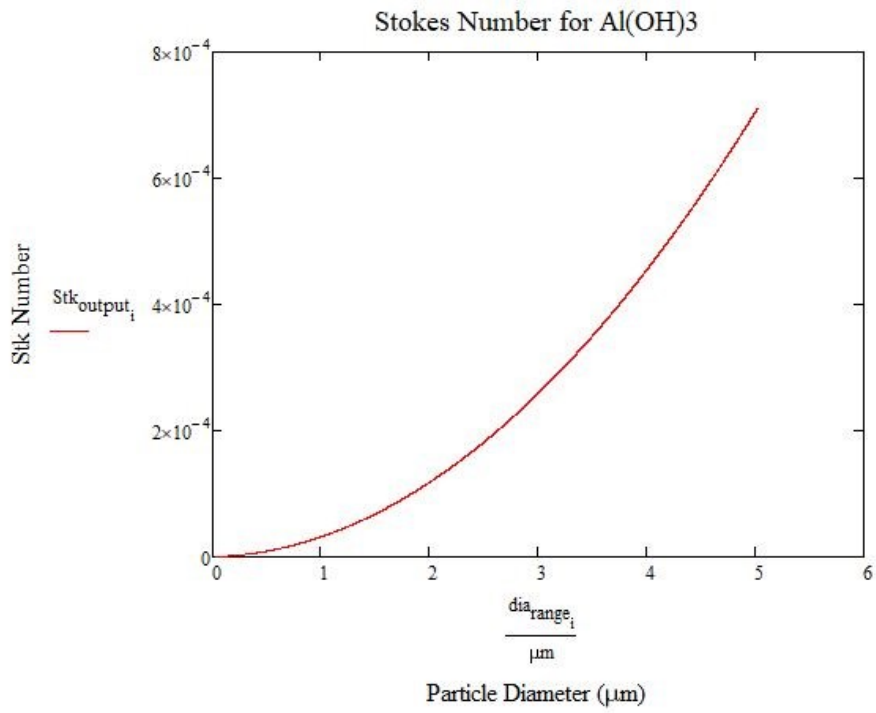


Figure 3.8 Stk Calculation for Al(OH)<sub>3</sub>

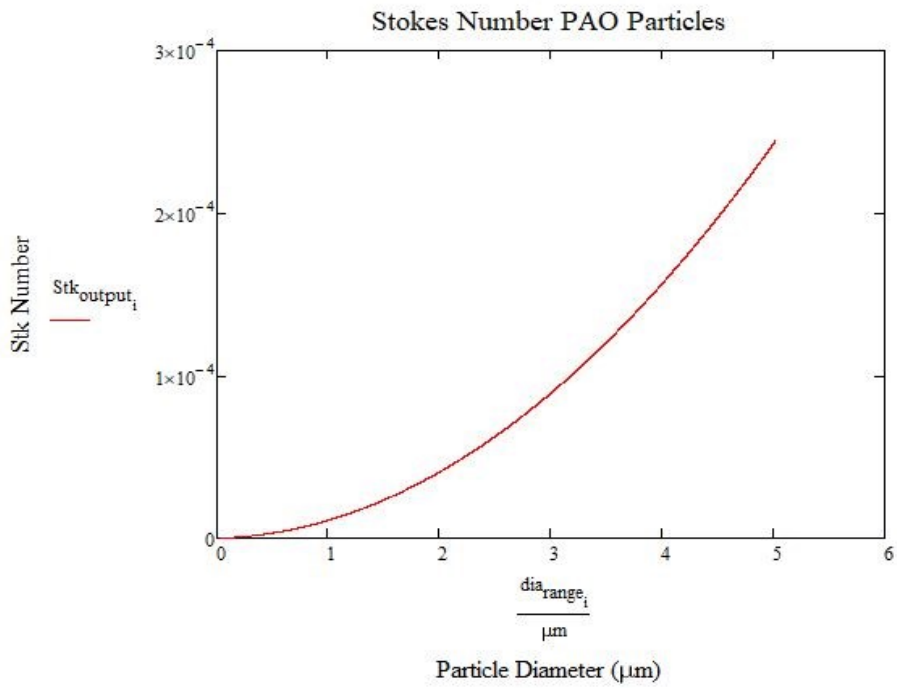


Figure 3.9 Stk Calculation for PAO

These calculations were performed at standard conditions with a 5 L/min sample flow rate, 0.5 cfm duct flow, arbitrarily picked 0.27-inch diameter sample probe, and the 4-inch duct diameter. Since  $\text{Al}(\text{OH})_3$  has a greater particle density (2.42 g/ccm) compared to PAO (0.833 g/ccm), the Stk for  $\text{Al}(\text{OH})_3$  is higher than PAO [11,12]. However, both yielded a Stk much less than the 0.01 threshold, making the conditions very efficient. To further show the efficiency of the concentration ratios for each particle type, Figures 3.10 and 3.11 show the concentration ratio for  $\text{Al}(\text{OH})_3$  and PAO, respectively, calculated using Equation 2.13. Duct flow rates of 0.5, 6, and 20 cfm were used for calculations to get a wide view of the concentration efficiencies for both sets of particles.

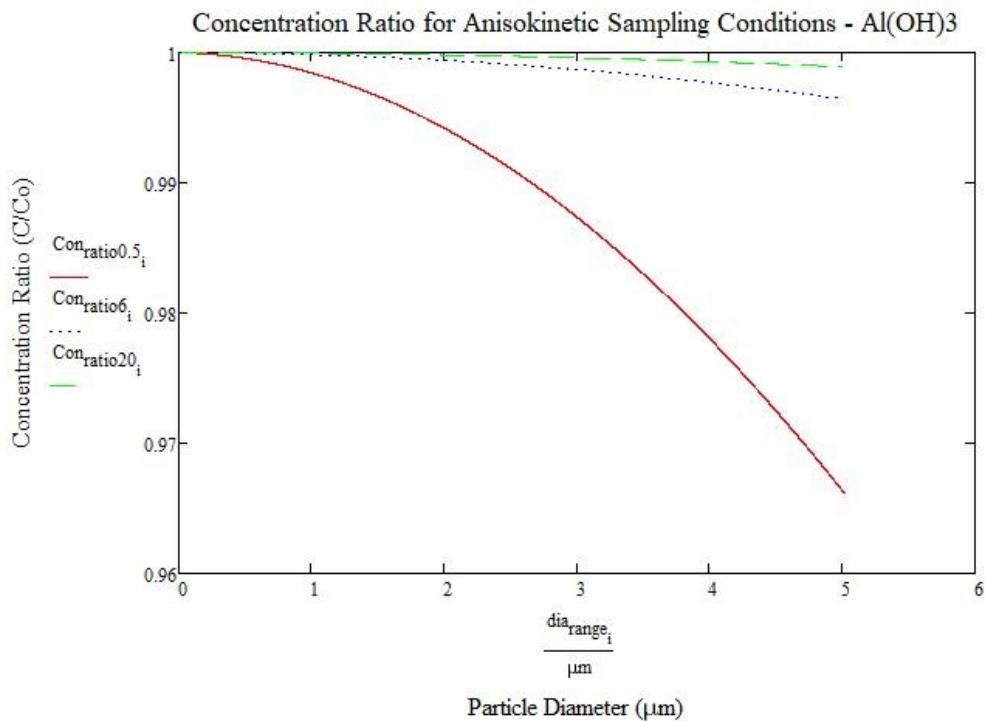


Figure 3.10 Concentration Ratios for  $\text{Al}(\text{OH})_3$

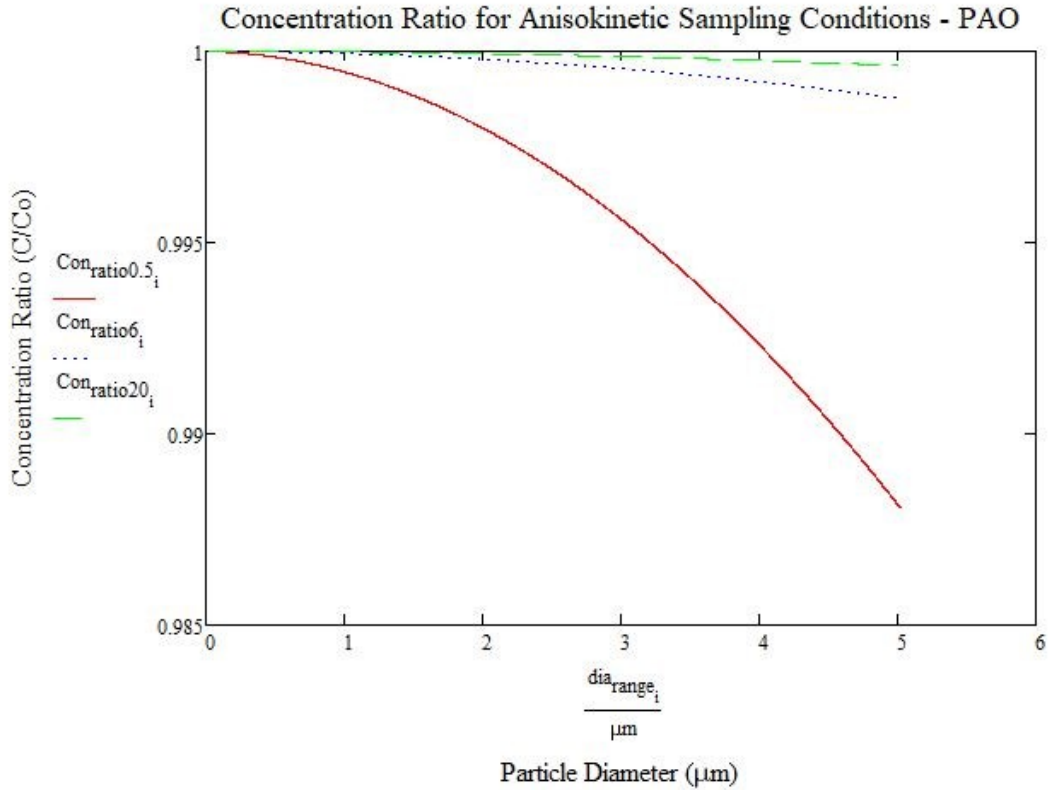


Figure 3.11 Concentration Ratios for PAO

For  $\text{Al}(\text{OH})_3$ , the least efficient particle was  $5.025 \mu\text{m}$  at  $0.5\text{cfm}$  with a concentration ratio of  $96.6\%$ . This was expected since the  $\text{Stk}$  should increase as the mass of the particle increases. For PAO, the least efficient particle was the same size and flow rate but with a better concentration ratio of  $98.8\%$ . The selected  $0.27\text{-inch}$  diameter probe accounts for only  $6.8\%$  of the flow area.

*Injection Assembly.* In order to promote a well mix of aerosols in the air stream, an injection manifold was designed and built in-house. The design was guided by the AG-1 standard for injection manifolds. The exit holes' total area is suggested to be  $1.25$  times the cross section of the manifold. A  $1\text{-inch}$  diameter manifold was selected resulting in  $36, 3/16\text{-inch}$

diameter exit holes. These perforations were placed in staggered rows, 45 degrees apart starting from above and below the main axis of the manifold. The spacing of the exit holes as well as the manifold was determined to be sufficient in turbulating the air and distribution of the aerosols using Analysis System (ANSYS) simulations. The machined injection manifold can be seen in Figure 3.12.



Figure 3.12 Injection Manifold Assembly.

This manifold is compatible for both liquid and solid aerosols, and requires compressed air to push the aerosols through the exit holes.

### 3.3 Test Stand Components

With the piping, heater, blower, sampling, and injection requirements calculated and designed, the rest of the SSTS components could be selected.

*Pre-and-Post-Filters.* To ensure the air entering the SSTS is free of any particles, ambient lab air enters the test stand through a pre-filter. Since the lab air is relatively clean, a 2 inch by 12 inch by 12 inch, high temperature, Minimum Efficiency Reporting Value (MERV) 13 filter is used to remove any particles that may be in the ambient air. For reference, a HEPA filter is considered to be MERV 17 or higher. A MERV 13 filter was also selected to limit the amount of dP that the blower would have to overcome to pull the desired flow. The same filter is also placed downstream in order to protect the mass flow meter and blower from any aerosols that pass through the test filter. These filters are rated for air flow temperatures up to 500°F. The type of filter used is shown in Figure 3.13, and the pre-and-post-filter housings are shown in Figures 3.14 and 3.15.



Figure 3.13 Pre-and-Post-Filter

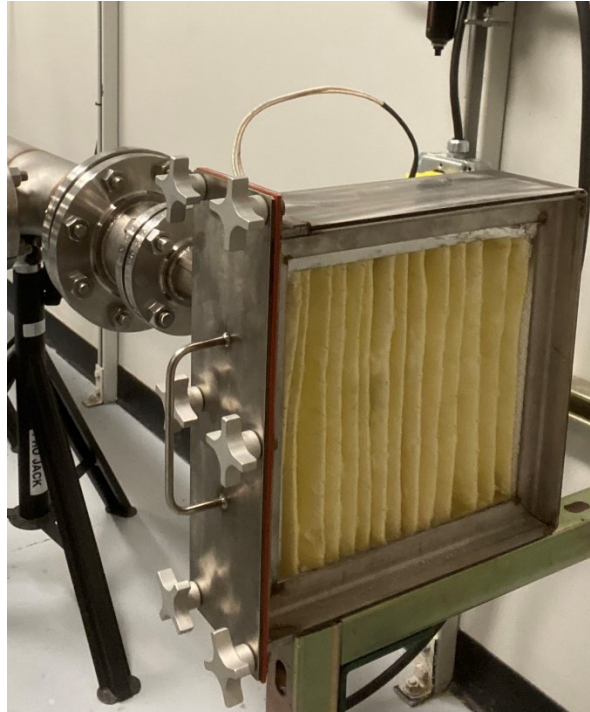


Figure 3.14 Pre-Filter Housing

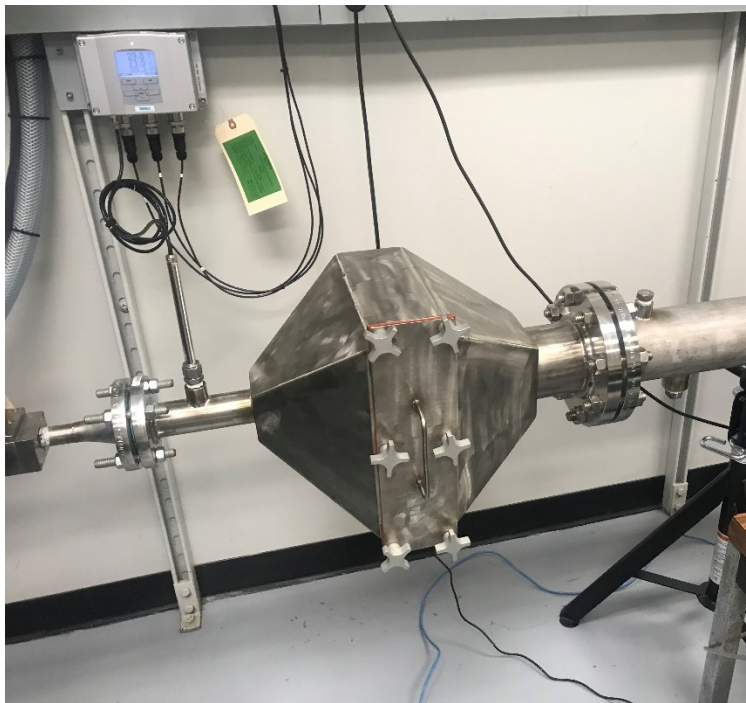


Figure 3.15 Post-Filter Housing



*Filter Coupon Holder.* A custom made test filter holder was machined in order to secure and seal the test filter inside of the SSTS. Two flanges were fitted to sandwich the test filter, gaskets, and filter backing. This assembly is shown in Figure 3.16.

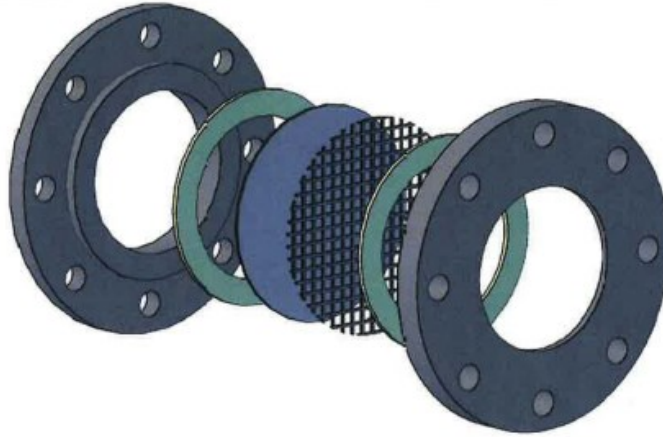


Figure 3.16 Coupon Holder Assembly.

*Controls and Data Recording.* The SSTS is controlled by a National Instrument (NI) LabVIEW program. This program is displayed on a lab computer, but the communications happen within a NI CompactDAQ. This CompactDAQ can be seen in Figure 3.17.





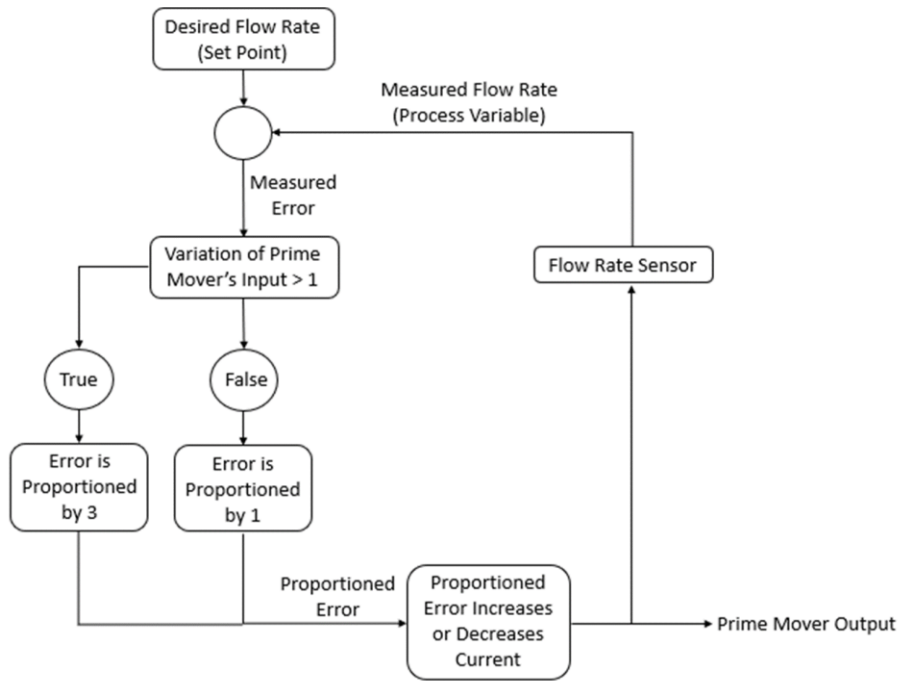


Figure 3.18 Control Loop for the VFD.

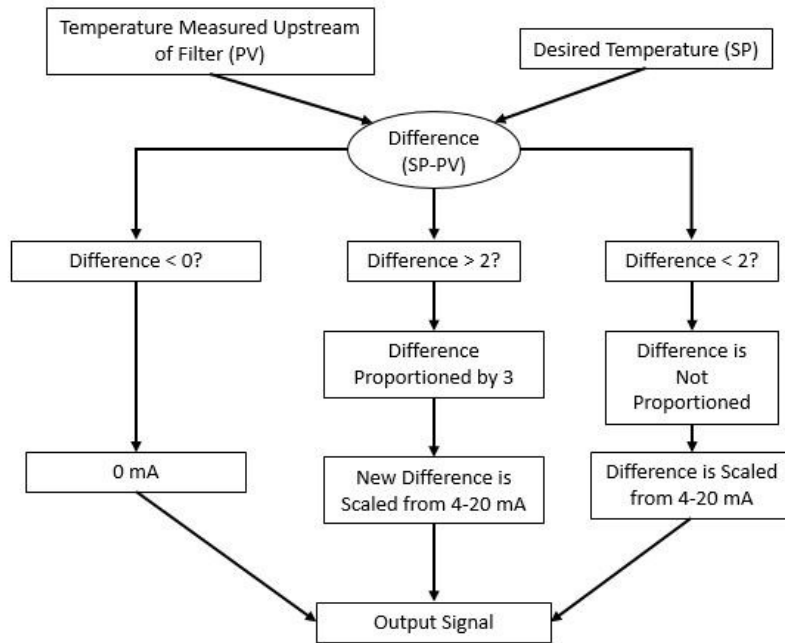


Figure 3.19 Control Loop for the Heater Relay.

The mass flow rate program takes the measured downstream standard flow rate and converts it to the actual cfm at the filter face using the air properties at the filter face. These calculations are shown in Figure 3.20.

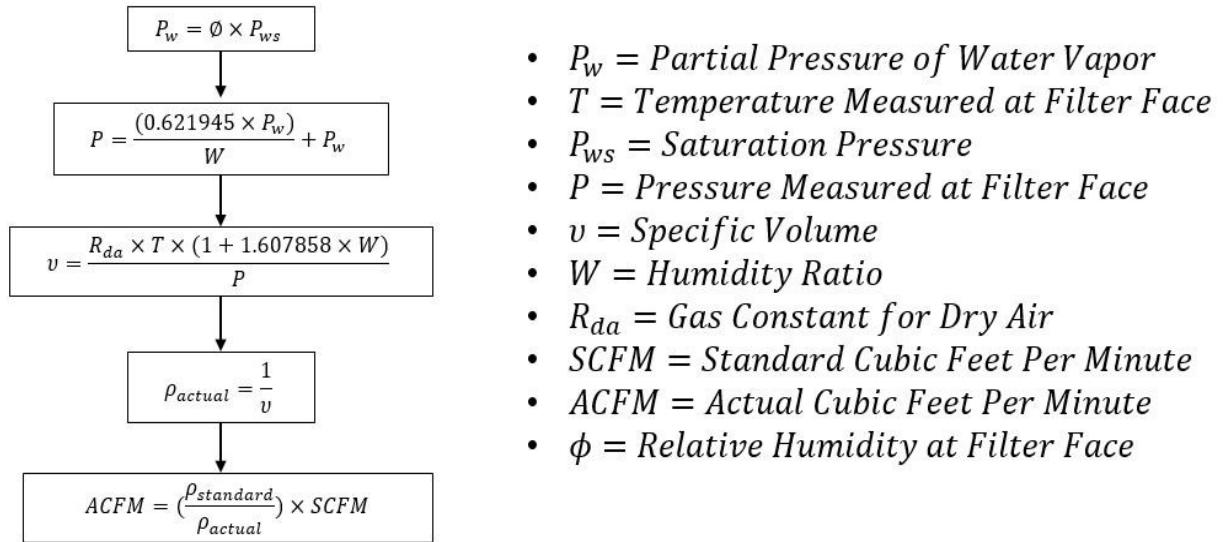


Figure 3.20 CFM to ACFM

The control panel for the test stand is shown in Figure 3.21. This panel is useful to view the real-time data to observe the data output of the SSTS. Having this ability provides the ability to monitor for any testing errors that may arise.

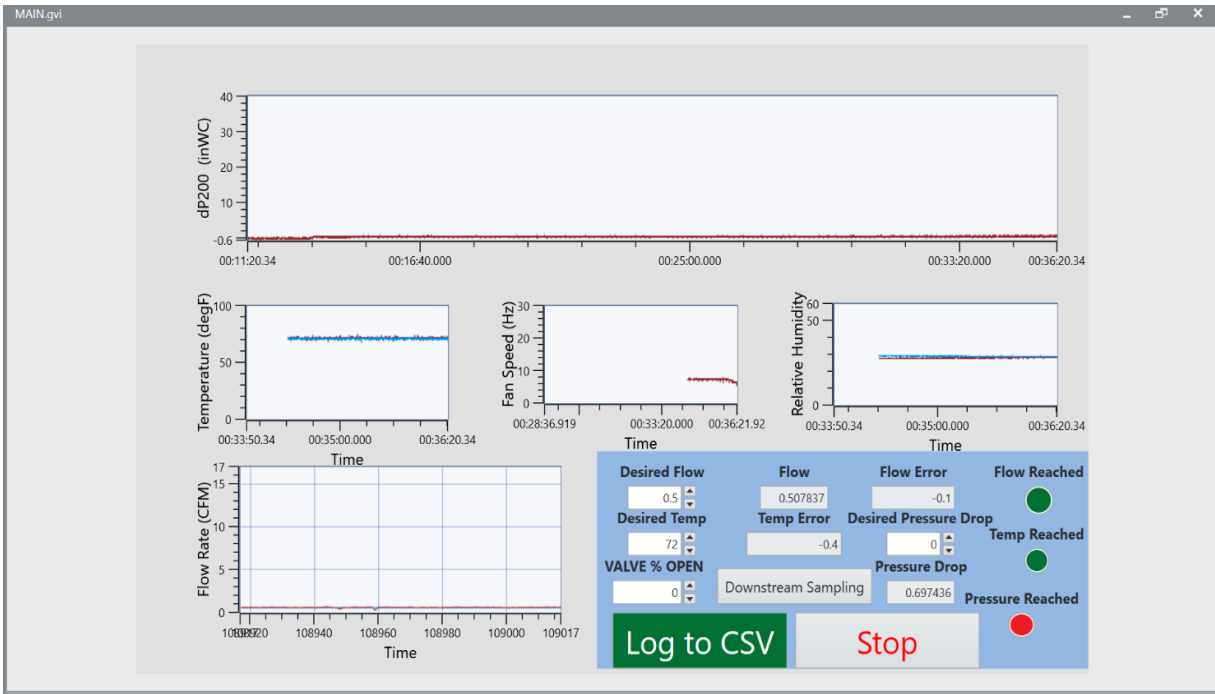


Figure 3.21 LabVIEW Control Panel.

All the data is recorded once the testing conditions have been met. The data is stored and presented in an Excel sheet at the conclusion of the test.

*Sample Train and Operation.* Since the SSTS only has one set of sampling instrumentation, the sampling has to be manually switched between upstream and downstream sampling. This is done by the use of a sampling train pictured in Figure 3.22.



Figure 3.22 Sampling Train

The sampling train is made up of two, three-way valves. These valves give the ability to direct the sample flow to the SMPS and LAS from either upstream, downstream, or the purge line. The purge line is used in order to move between upstream or downstream sampling since the instruments must first be purged of any remaining particles still inside the instrument. The purge pulls lab air through a HEPA capsule. When sampling downstream, the control program has a setting to account for the change of sampling location. This is because the sample probes pull a flow rate of 5 L/min (0.177cfm). When sampling upstream, an additional 5 L/min is pulled along with the set flow rate. When sampling downstream, the additional flow rate from the sample probe is accounted for by decreasing the set flow rate by 5 L/min. This system ensures

that whether sampling is happening upstream or downstream, the flow rate at the filter face remains constant. An illustration of the two scenarios is shown in Figure 3. 23.

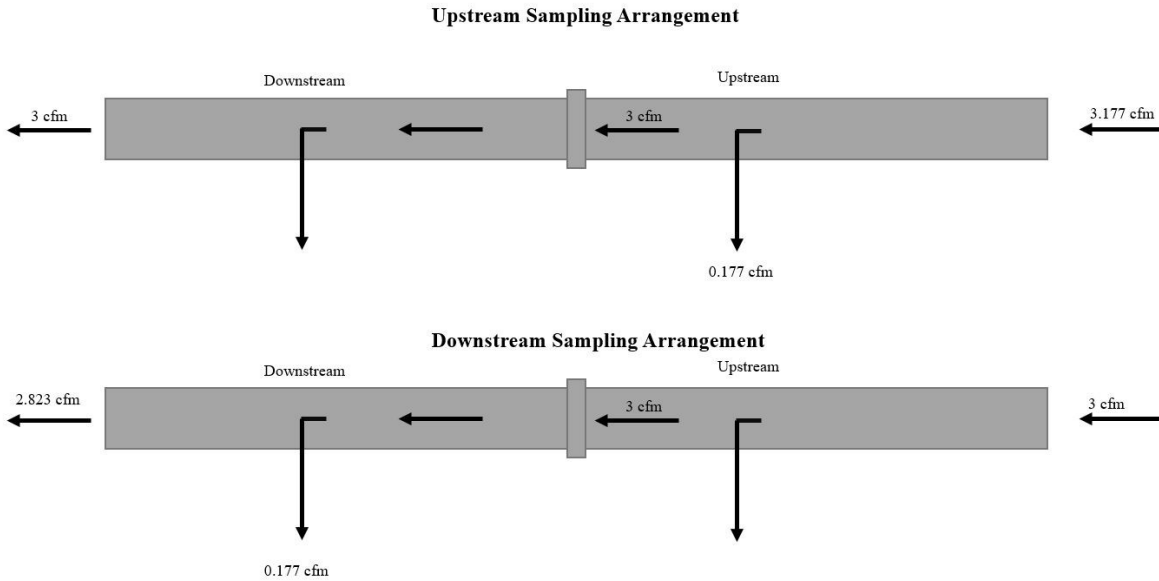


Figure 3.23 Upstream and Downstream Flow Conservation

Sampling upstream slightly affects the upstream concentration as it pulls in more air from the lab compared to the downstream setting, but the flow rate and pressure drop at the filter face was deemed more important to hold steady. The 5 L/min sample line is pulled by both instruments and a vacuum pump that is regulated by a mass flow controller. The SMPS pulls a flow rate of 0.3 L/min, and the LAS pulls a flow rate of 0.05 L/min. The mass flow controller is set to limit the vacuum pump to pull a flow rate of 4.65 L/min to bring the total flow rate to the required 5 L/min for the diluters. The vacuum pump and mass flow controller can be seen in Figure 3.24.

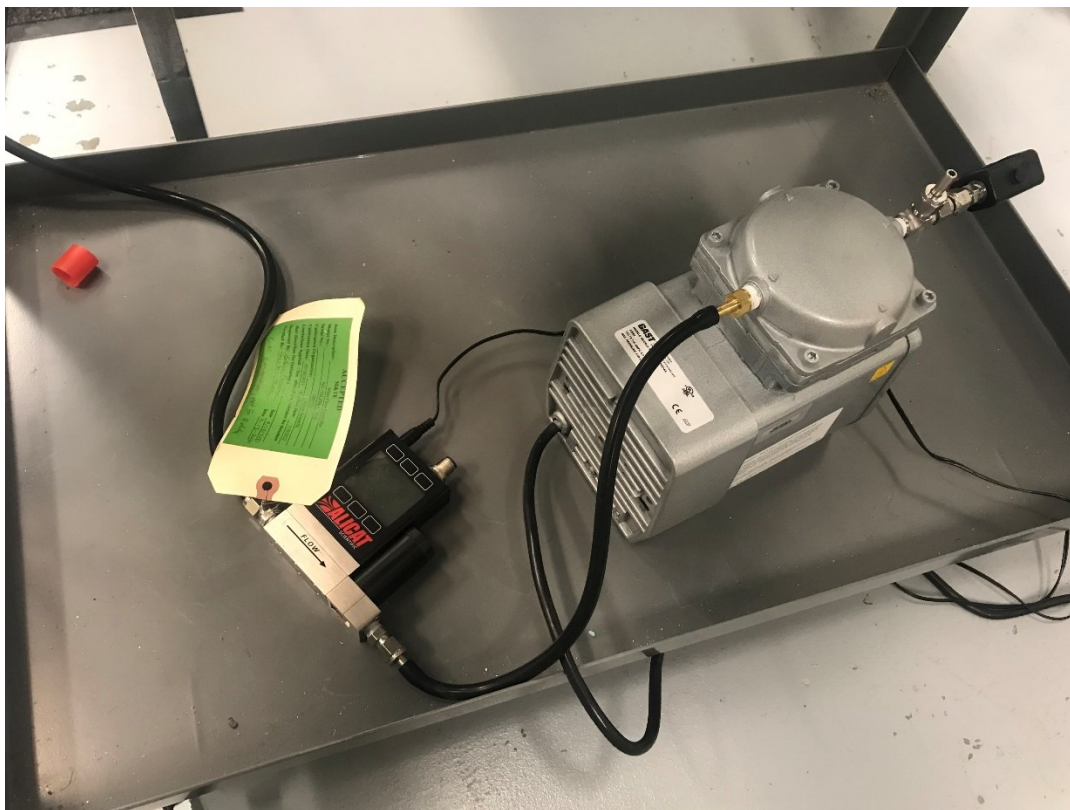


Figure 3.24 Sampling Vacuum Pump and Mass Flow Controller

The flow is split twice using a flow splitter. First, the flow is split between the instrumentation and vacuum pump. Then, the flow is split between the LAS and SMPS. The flow splitter can be seen in Figure 3.25, and a simple diagram of the sampling system can be seen in Figure 2.26.



Figure 3.25 Flow Splitter

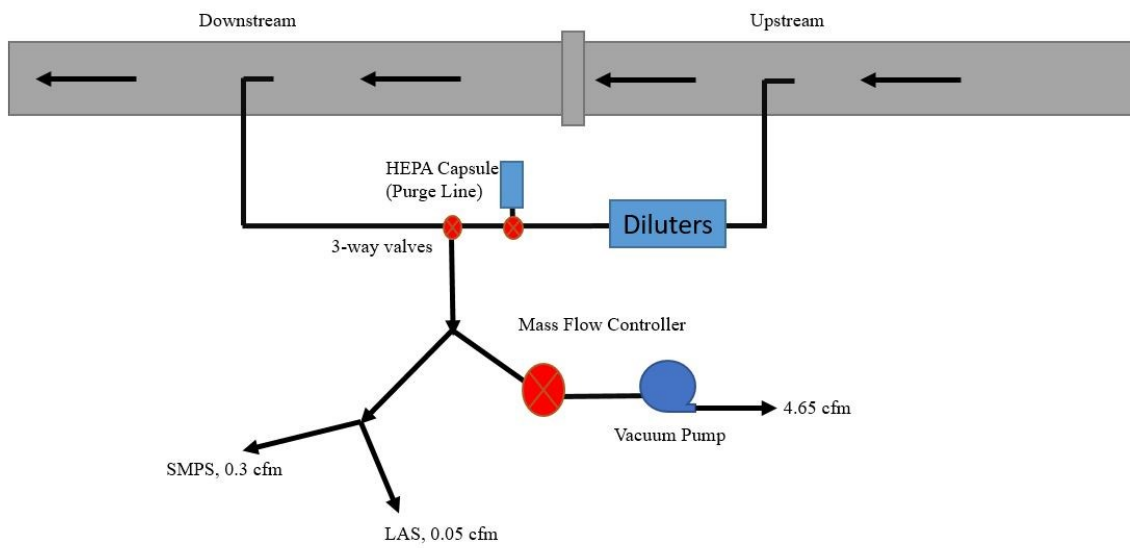


Figure 3.26 Schematic of the SSTS Sampling System

*Powder Feeder.* In order to generate solid particle aerosols, a powder feeder is commonly used. Traditionally at ICET, a twin screw powder feeder with a VFD driven motor is used in order to feed powder into the injection assembly. However, the twin screw assembly is used to feed at much higher rates than what was anticipated for the SSTS. Therefore, a single screw powder feeder was acquired. This powder feeder can be seen in Figure 3.27.



Figure 3.27 Powder Feeder for  $\text{Al}(\text{OH})_3$  and ARD.

The powder feeder turns the screw at the feed rate set on the control panel and moves powder to the outlet where the powder is pulled into a vacuum nozzle that is driven by



compressed air. The compressed air is measured using a pressure gauge attached to the vacuum nozzle. The pressure gauge and vacuum nozzle can be seen attached to the injection manifold in Figure 3.12. The compressed air breaks up the powder chunks into a cloud of particles. The cloud is pushed through the injection manifold and pulled through the test stand.

*Atomizer.* To generate liquid aerosols, an atomizer is used. An atomizer uses compressed air to generate the cloud of particles similar to the vacuum nozzle. However, instead of a vacuum nozzle, the compressed air is pushed through an orifice. The liquid is pulled up by the air and blown into an aerosol cloud. After, the cloud is pushed through the outlet and through the injection manifold. This process is represented in Figure 3.28 [13].

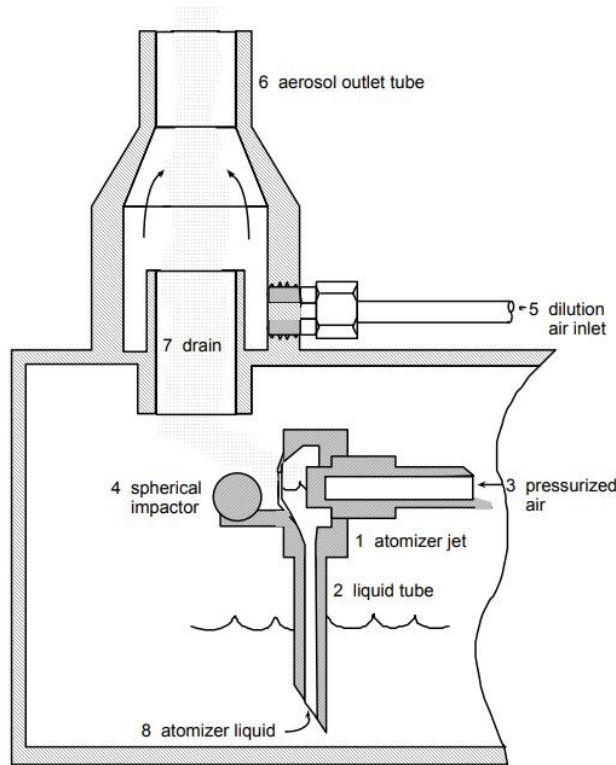


Figure 3.28 Atomizer schematic from TSI.

An atomizer that could provide the number of aerosols needed to inject into the SSTS was provided by ICET. This atomizer is shown in Figure 3.29.

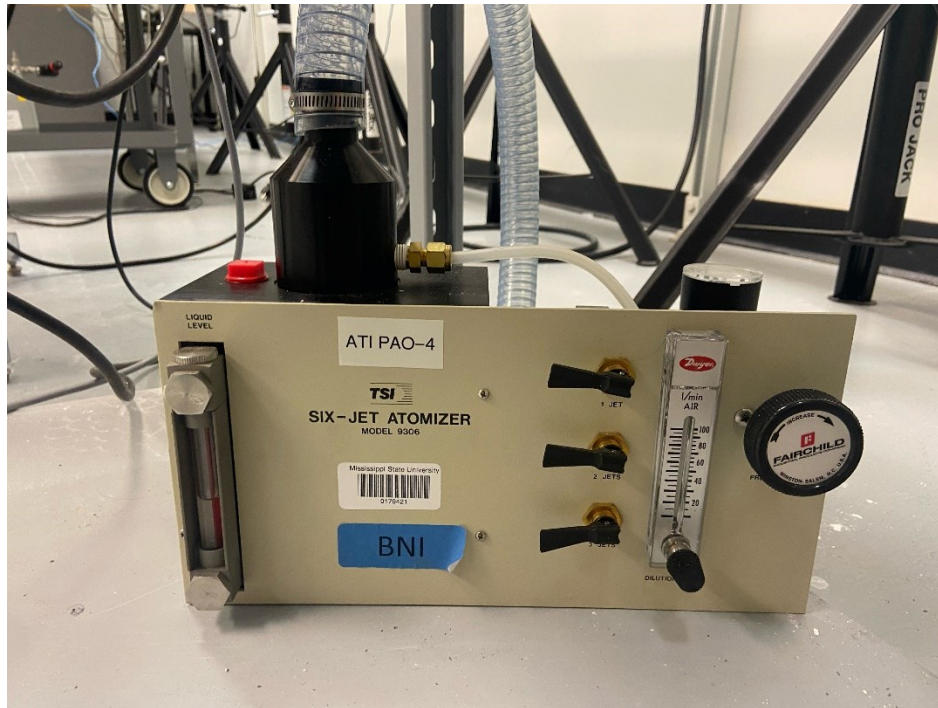


Figure 3.29 Atomizer for PAO.

*Upstream Instrumentation.* At the filter face, the air flow's temperature, humidity, and static pressure are all measured. These values are important in knowing the state of the air and mechanical properties of particles as they pass through the filter face. In knowing these values, the ACFM can be calculated and used in the previously mentioned flow correction loop. These instruments are shown in Figure 3.30.

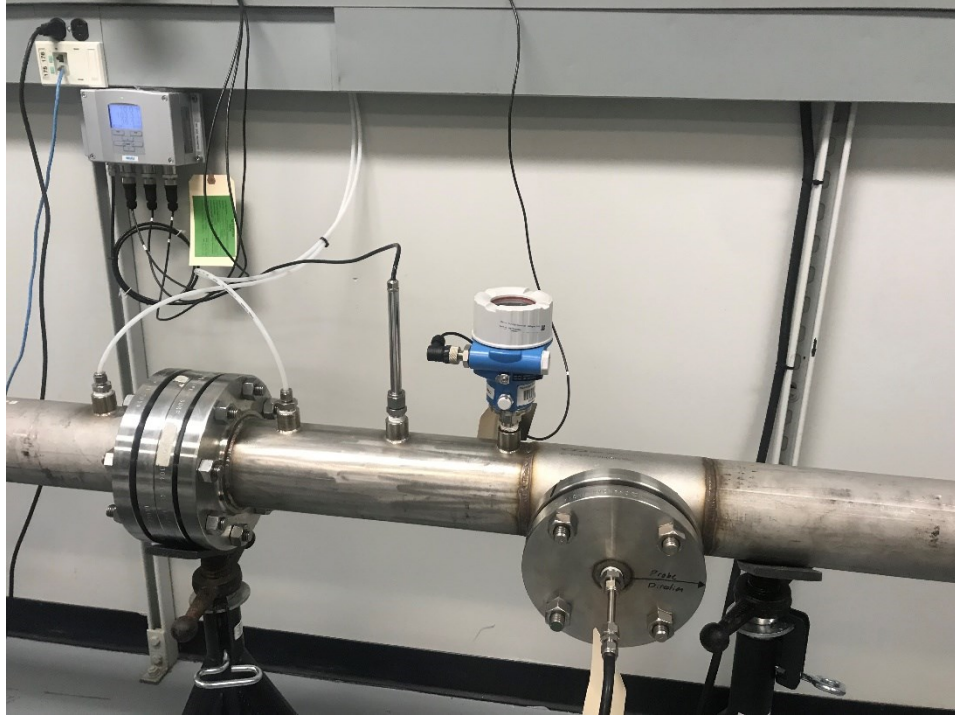


Figure 3.30 Upstream Temperature and RH Probe and Static Pressure Transducer.

*Differential Pressure Measurement.* The dP sensor is one of the most important measurements in the SSTS. This measurement must be highly accurate in order to evaluate the relationship between the mass loaded and dP. The selected dP sensor is capable of measuring 40 inWC which is greater than the maximum testing value of 35 inWC. If the test filter experiences a dP greater than 38 inWC, the program automatically shuts the blower off in order to protect the dP sensor. This sensor is shown in Figure 3.31. The upstream and downstream pressure locations can be best seen in Figure 3.30 on either side of the test coupon.

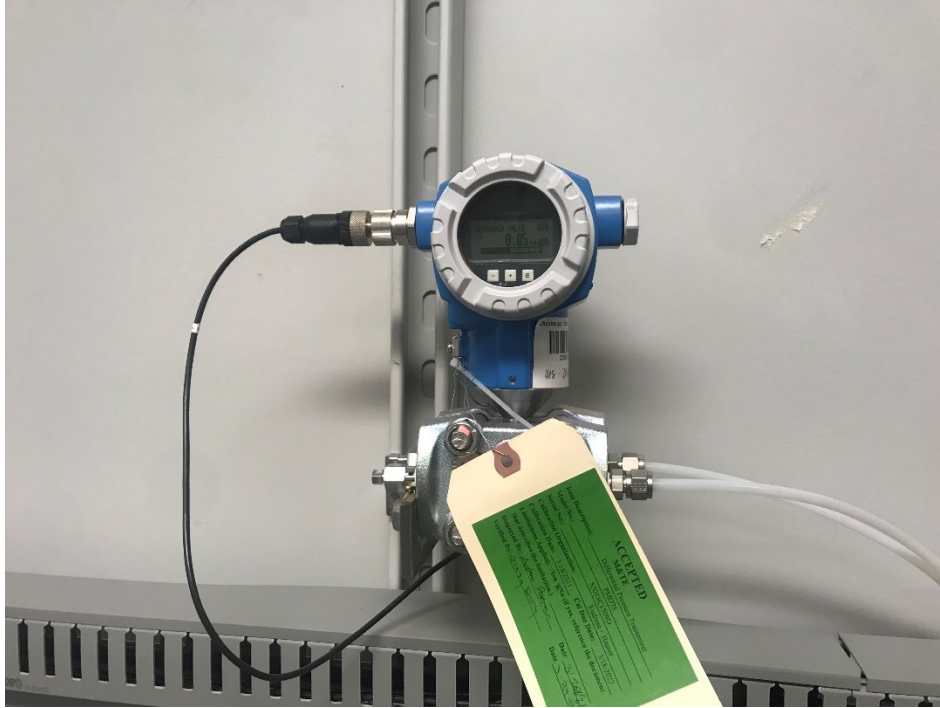


Figure 3.31 dP Sensor for Test Filter.

*Downstream Instrumentation.* After the post-filter, the remaining instrumentation is the mass flow meter and downstream temperature and humidity probe. The selected mass flow meter can measure a flow range of 0 to 17 cfm and can only be in air flow temperatures less than 212°F. To ensure the mass flow meter does not overheat, the downstream temperature probe monitors the temperature of the flow. If the downstream temperature reaches 200°F, the program automatically cuts off the heater as a precaution. The mass flow meter and downstream temperature probe are pictured in Figure 3.32.

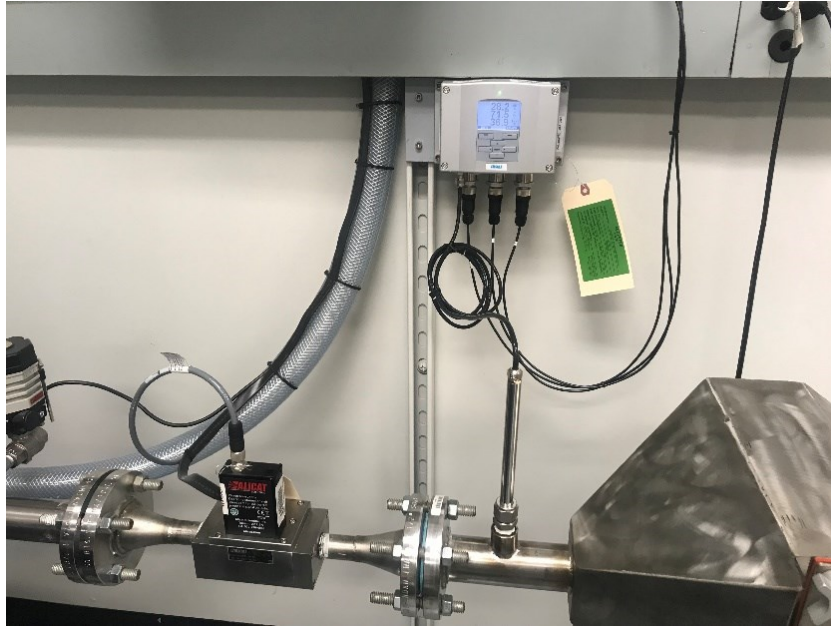


Figure 3.32 Downstream Temperature and Humidity Probe and Mass Flow Meter

*Make-up air valve.* A make-up air valve with an electronic actuator was installed after the mass flow meter and before the blower in order to provide additional air for low flow test. Make-up air is needed for whenever the set flow causes the frequency to fall below 10% of the maximum speed. In this case, the pump is a 60 Hz motor. The make-up air valve forces the blower to require more than 6 Hz in order to pull the selected flow. The make-up air valve and actuator can be found in Figure 3.30.





Figure 3.33 Make-up Air Valve and Actuator

Pictured below in Figure 3.31 is the completed and labeled SSTS.

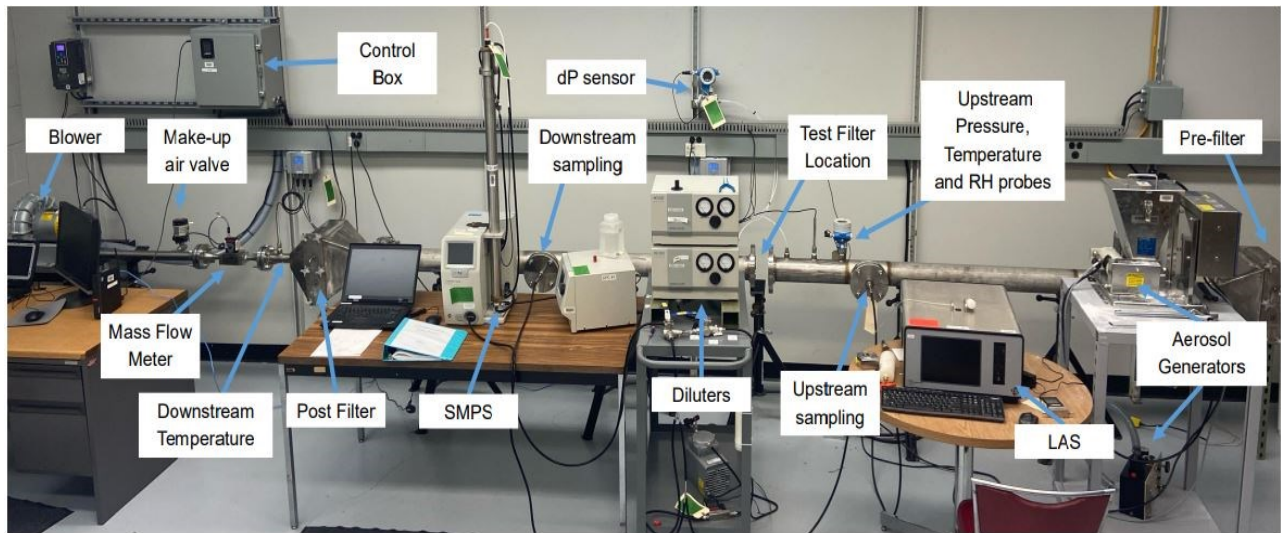


Figure 3.34 Completed SSTS Labeled

Table 3.3 provides a summary of the SSTS instrumentation which includes their respective makes, models, ranges, and uncertainties.

Table 3.3 SSTS Instrumentation

<b>Instrument</b>	<b>Manufacturer</b>	<b>Model</b>	<b>Range</b>	<b>Accuracy</b>
SMPS	TSI Inc.	EC – 3082 CPC – 3775	0.024nm – 1 $\mu$ m 0 – 10 <sup>7</sup> particles/ccm	$\pm$ 10% at <50,000 particles/cm <sup>3</sup> $\pm$ 20% at < 10,000,000 particles/cm <sup>3</sup>
LAS	TSI Inc.	3340	0.09nm – 7.5 $\mu$ m 0 – 3,600 particles/ccm	<5% efficient for a particle diameter of 0.1 $\mu$ m
Static Pressure Gauge	Endress+Hauser	PMC51	1.5 psi gauge	$\pm$ 0.075% of span
Temperature and Humidity Probe (2)	Vaisala	HTM335	-40 – 365°F, 0 – 100% RH	$\pm$ 0.18°F, $\pm$ 0.5 %RH (0-40 %RH) $\pm$ 0.8 %RH (40-95 %RH)
dP Gauge	Endress+Hauser	PMD75	0 – 40 inWC	$\pm$ 0.035% of span
Mass Flow Meter	Alicat	500SLPM	0 – 17.6 cfm (0 – 500 L/min)	$\pm$ 0.32% of reading or $\pm$ 0.02% of full scale (whichever is greater)
Mass Flow Controller	Alicat	5SLP	0 – 0.177 cfm (0 – 5 L/min)	$\pm$ 0.5% of reading or $\pm$ 0.1% of full scale (whichever is greater)

The general uncertainty of the flowrate being pulled through the sample line was calculated to be 6.3% ( $\pm$ 0.32 L/min) using both the Monte Carlo and Taylor Series methods for

uncertainty. This uncertainty in addition to the accuracy of the sampling instrumentation should be taken into account when evaluating the sampling data. The general uncertainty for the standard flowrate going through the duct can be taken from accuracy of the mass flow meter in Table 3.3. The actual uncertainty is assumed to be greater, however, as the standard mass flow rate is converted to the actual flowrate using the humidity, temperature, and pressure measured at the filter face.



## CHAPTER IV

### RESULTS AND DISCUSSION

The following results and verifications were performed in order to characterize the SSTS. This characterization was important to determine how well the SSTS met the design criteria, verify the design calculations, and evaluate the overall performance of the test stand. PAO was used for the diluter characterization and traverse measurements due to the consistent aerosol production from the atomizer relative to the powder feeder. PAO is also more spherical compared to the powders which increases the accuracy. Only the SMPS was used for the characterization of diluters, sampling efficiency, and flow development due to the unknown concentrations that could potentially damage the LAS.

#### **4.1 Air Flow Condition Capabilities**

For both the volumetric flow rate and temperature, the selected mass flow meter was the limiting factor of the test stand. The maximum flow rate that the mass flow meter can handle is 500 L/min (17.657 cfm). Despite not reaching the desired 20 cfm, this mass flow meter was selected due to cost, familiarity with the company, and accuracy. The measured air flow rates for 0.5 cfm and 17 cfm can be seen in Figures 4.1 and 4.2.

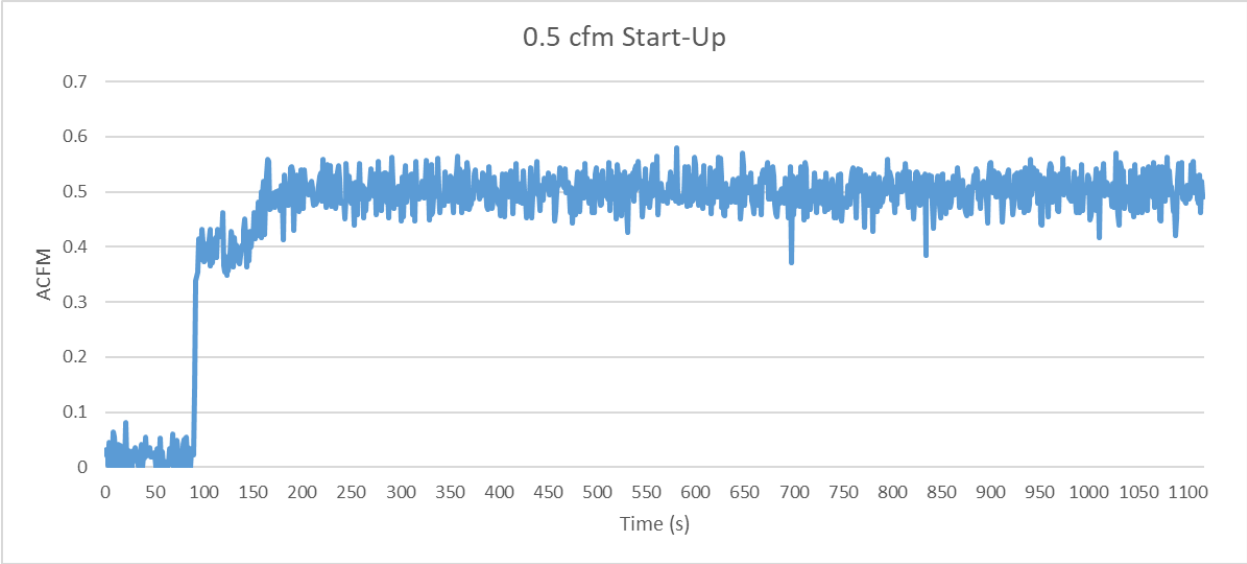


Figure 4.1 0.5 cfm Flow Measurement

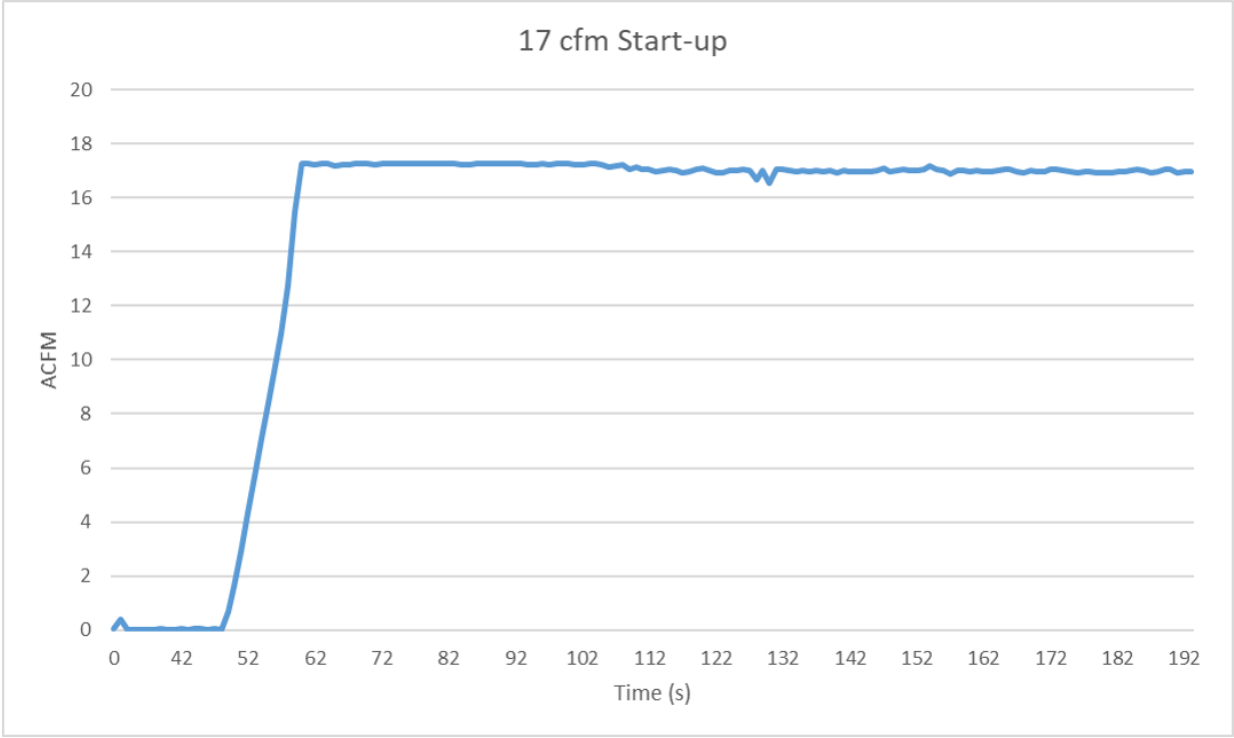


Figure 4.2 17 cfm Flow Measurement

It can be easily observed that the low flow is much more challenging to maintain compared to high flow setting. This is due to the correction time intervals not being fast enough in order to hold the flow rate steady. There is certainly room for improvement, but this proved to not be a large issue when running tests.

This mass flow meter is the company's high temperature option, but even this model can only withstand air temperatures of 212°F. However, the 250°F air temperature is the desired temperature at the test filter face. In preliminary testing, most of the heat in the air dissipates as it moves through the downstream portion of test stand by the time it reaches the mass flow meter. If the tests were long enough, the downstream portion of the test stand would eventually heat up and allow the air flow temperature to reach the maximum for the flow meter. In order to assure this does not happen, the program is designed to cut the heater coil off if the downstream temperature probe reaches a temperature greater than 200°F. Another safety feature included in the program is that the heater coil will not turn on unless the blower is running. This ensures that the heater is able to be cooled and not burn up. The temperature measurement at the filter face, as well as the downstream temperature for 17 cfm, is shown in Figure 4.3.

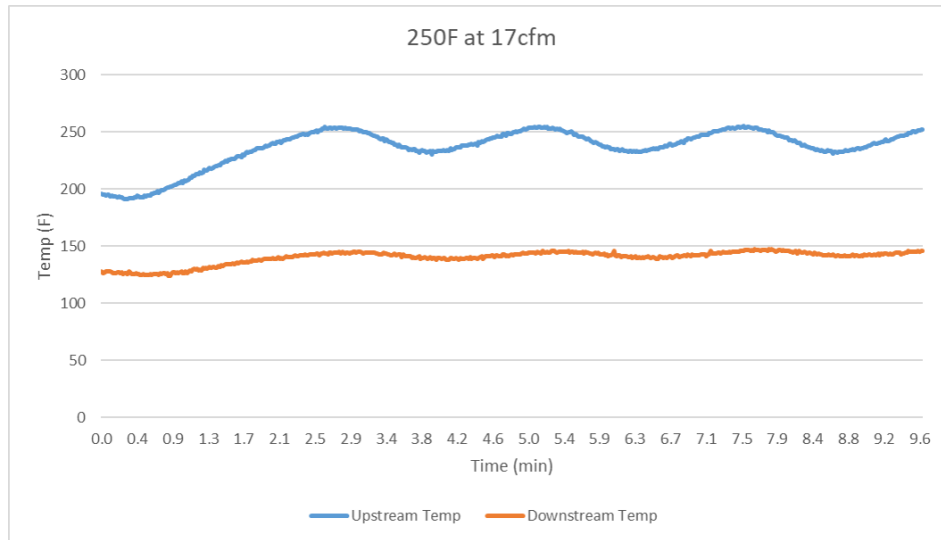


Figure 4.3 17 cfm Temperature Measurement

The control loop is unable to hold a near steady state condition. This is due to the temperature being recorded in one location, and the heat being controlled in another leading to a large response time. Figure 4.4 provides a comparison of a filter that experienced 250°F, 17 cfm air flow conditions, and an unused filter coupon.



Figure 4.4 New vs Baked Filter Coupon

The heater coil was unable to perform properly at the low flow conditions due to not enough air passing through the coil to cool it down.

#### 4.2 Diluter Characterization

One of the most important components of the sampling system is the diluter setup. Specifically, knowing the actual dilution factor is key to accurately determining the upstream aerosol concentration. This can be used to know the filter efficiency, and the mass deposited onto the test filter. Once again, the expected upstream concentration between  $10^5$  to  $10^6$  particles/ccm must be diluted due to the LAS only being able to sample a maximum concentration of 3600 particles/ccm. Therefore, two diluters in series are required. A 20:1 and 100:1 diluter arrangement is used to provide a nominal dilution factor of 2000:1. However, the actual dilution factor must be known in order to know what the actual concentration is upstream. In order to do this, the SMPS is used to sample upstream with both diluters, only the 20:1 diluter, and then only

the 100:1 diluter. Using the average concentration from each of these sample groups, the resulting difference in factors can be found. Six samples with the SMPS were taken using both diluters at a selected velocity of 30 ft/min for a baseline test. The average concentration was 1650 particles/ccm. Figure 4.5 shows the average particle distribution.

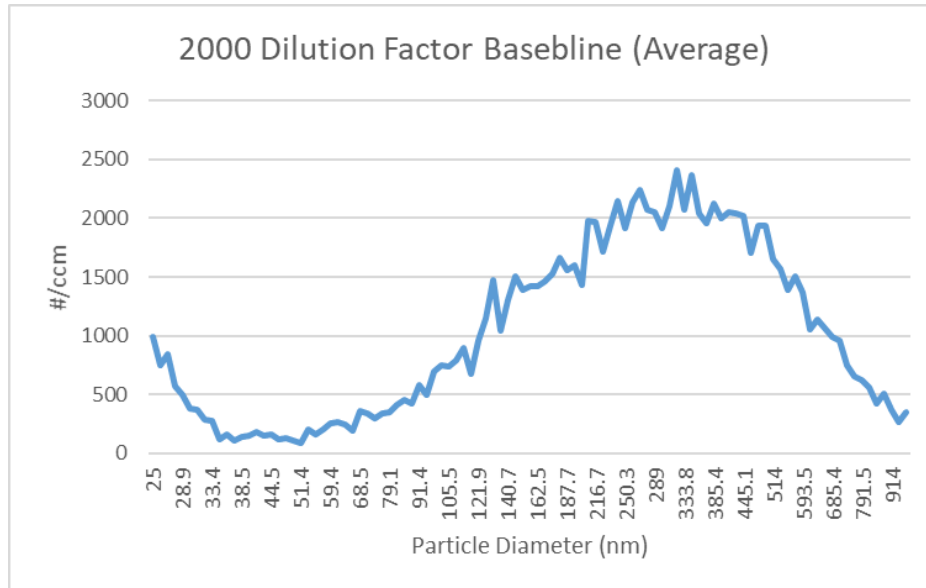


Figure 4.5 Diluter Characterization Baseline Test

Next, the 20:1 diluter was removed and only the 100:1 diluter was used to sample the upstream concentration. This yielded an average concentration of 1.64E+04 particles/ccm over 4 samples. The distribution curve is shown in Figure 4.6.

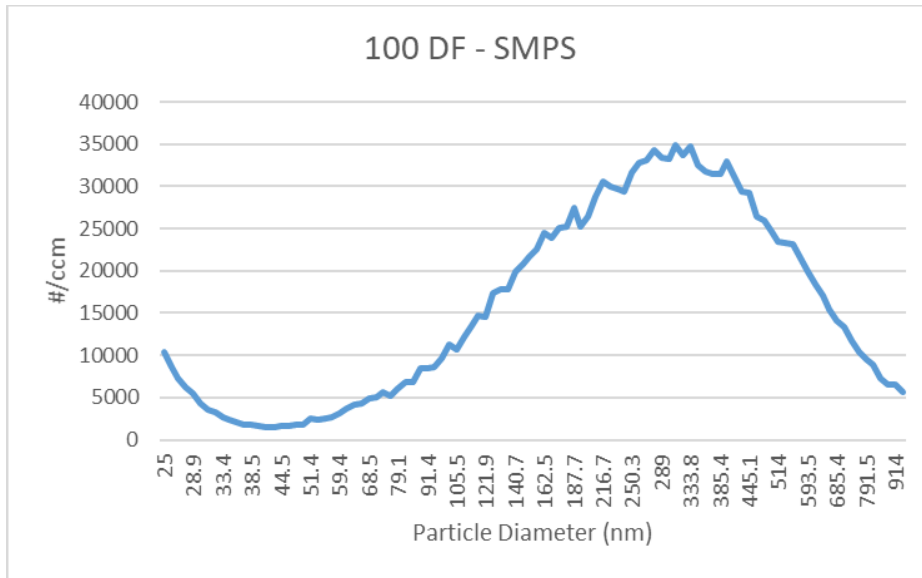


Figure 4.6 100:1 Dilution Particle Distribution

By dividing the average concentration of the 100:1 samples by the 2000:1 samples, the dilution factor for the 20:1 diluter could be found. This actual dilution factor was determined to be 15.26. Finally, the same process was performed instead with the 20:1 as the only diluter in the system. This yielded an average concentration of  $1.55E+05$  particles/ccm over 4 samples. The particle distribution curve is shown in Figure 4.7. It is interesting to note the increasing resolution that happens as the concentration is diluted less and less. This is likely due to the particle losses associated with the additional transportation and wall deposition.

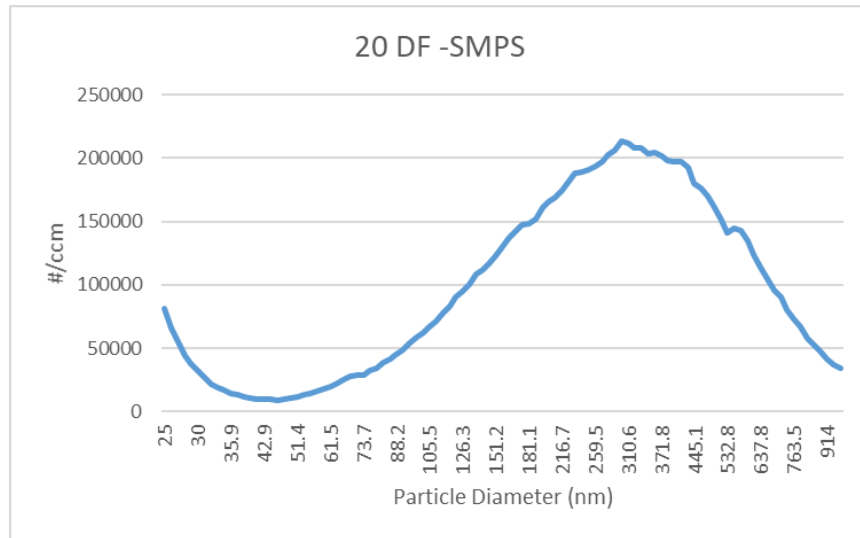


Figure 4.7 20:1 Dilution Particle Distribution

By once again dividing the average 20:1 concentration by the 2000:1 samples, the actual dilution factor for the 100:1 diluter was found to be 93.93. Multiplying the two actual dilution factors for the diluters resulted in an actual dilution factor of 1433.5 compared to the nominal value of 2000. Now with this actual dilution factor, the average concentration and particle distribution curve of the original 2000:1 samples can be scaled to represent the actual upstream concentration inside of the test stand. The actual concentration of the 2000:1 sample set could now be determined to be 2.38E+06, and the scaled particle distribution curve can be seen in Figure 4.8.



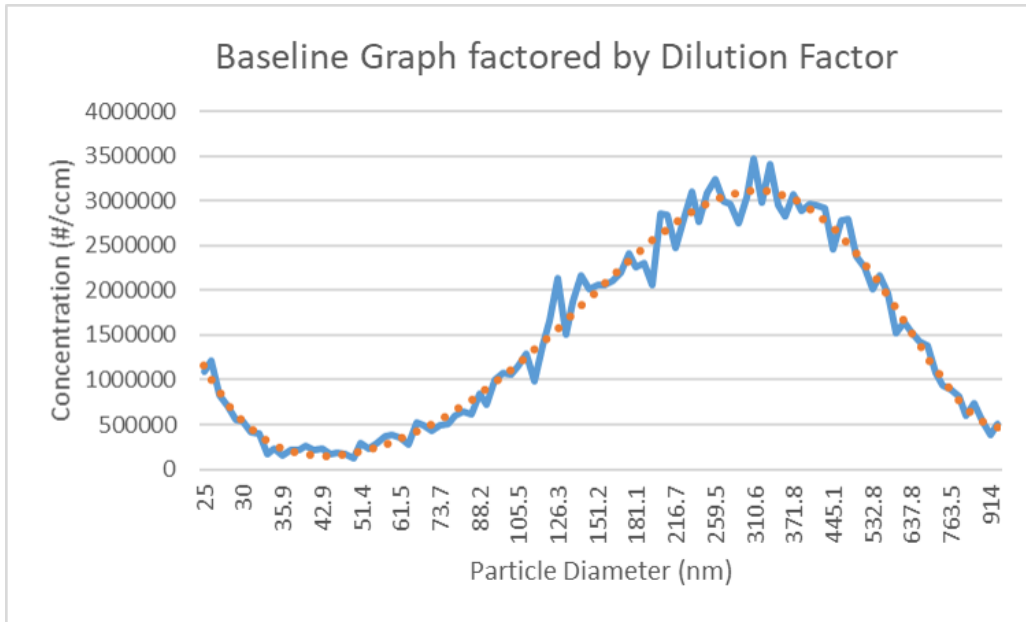


Figure 4.8 Scaled 2000:1 Particle Distribution

To further provide a visual of the scaling factors of the different diluters, Figure 4.9 is provided. This plot shows all three particle distribution curves on a logarithmic scale regarding the concentration.

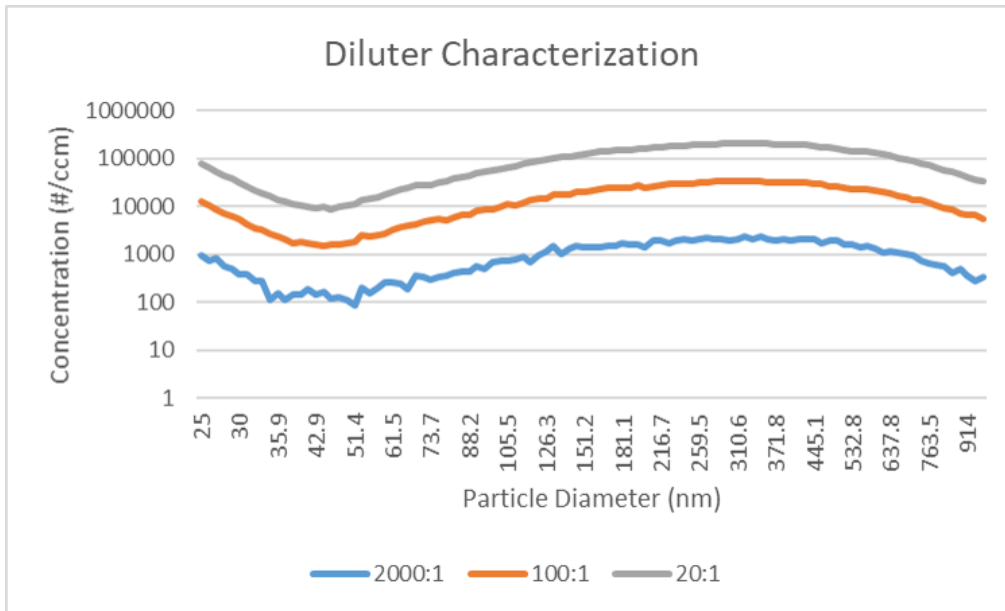


Figure 4.9 Diluter Characterization Distributions

### 4.3 Sampling Efficiency Verification

In order to verify that the Stk and sampling efficiency calculations performed are correct, a comparison of using two different probe sizes was performed. This would verify the assumption that the anisokinetic conditions would have minimal effect on the sampling if the two different probe sizes produced the same average concentration. The two selected probe sizes were a 0.27-inch ID and 0.67-inch ID. These two probes are pictured in Figures 4.10 and 4.11, respectively.



Figure 4.10 0.27-inch ID Sampling Probe

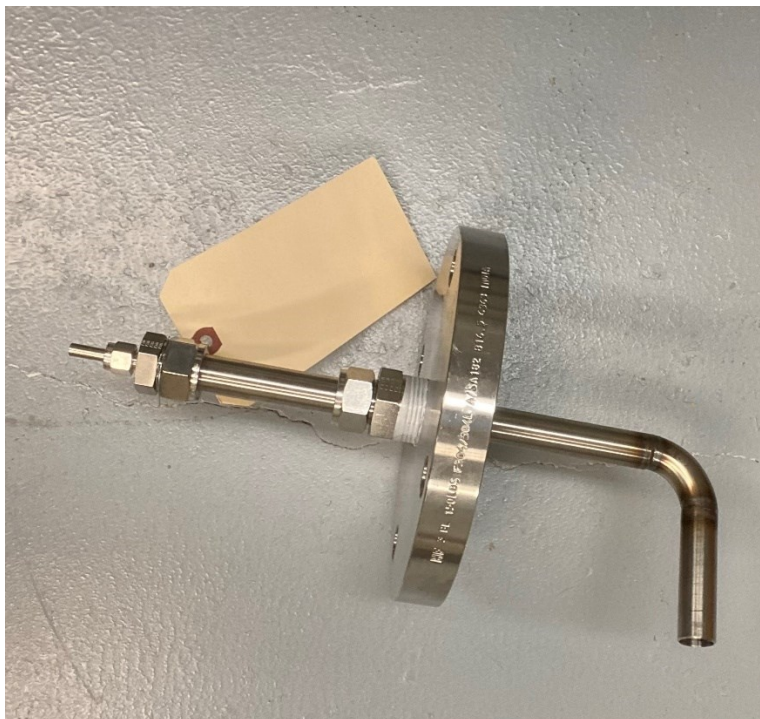


Figure 4.11 0.67-inch ID Sampling Probe

Both sample probes pulled the same 5 L/min flow rate. This equated to the 0.27-inch probe pulling an air velocity of 444 ft/min, while the 0.67-inch pulled an air velocity of 72.73 ft/min. With these drastically different air speeds, if the concentrations are similar, it could be verified that the anisokinetic conditions have a minimal effect on the sampling efficiency. A duct flow rate of 0.5 cfm was selected to perform this test since the calculations resulted in this flow rate being the least efficient. The isokinetic flow rate for the 0.67-inch probe is 7.165 cfm, but this flowrate is within the non-laminar zone and would not yield accurate results. Five samples of both probes were taken under the same conditions. The average particle distribution curves for each probe can be seen in Figure 4.12.

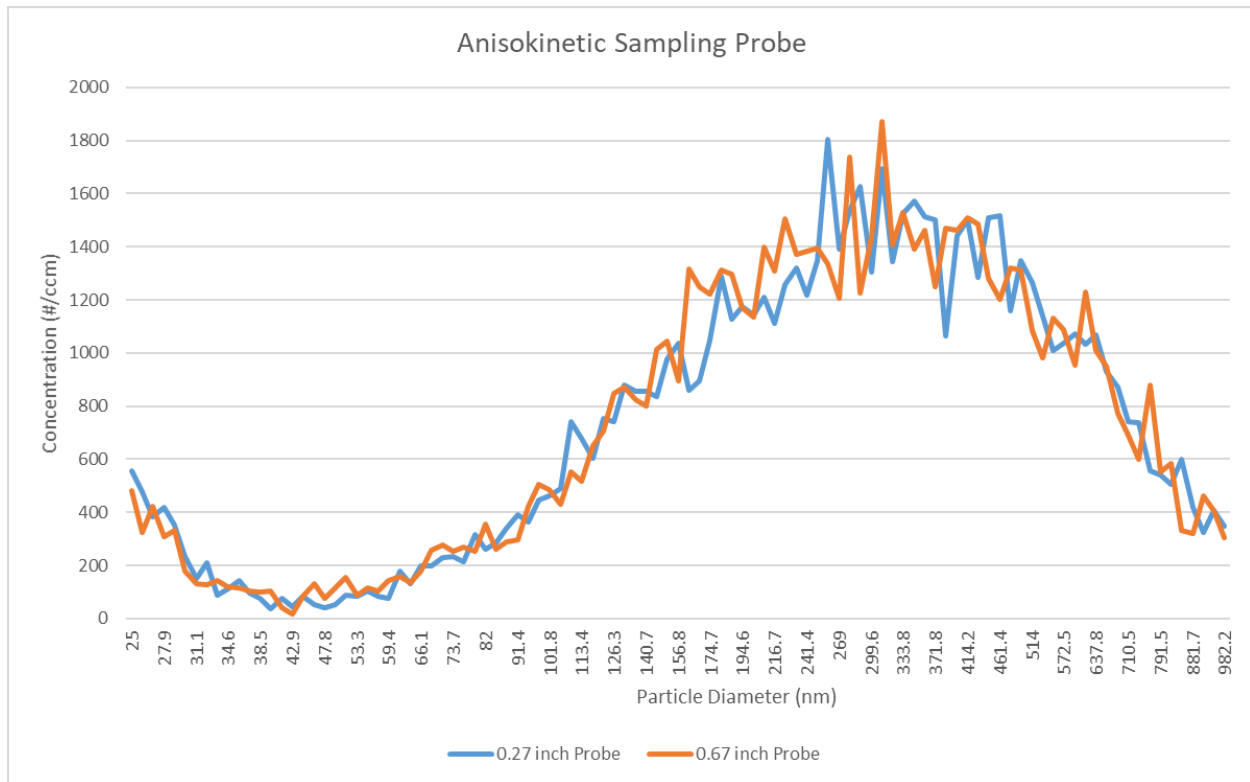


Figure 4.12 Anisokinetic Sampling Condition Test

It can be observed that the two different probe sizes provided very similar particle distribution curves. The average concentration of the 0.27-inch probe sample set was 1170 particles/ccm compared to the average concentration of the 0.67-inch probe sample set was 1190 particles/ccm. These average concentrations are quite similar, and the slight increase in concentration for the 0.67-inch probe can be potentially be accounted by considering either noise in the data, or the difference in transportation losses due to different velocities. Overall, this concludes that the previous design calculations of the Stk and sampling efficiency were correct.

#### 4.4 Well Mixing of Aerosols Verification

In order to determine that the 10 duct diameters were enough pipe length to allow the air flow to develop, travers sampling measurements were taken across the diameter of the duct. Two

measurements were taken every 0.5-inch of the 4-inch duct for the slowest available flow rate of 0.5 cfm. Due to the shorter nature of the 6 cfm test, only one measurement at each 0.5-inch spot was taken. A visual of the location of the traverse measurement is shown in Figure 4.13.

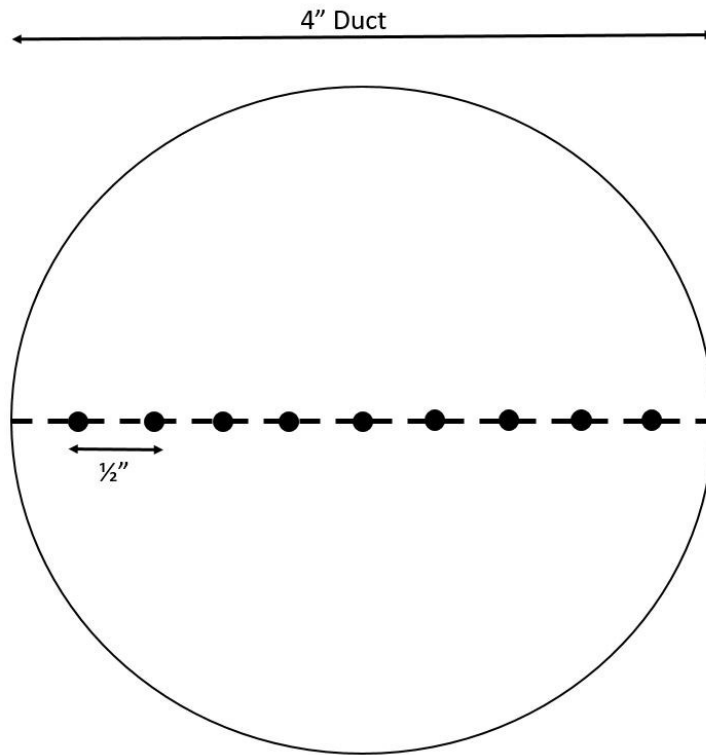


Figure 4.13 Diagram of Traverse Measurement in the Duct

A custom probe had to be manufactured that was long enough to reach each side of the duct to allow for position adjustment. This custom probe is shown in Figure 4.14. This probe has the ability to slide during the test which helps to ensure that the conditions were consistent across each sample.

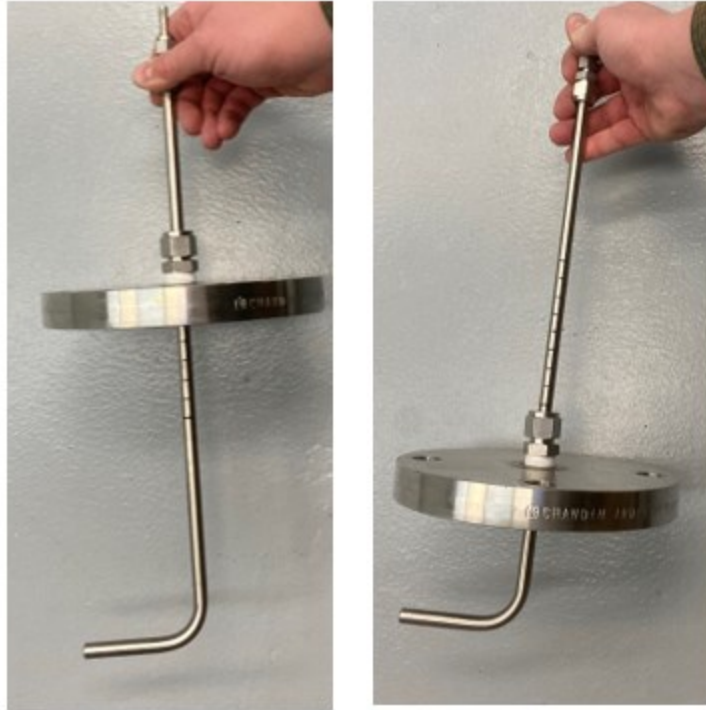


Figure 4.14 Traverse Sample Probe

The SMPS results of the traverse samples for 0.5 cfm and 6 cfm are shown in Figures 4.15 and 4.16, respectively.

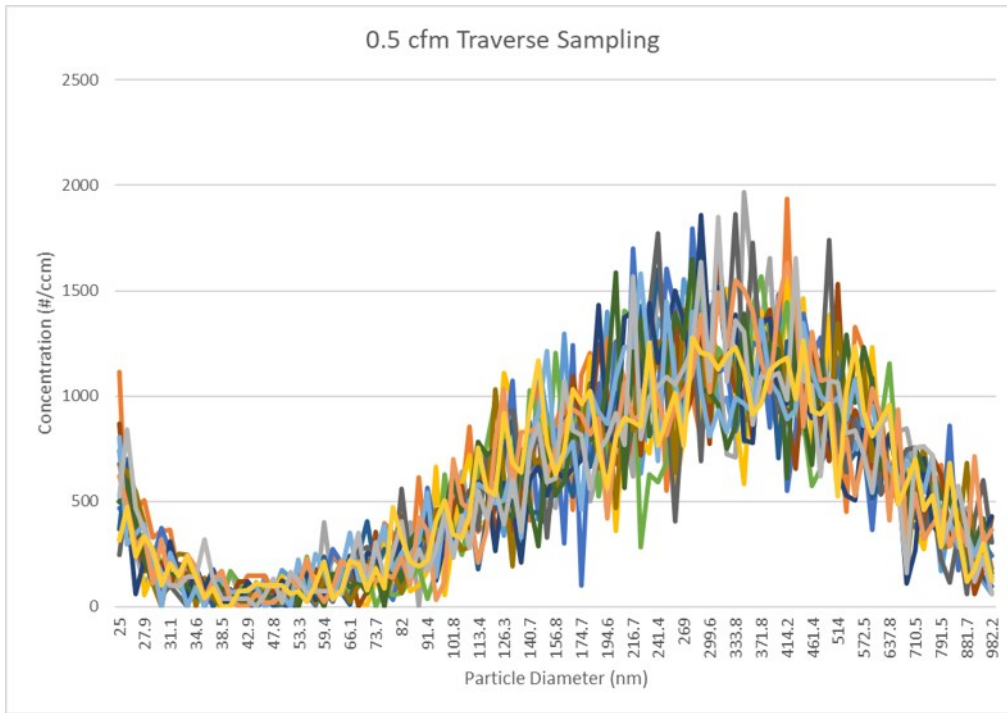


Figure 4.15 0.5 cfm SMPS Traverse Sample Measurements

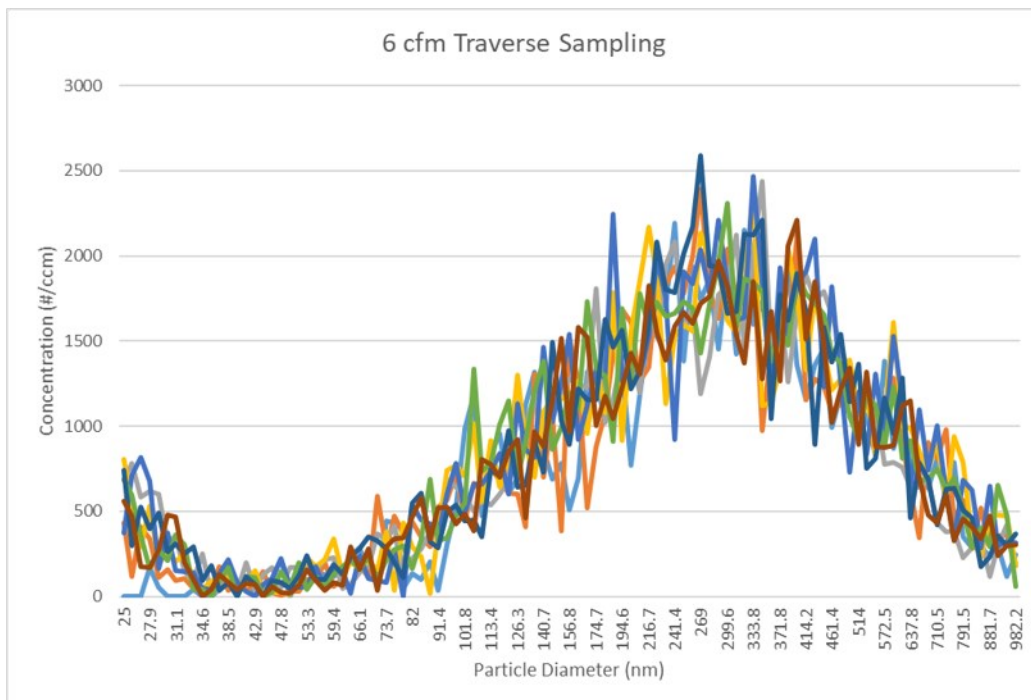


Figure 4.16 6 cfm SMPS Traverse Sample Measurements



As expected, the slower flow rate of 0.5 provided a lesser developed flow compared to the faster 6 cfm flow rate. However, both traverse measurements were deemed to be mixed enough to be able to obtain the average concentration of the injected aerosols during the test period.

#### **4.5 Filter Efficiency Results**

As previously mentioned, an important characteristic of any filter media is its particle capture efficiency. The procedure used to perform filter efficiency tests for the SSTS can be found in Appendix B. In short, five samples are taken downstream at the start of the test then five samples upstream after purging the instrumentation. For efficiency test, PAO is used as the challenge aerosol. Both the LAS and SMPS were used to compare the results to one another. The upstream samples were scaled by the previously derived dilution factor of 1433.5. The downstream samples were not diluted, as the concentration is low enough for both instruments after the particle have passed through the filtration media. The Most Penetrating Particle Size (MPPS) and the filter's efficiency and penetration fraction of this particle were calculated along with the filtering efficiency and penetration fraction of the 0.3  $\mu\text{m}$  particle. For the sake of characterization, four different air velocities were tested to determine what the controls needed to be to successfully perform the test. These air velocities include 5, 15, 31.7, and 45 ft/min (0.495, 1.477, 3, and 4.4 cfm). The following Tables and Figures provide a summary of the respective air velocity testing results.

Figure 4.17 provides the particle size distribution of the upstream and downstream samples from both the LAS and SMPS for 5 ft/min. Figure 4.18 provides the penetration fraction plot for both the LAS and SMPS.

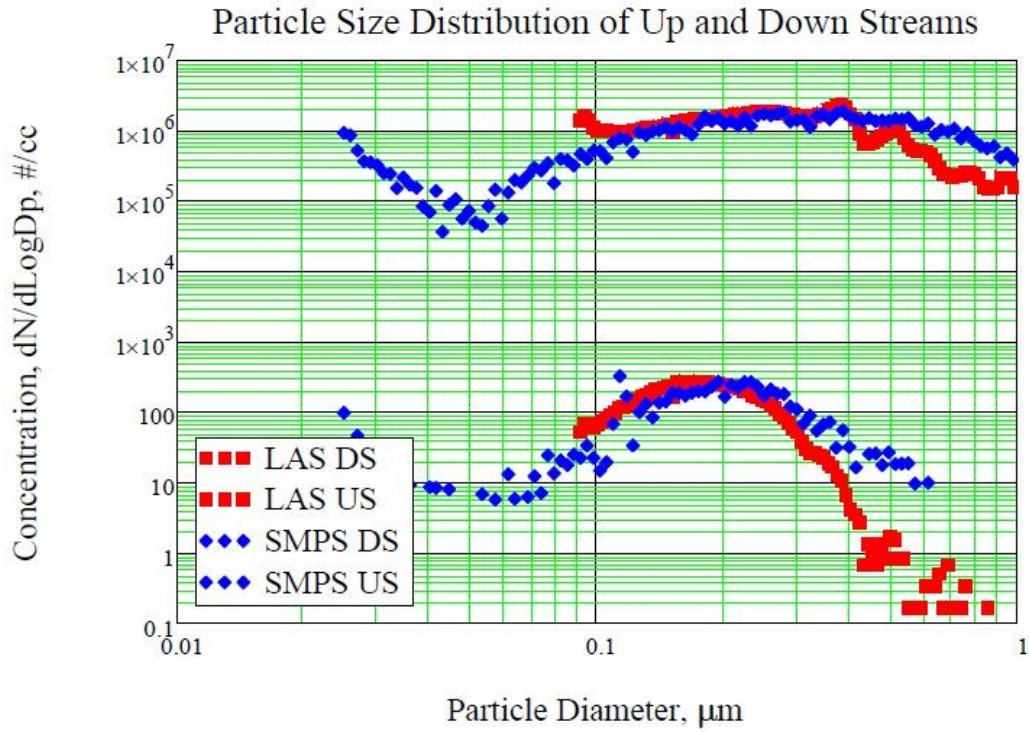


Figure 4.17 5 ft/min Up and Downstream Particle Distributions per LAS and SMPS

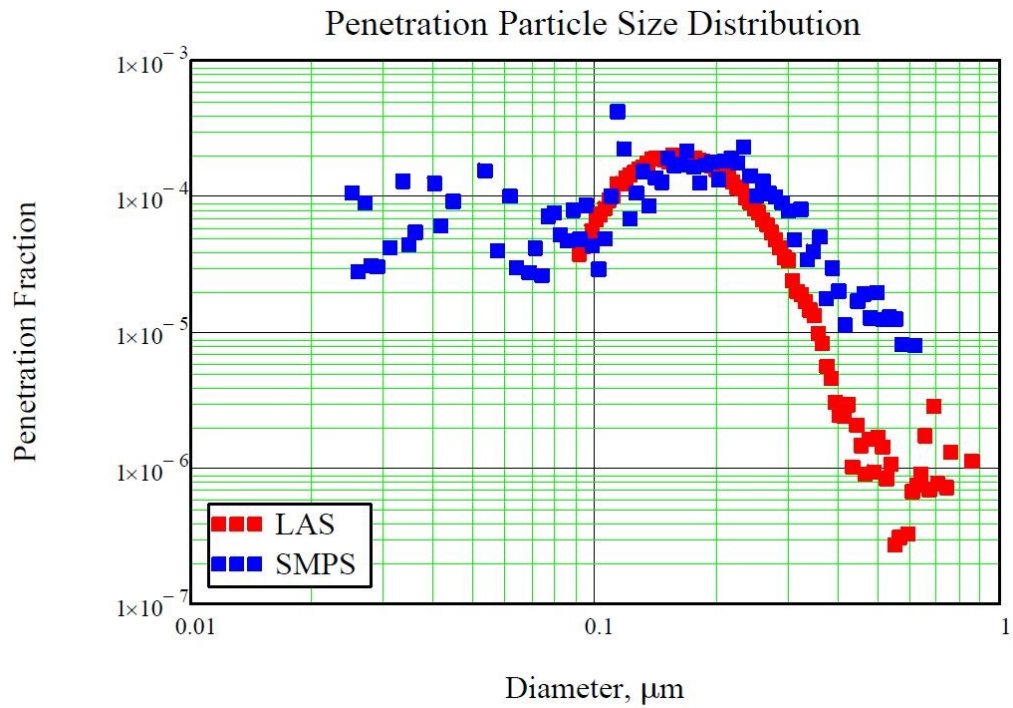


Figure 4.18 LAS and SMPS Penetration Distribution for 5 ft/min

Table 4.1 provides a summary of the testing results for the 5 ft/min filtering efficiency test. The initial and final dP for this test were 0.614 inWC and 0.804 inWC, respectively. The compressed air for the atomizer was set to 8 psi.

Table 4.1 5 ft/min Filter Efficiency Test Results

	LAS	SMPS
<b>0.3 <math>\mu\text{m}</math> Penetration Fraction</b>	5.42E-05	7.373E-05
<b>0.3 <math>\mu\text{m}</math> Filtering Efficiency</b>	99.9946%	99.9926%
<b>MPPS (<math>\mu\text{m}</math>)</b>	0.1605	0.1663
<b>MPPS Penetration Fraction</b>	1.9847E-04	1.7464E-04
<b>MPPS Filtering Efficiency</b>	99.98015%	99.98254%

While the HEPA filter media by itself does not require it to be 99.97% for 0.3  $\mu\text{m}$ , at 5 ft/min, the selected filter media was extremely efficient against this particle. The results and particle distributions were as expected when compared to previously acquired data. The LAS and SMPS samples produced similar efficiency results for both particles.

Figure 4.19 provides the particle size distribution of the upstream and downstream samples from both the LAS and SMPS for 15 ft/min air velocity. Figure 4.20 provides the penetration fraction plots for both the LAS and SMPS.

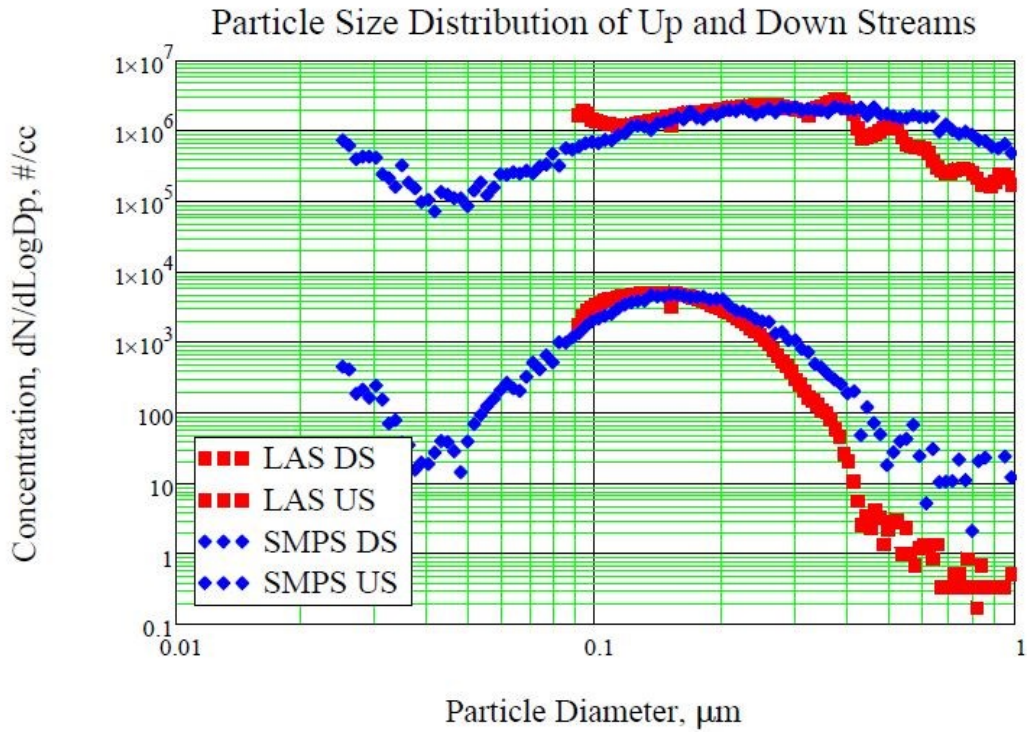


Figure 4.19 15 ft/min Up and Downstream Particle Distributions per LAS and SMPS

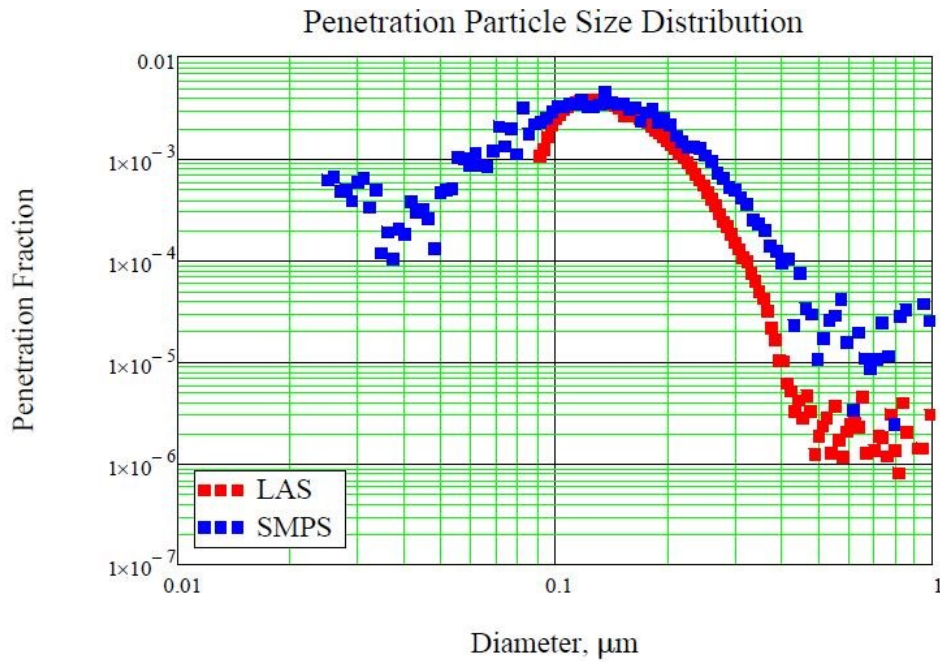


Figure 4.20 LAS and SMPS Penetration Distribution for 15 ft/min

Table 4.2 provides a summary of the testing results for the 15 ft/min filtering efficiency test. The initial and final dP for this test were 1.264 inWC and 5.602 inWC, respectively. The compressed air for the atomizer was set to 8 psi.

Table 4.2 15 ft/min Filter Efficiency Test Results

	<b>LAS</b>	<b>SMPS</b>
<b>0.3 <math>\mu\text{m}</math> Penetration Fraction</b>	3.0751E-04	4.885E-04
<b>0.3 <math>\mu\text{m}</math> Filtering Efficiency</b>	99.9692%	99.9512%
<b>MPPS (<math>\mu\text{m}</math>)</b>	0.1314	0.1276
<b>MPPS Penetration Fraction</b>	3.653E-03	3.5506E-03
<b>MPPS Filtering Efficiency</b>	99.6347%	99.64494%

At 15 ft/min, the HEPA filter material slightly missed the HEPA filter requirements of 99.97% efficient against the 0.3  $\mu\text{m}$  particle. Again, this is not a requirement for standalone filter media, but it is worth noting that the overall efficiency of the media decreases with increased velocity, as expected.

Figure 4.21 provides the particle size distribution of the upstream and downstream samples from both the LAS and SMPS for 31.7 ft/min air velocity. Figure 4.22 provides the penetration fraction plots for both the LAS and SMPS.

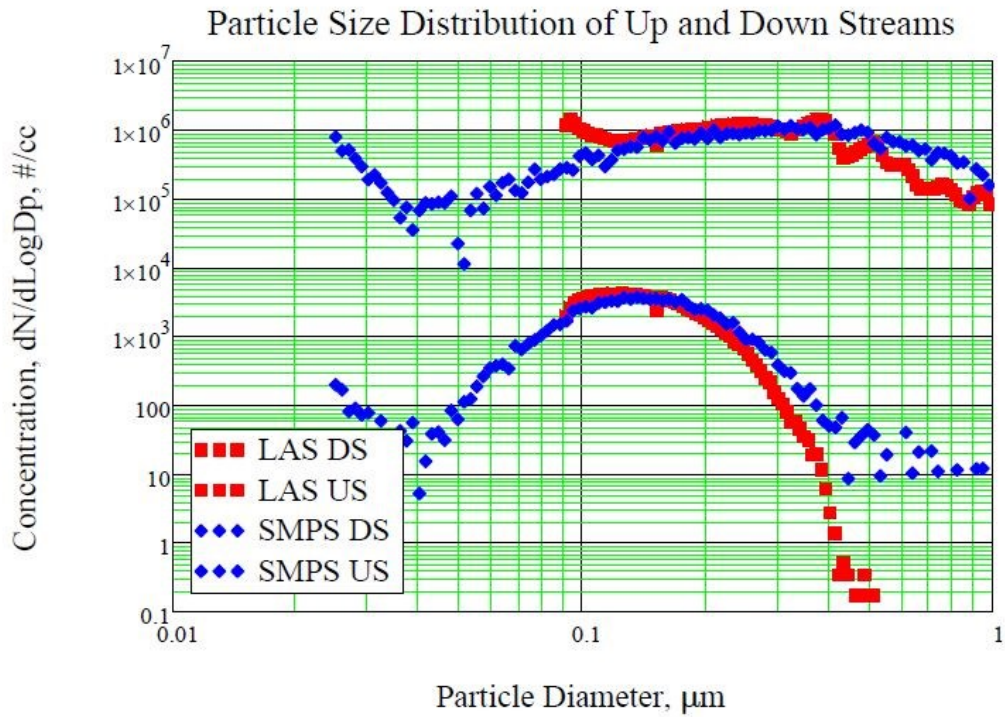


Figure 4.21 31.7 ft/min Up and Downstream Particle Distributions per LAS and SMPS

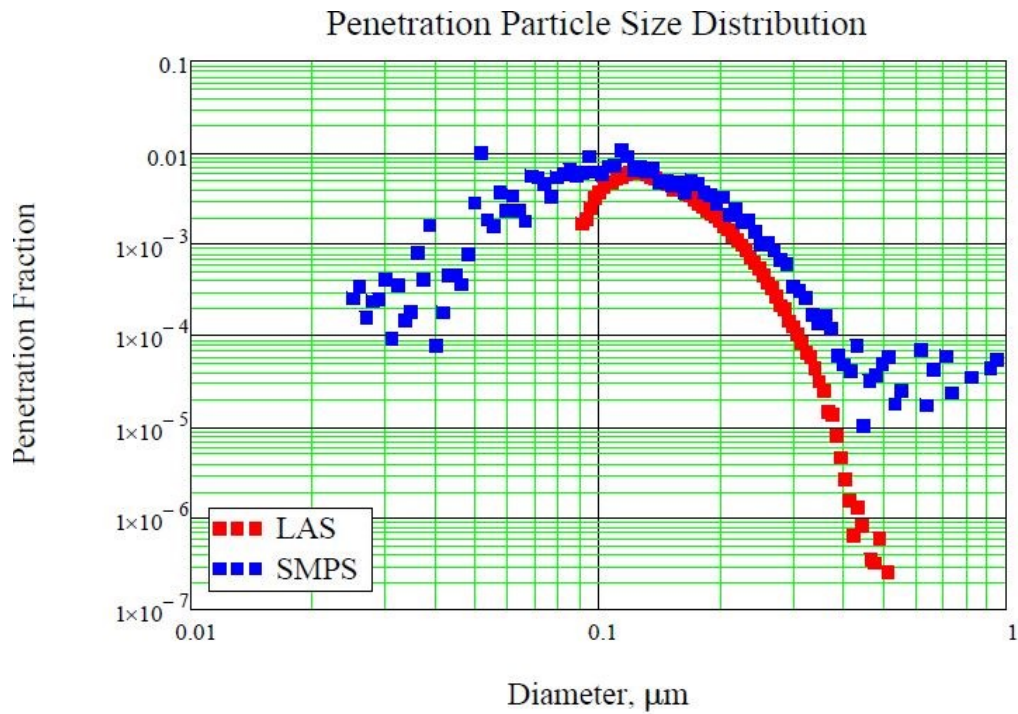


Figure 4.22 LAS and SMPS Penetration Distribution for 31.7 ft/min



Table 4.3 provides a summary of the testing results for the 31.7 ft/min filtering efficiency test. The initial and final dP for this test were 3.534 inWC and 7.036 inWC, respectively. The compressed air for the atomizer was set to 8 psi.

Table 4.3 31.7 ft/min Filter Efficiency Test Results

	<b>LAS</b>	<b>SMPS</b>
<b>0.3 <math>\mu\text{m}</math> Penetration Fraction</b>	2.8064E-04	4.235E-04
<b>0.3 <math>\mu\text{m}</math> Filtering Efficiency</b>	99.9719%	99.9577%
<b>MPPS (<math>\mu\text{m}</math>)</b>	0.1284	0.107
<b>MPPS Penetration Fraction</b>	5.6401E-03	7.069E-03
<b>MPPS Filtering Efficiency</b>	99.43599%	99.2931%

Once again, the overall filtering efficiency decreased with the increased air velocity as expected.

Figure 4.23 provides the particle size distribution of the upstream and downstream samples from both the LAS and SMPS for 45 ft/min air velocity. Figure 4.24 provides the penetration fraction plots for both the LAS and SMPS.

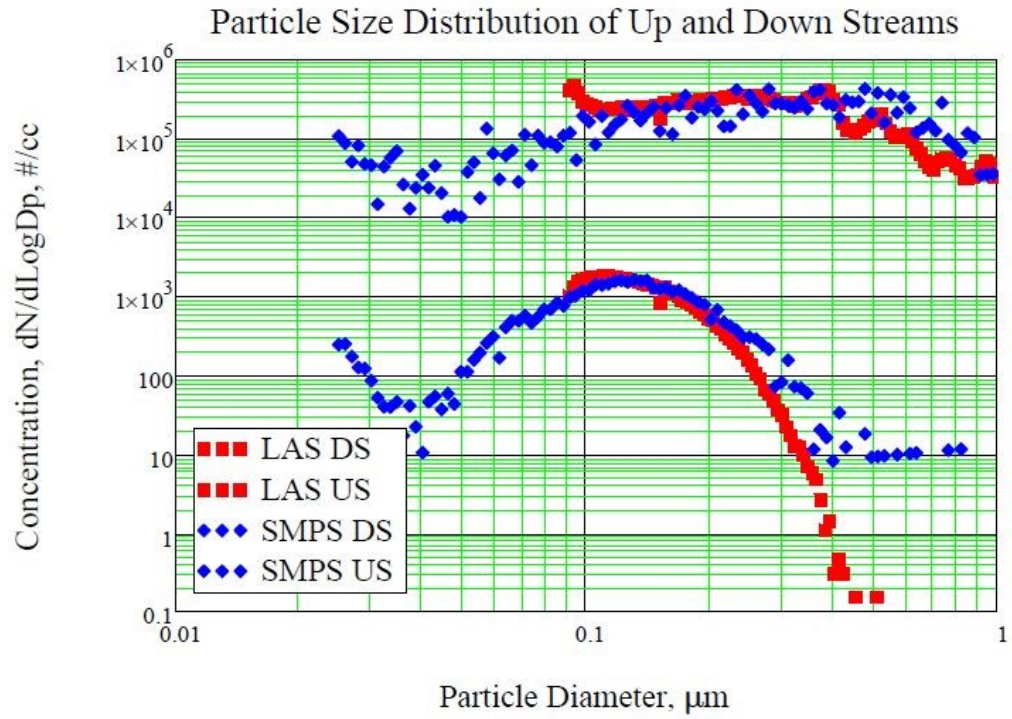


Figure 4.23 45 ft/min Up and Downstream Particle Distributions per LAS and SMPS

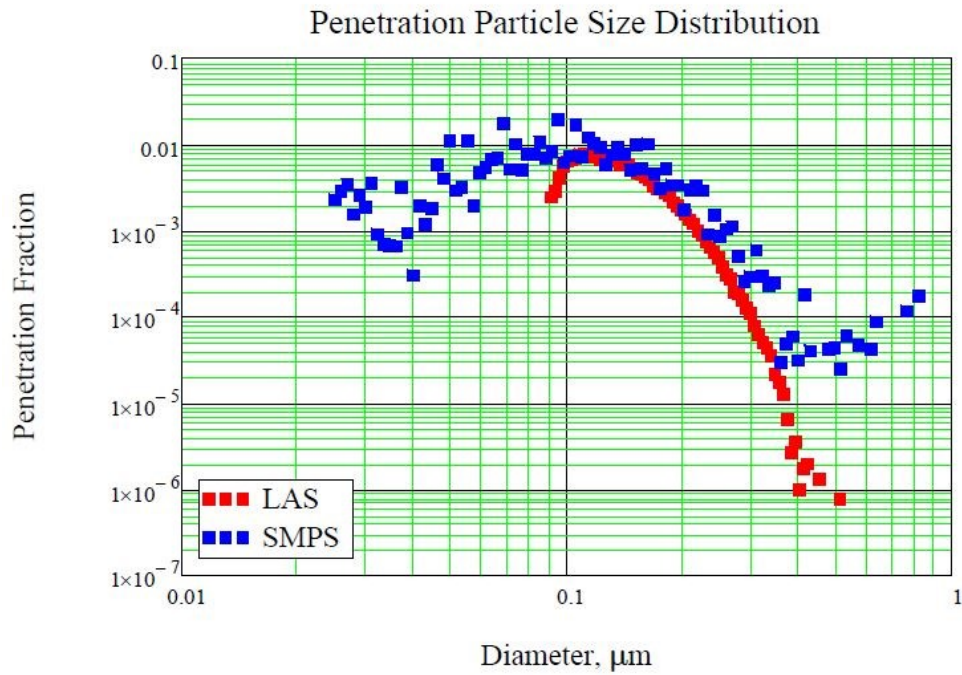


Figure 4.24 LAS and SMPS Penetration Distribution for 45 ft/min



Table 4.3 provides a summary of the testing results for the 45 ft/min filtering efficiency test. The initial and final dP for this test were 5.351 inWC and 7.41 inWC, respectively. The compressed air for the atomizer was set to 6 psi. The psi had to be reduced from 8psi due to the concentration being too high downstream for the LAS to function properly.

Table 4.4 45 ft/min Filter Efficiency Test Results

	<b>LAS</b>	<b>SMPS</b>
<b>0.3 μm Penetration Fraction</b>	2.3732E-04	3.254E-04
<b>0.3 μm Filtering Efficiency</b>	99.9763%	99.9675%
<b>MPPS (μm)</b>	0.1215	0.128
<b>MPPS Penetration Fraction</b>	7.1568E-03	1.01E-02
<b>MPPS Filtering Efficiency</b>	99.28432%	98.98651%

Overall, the filter efficiency characterization testing was successful. The results proved that the SSTS was capable of performing penetration testing and able to provide meaningful data about the test media properties.

#### 4.6 Filter Loading Results

The next type of test that can be performed using the SSTS is a loading test. The procedure used to perform filter loading tests for the SSTS can be found in Appendix C. Unlike a penetration test, only upstream samples are taken during the test. Both Al(OH)<sub>3</sub> and ARD are typical aerosols used to load the test filter. Only the SMPS was used to sample the loading test and to calculate the mass loaded onto the filter. This is because the SMPS records each samples total concentration, and there were concerns about using powder with the LAS. The dP of the test filter is also shown as a function of the mass loaded. The upstream samples were scaled by the

previously characterized dilution factor of 1433.5. Once again, for the sake of characterization, four different air velocities were tested to determine what the controls needed to be to successfully perform the test. These air velocities include 5, 10, 30, and 45 ft/min (0.495, 1.0, 2.955, and 4.4 cfm). The following figures provide a summary of the respective air velocity testing results.

Figure 4.25 provides the particle size distribution of the upstream samples from both the LAS and SMPS for 5 ft/min air velocity. Figure 4.26 provides dP and mass loaded plot while Figure 4.27 shows the dP as a function of mass loaded. The initial and final dP for this test were 0.524 inWC and 1.667 inWC, respectively. The compressed air for the vacuum nozzle was set to 12 psi.

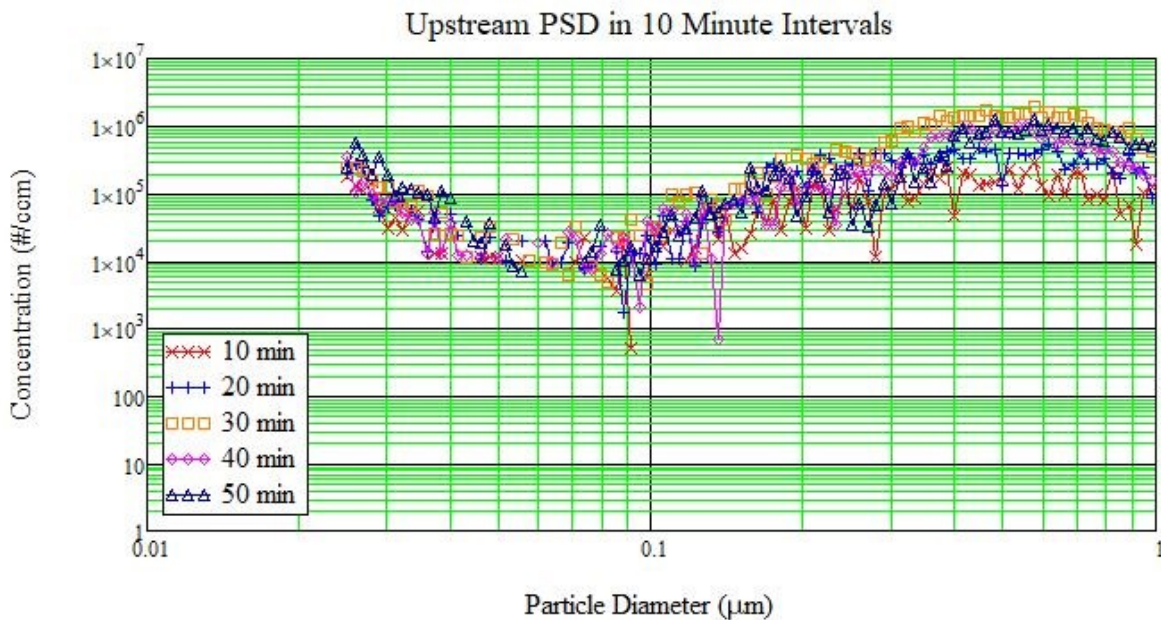


Figure 4.25  $\text{Al}(\text{OH})_3$  Particle Size Distributions for 5 ft/min Loading Test

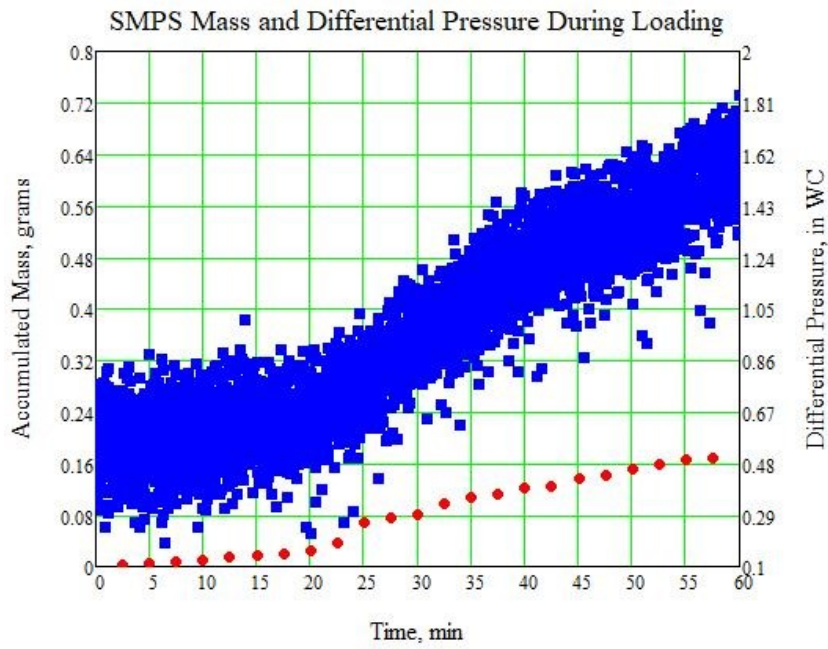


Figure 4.26 dP and Mass Loaded for 5 ft/min

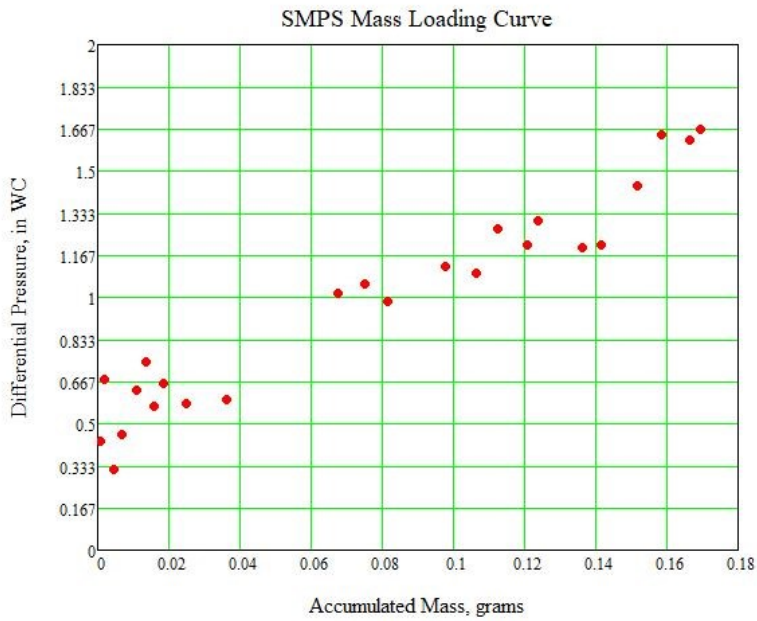


Figure 4.27 Mass Loading Curve for 5 ft/min

Due to the low flow rate, a low pressure from the compressed air must be used. This causes challenges in maintaining a constant feed rate as can be seen in the previous figures.

Figure 4.28 provides the particle size distribution of the upstream samples from both the LAS and SMPS for 10 ft/min air velocity. Figure 4.29 provides dP and mass loaded plot while Figure 4.30 shows the dP as a function of mass loaded. The initial and final dP for this test were 1.483 inWC and 6.752 inWC, respectively. The compressed air for the vacuum nozzle was set to 14 psi.

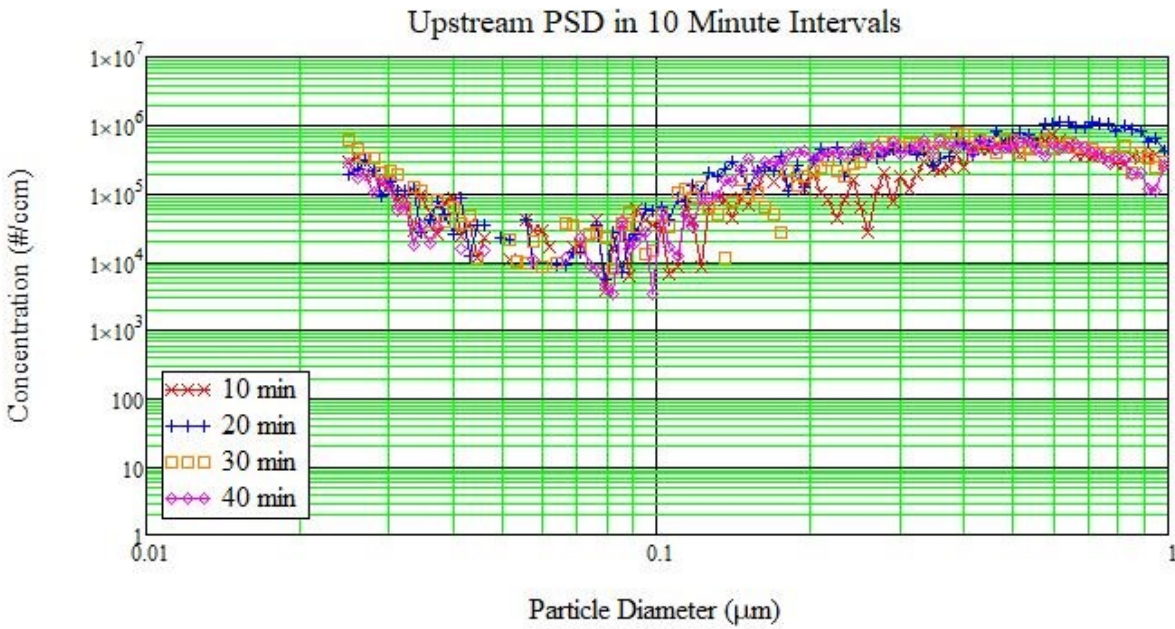


Figure 4.28 Al(OH)<sub>3</sub> Particle Size Distributions for 10 ft/min Loading Test

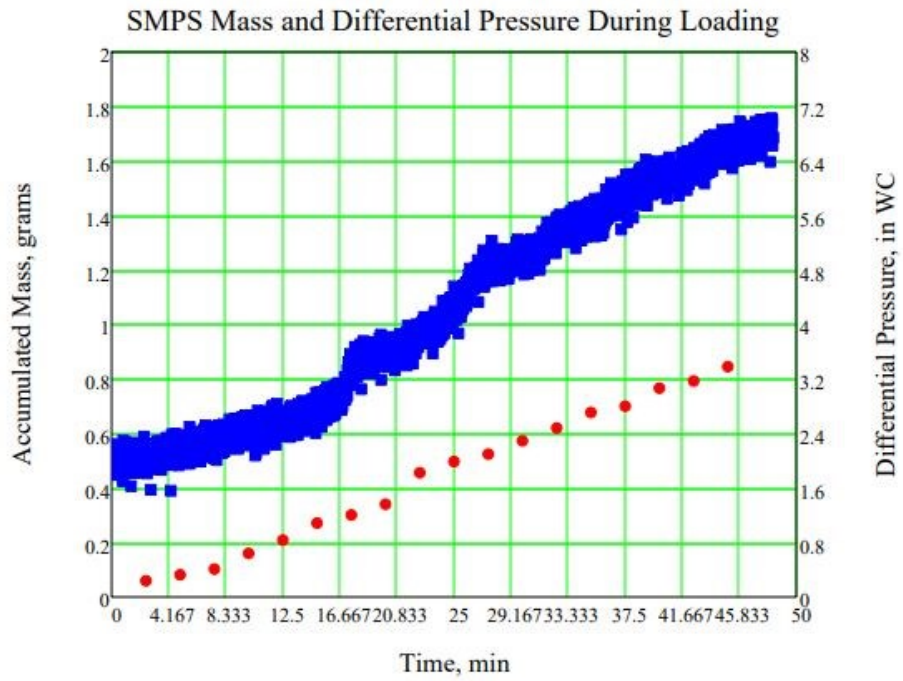


Figure 4.29 dP and Mass Loaded for 10 ft/min

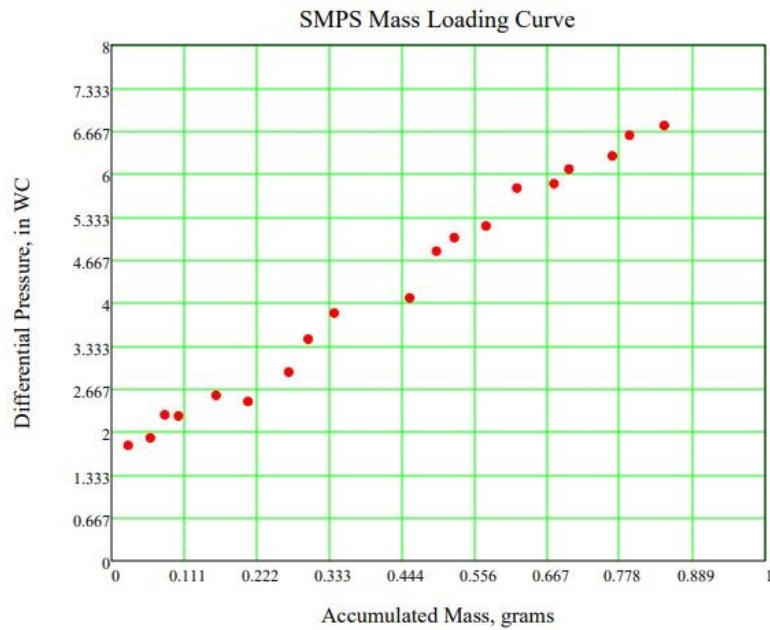


Figure 4.30 Mass Loading Curve for 10 ft/min

Figure 4.31 provides the particle size distribution of the upstream samples from both the LAS and SMPS for 30 ft/min air velocity. Figure 4.32 provides dP and mass loaded plot while Figure 4.33 shows the dP as a function of mass loaded. The initial and final dP for this test were 3.406 inWC and 24.226 inWC, respectively. The compressed air for the vacuum nozzle was set to 18 psi.

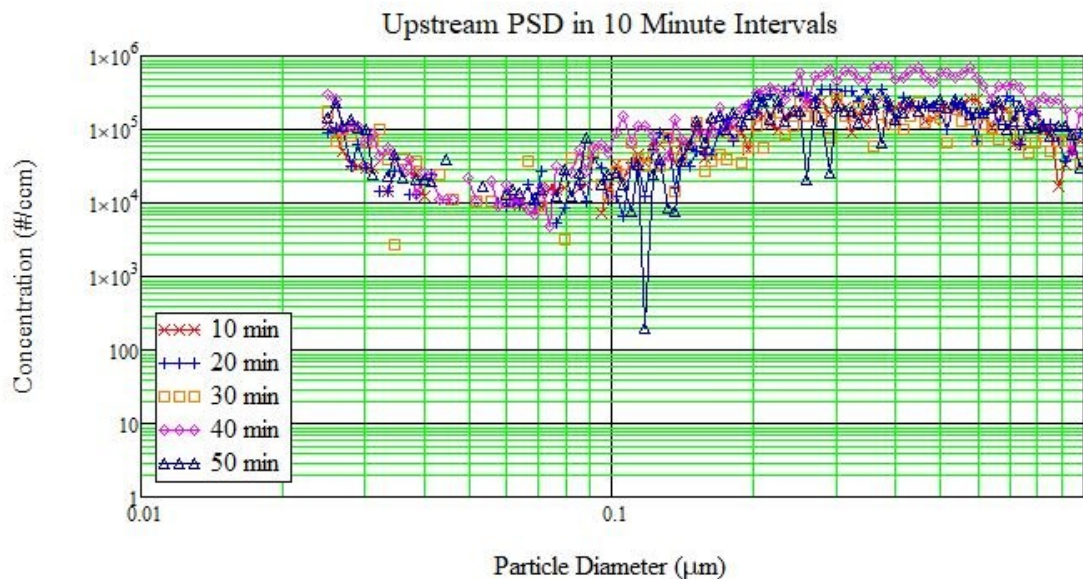


Figure 4.31 Al(OH)<sub>3</sub> Particle Size Distributions for 30 ft/min Loading Test



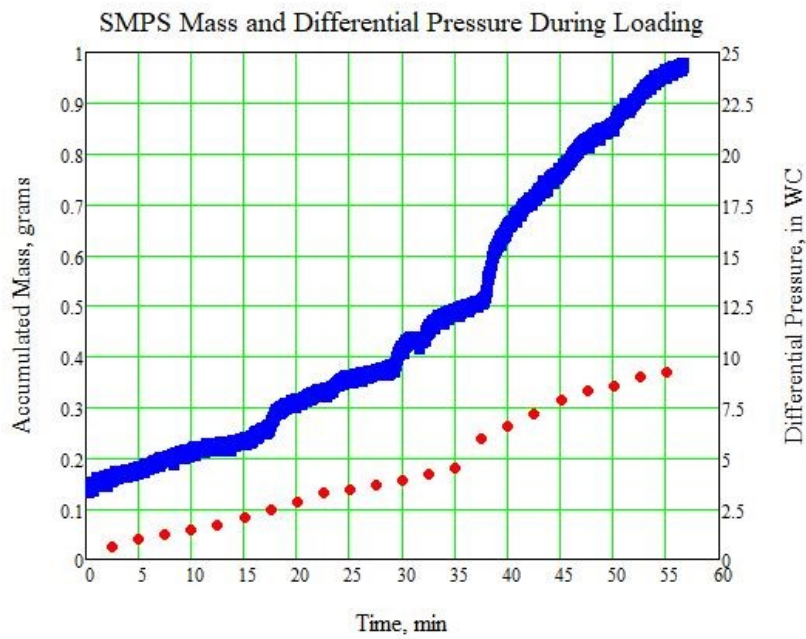


Figure 4.32 dP and Mass Loaded for 30 ft/min

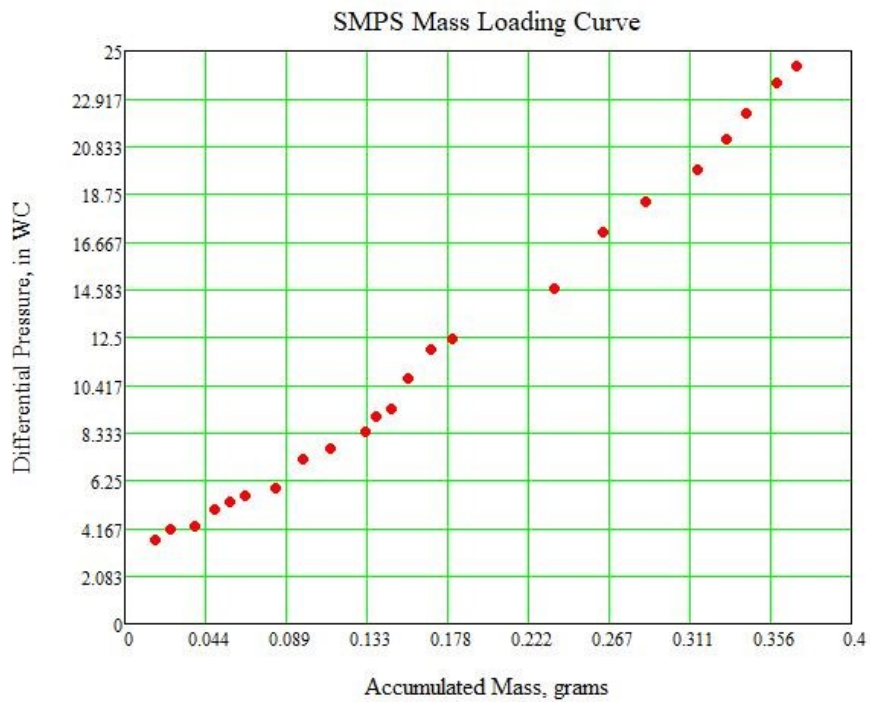


Figure 4.33 Mass Loading Curve for 30 ft/min

The 45 ft/min test did not provide enough samples to reduce into a mass loading diagram due to a dP spike across the filter at the same concentration as the previous test. The concentration could not be reduced as any less would not be enough to obtain an accurate distribution. The initial and final dP for this test were 5.331 inWC and 33.252 inWC, respectively. The compressed air for the vacuum nozzle was set to 26 psi. Figure 4.34 provides the one sample of the particle size distribution, and Figure 4.35 provides the dP curve with respect to time.

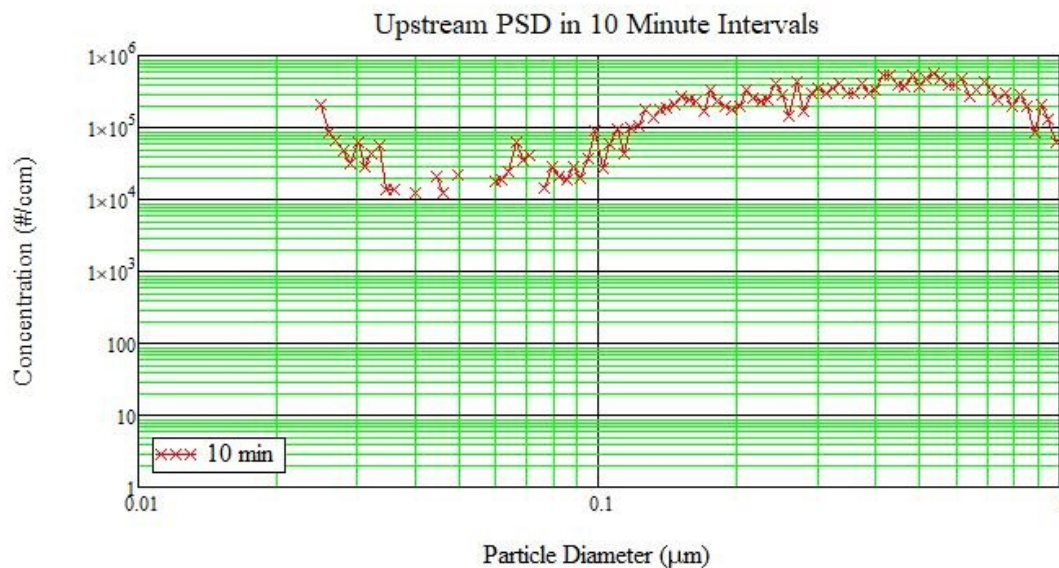


Figure 4.34  $\text{Al}(\text{OH})_3$  Particle Size Distribution for 45 ft/min Loading Test



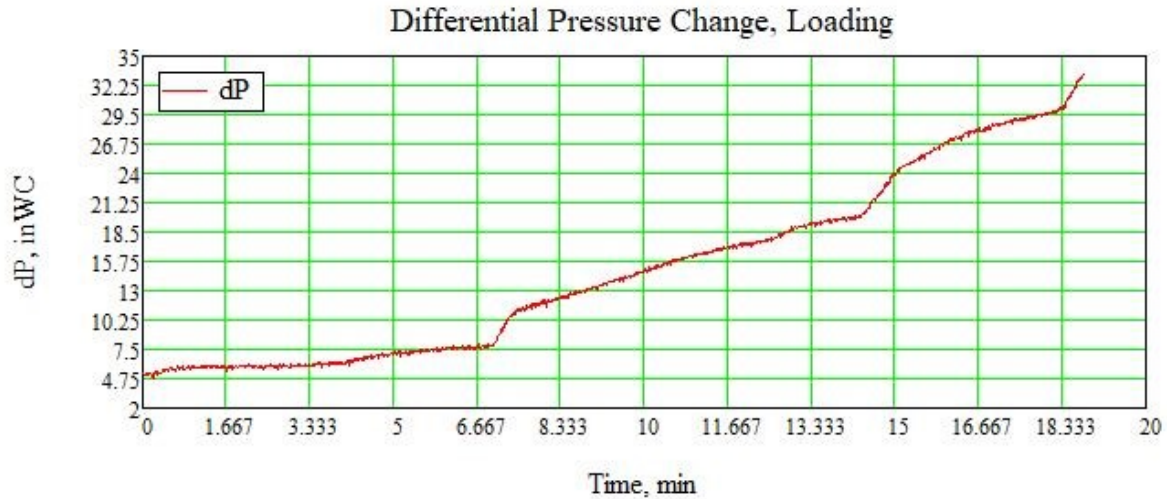


Figure 4.35 dP for 45 ft/min Loading Test

The performed loading test proved to be able to provide meaningful data about the mass loaded and dP for the test filter. For the selected HEPA media, a velocity range of 5 to 30 ft/min can be performed. Other less efficient filter medias may be able to be tested at high flow rates. The powder and injection assembly is capable of producing a fairly constant feed rate, but for a lengthy test, clogging in the injection manifold and vacuum nozzle can become an issue due to the powders properties.

## CHAPTER V

### CONCLUSIONS

The intent of this work was to design, construct, and characterize the capabilities of a test stand that could perform penetration and loading test on various filter medias on a small scale. This was accomplished with the SSTS. A thorough design of the test stand was done in order to best satisfy the design criteria. However, these design criteria provided a series of issues that had to be addressed through different design calculations, compromises, and verifications. These issues, and what was required to overcome them, will hopefully be applied to future test stand developments at ICET.

The original goal for the maximum flow rate was 20 cfm, but there were difficulties in attempting to find a flow meter that was capable for the high temperature flow rates. Another criterion that limited the flow meter options was the selected vendor list. In order to provide Quality Assured (QA) data, ICET only procures instrumentation from approved, audited vendors. With these limitations and attempts to stay under a certain price limit, a flow meter with a maximum flow rate of 17.6 cfm and temperature of 212°F was selected. This flowmeter was a good compromise of the criteria and what was available.

The next challenge was presented with the 4-inch duct diameter requirement. This requirement led to turbulent conditions after only 5 cfm flow rate according to the *Re* number calculations. In addition, the increased air velocity made obtaining isokinetic sampling conditions virtually impossible for the slower flows with reasonably size sampling probes.

However, this issue was eluded by a detailed calculation of the particles Stk and verification using different sampling probes. There are still errors involved with the anisokinetic conditions, but there is great confidence that the samples provide an adequate representation of the concentration in the duct that the test filter experiences.

Finally, the last challenge faced was maintaining an elevated temperature for the air flow. This was largely due to the temperature being measured further downstream than the heater coil and the transient nature of the heating process. This caused the temperature to rise and fall over the given period of time due to the control scheme. Also, the heater coil was unable to work at flows lower than 17 cfm. When attempting to test the heater with the lower flows, the coil would begin to overheat. Both of these issues were acceptable; however, as the intent of the elevated temperature is to essentially “bake” the filter for a period of time. Then, once everything cooled down, the “baked” filter would be tested normally. This allows the high flow and varying temperature to be sufficient in simply changing the filters characteristics.

In regards to what could be improved, the selected powder feeder had difficulties providing a consistent feed rate. This was due to the powder’s characteristics, as well as the small-scale system. The powder had a tendency easily clump together and form a bridge above the screw. This led to constant attention being required to ensure that the powder bridge was broken up as it began to form. The powder would also clog certain components of the injection system over time, specifically in the vacuum nozzle. On the larger scale test stands, the compressed air for the vacuum nozzle is set to 60 psi in order to ensure that the powder is broken up. However, for the SSTS, the maximum compressed air settings ranged from 8 to 26 psi. Other injection methods should be explored for smaller scale applications.

The LabVIEW program and station can also be improved. As more and more data is stored, the program begins to lag and struggle to compute the loops. A more powerful computer and efficient programming is recommended over the long term, especially when lengthy loading tests are being performed. The heater loop should also be adjusted to better handle the low flow settings. This can be done by adjusting the voltage output to the heater and the pulse time.

Overall, the development of the SSTS required a few compromises and design calculations to best satisfy the design criteria. The SSTS can perform excellent and consistent filter efficiency testing, with low testing times. The loading testing certainly has room for improvement but is still capable of providing good data that can be used for a multitude of other research projects. The SSTS is an ideal option to perform tests on prototype medias such as carbon fiber and electrospun media, as well as other types such as ceramics and metal media due to the SSTS's modular capabilities. In regards to future work, the SSTS hopes to provide data for the previously mentioned filter medias and generate filter loading models to predict the filters expected life. In order to obtain these goals, the next step for the SSTS is to begin the process of being a QA test stand. This includes calibrating all of the instrumentation through an ICET, audited company and going through a series of document reviews. Once the test stand has achieved this, official testing can be done.

## REFERENCES

- [1] (DOE), D. of E., 2003, “History of the Development of Air Cleaning Technology in the Nuclear Industry,” *Nuclear Air Cleaning Handbook (DOE-HDBK-1169-2003)*, pp. 1–18.
- [2] Bergman, W., 2006, “HEPA Filter Particle Loading,” Stanwood, WA, pp. 1–30.
- [3] Berry, G., Parsons, A., Morgan, M., Rickert, J., and Cho, H., 2022, “A Review of Methods to Reduce the Probability of the Airborne Spread of COVID-19 in Ventilation Systems and Enclosed Spaces,” *Environ. Res.*, **203**, p. 111765.
- [4] Novick, V. J., Monson, P. R., and Ellison, P. E., 1992, “The Effect of Solid Particle Mass Loading on the Pressure Drop of HEPA Filters,” *J. Aerosol Sci.*, **23**(6), pp. 657–665.
- [5] Hinds, W. C., 1999, *Aerosol Technology: Properties, Behavior, and Measurement of Airborne Particles*, John Wiley & Sons, Inc.
- [6] Erickson, K., Singh, M., and Osmondson, B., 2007, “Measuring Nanoparticle Size Distributions in Real-Time: Key Factors for Accuracy,” 2007 NSTI Nanotechnol. Conf. Trade Show - NSTI Nanotech 2007, *Tech. Proc.*, **4**(1), pp. 179–182.
- [7] Inc., TSI., 2007, “Scanning Mobility Particle Sizer™,” **48**(4), pp. 239–253.
- [8] 2007, “Model 3775 Condensation Particle,” *ReVision*, (April).
- [9] Inc., TSI., 2009, “Model 3340 Laser Aerosol Spectrometer,” *Indoor Environ.*, (June), pp. 1–37.
- [10] Inc., TSI., 2012, “Aerosol Diluter Model 3302a : Rp-3302a,” p. 67877200.
- [11] Properties, P., and Properties, C., 2018, “FILLERS – ORIGIN , CHEMICAL COMPOSITION , PROPERTIES , AND MORPHOLOGY,” **220**.
- [12] Applications, I., Conduc-, T., Fluid, B., Tribology, I., and Series, I. E., 2011, “Poly-Alpha-Olefins Tribochemistry of Lubricating Oils Rheology Control.”
- [13] TSI Inc., TSI, 2003, “Model 9306A Six-Jet Atomizer Instruction Manual,” (February), p. 12.

## APPENDIX A

### PRELIMINARY DESIGN OF THE SMALL-SCALE FILTRATION TEST STAND

# Preliminary Design of the Small-Scale Filtration Test Stand

20-DD-HEPA-SSTS-002

Revision 0

January 11, 2020

This document is a preliminary design overview of the Small-Scale Test Stand, which is intended for the express purpose of serving as a test apparatus operated by student researchers for filtration testing. The document includes design parameters, design decisions, system components, and system functions.

Principal Investigator:

*Jamie Bukert for Charles A. Waggoner*

Dr. Charles A. Waggoner, Director  
Institute for Clean Energy Technology  
Mississippi State University  
205 Research Park  
Starkville, MS 39759  
(662) 325-2105  
Fax: (662) 325-8465  
[waggoner@icet.msstate.edu](mailto:waggoner@icet.msstate.edu)

Uncontrolled Document if Printed

## Preliminary Design of the Small-Scale Filtration Test Stand

Document Number: 20-DD-HEPA-SSTS-002

Version Number: 0

Revision Number: 0

Authored by: Gentry Berry  Date: 1-13-2021

Major Professor: Dr. Heejin Cho  Date: 1-14-2021

Checked By (Subject Matter Expert): John Wilson  Date: 1/19/2020

Reviewed By (Quality Assurance): LeAnn McMullen  Date: 1/13/2021

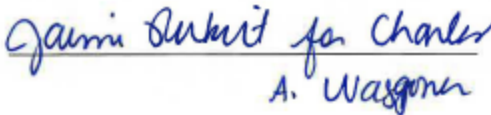
Reviewed By (Health and Safety): N/A \_\_\_\_\_ Date: N/A

Reviewed By (Environmental): N/A \_\_\_\_\_ Date: N/A

Reviewed By (Engineering): Jay McCown  Date: 1/14/21

Approved By: Jaime Rickert for Charles A. Waggoner

Approver's Position: Principal Investigator

Approver's Signature:  Date: 1/19/21

ii

Uncontrolled Document if Printed



### Document Change Record

Date	Revision Number	Change Made	Section	Pages

## Table of Contents

List of Figures .....	v
I. Background .....	1
II. Performance Objectives .....	2
III. Flow Path Description .....	3
IV. Instrumentation and Control .....	8
Appendix A. Concept Drawings .....	11
Appendix B. Small Scale Test Heat Transfer Analysis .....	16
Appendix B. Small Scale Test Stand Heating Coil Size Estimate .....	21
Appendix B. Small Scale Test Stand Head Loss Estimate .....	24
Appendix B. Small Scale Test Stand Reynolds Number Estimate.....	28

List of Figures

Figure 1. PID of the SSTS .....8  
Figure A.1. Preliminary model of the SSTS .....11  
Figure A.2. Annotated drawing of the SSTS model .....12  
Figure A.3. Preliminary PID of the SSTS .....13  
Figure A.4. Test article holder .....14  
Figure A.5. Room 282 proposed layout.....15  
Figure B.1. Gast product specification .....29

## **I. Background**

This document describes the preliminary design of the Small-Scale Filtration Test Stand (SSTS) at the Institute for Clean Energy Technology (ICET) at Mississippi State University. The purpose of this document is to serve as a description of the current design proposed for the SSTS in order to facilitate in future assembly and ongoing improvement.

A design for new testing equipment was conceptualized based upon common operating conditions found in related research in order to expand upon the capability already installed at ICET. The function of the SSTS is to provide conditioned, particle laden air to the test article while continuously measuring the aerosol characteristics and performance characteristics of the test article. These goals will be achieved by broadly defining the performance characteristics of a test article as the Pressure Drop ( $dP$ ) and Particle Capture Efficiency (simply capture efficiency or filtering efficiency) of said article induced by the loading of particles onto the media over time. The  $dP$  between points immediately upstream and downstream of the test article is constantly measured with respect to time in order to capture this performance characteristic. The filtering efficiency of the test article is measured by isokinetically sampling a representative portion of the airstream and measuring the distribution of known particle types based upon their diameter or mass and respective counts. An assumption is introduced here that the Particle Size Distribution (PSD) and concentration are considered to remain constant in the time between consecutive samples. This is relevant as the particle sampling will alternate between upstream sampling and downstream sampling and is not anticipated to remain at constant values throughout the entirety of the tests. Knowing these few characteristics with respect to time will allow for a comprehensive analysis of the performance of the test article, i.e., the evolution of  $dP$  across the test article as a function of mass loading or the analysis of variables indicating imminent filter failure.

The SSTS is anticipated to be primarily used for testing flat-sheet High Efficiency Particulate Air (HEPA) media, but may also potentially be retrofitted for use with small axial-flow filters, sintered metal filters, and ceramic filters if the appropriate modifications are added. Given common filtration velocities in current research (approximately 1-100 ft/min) and the

standard maximum filtration velocity for HEPA filters as defined by the AG-1 standard (5 ft/min), a test duct of 4 inches in diameter (ID) was selected with a maximum volumetric flow rate of 20 Actual Cubic Feet per Minute (ACFM). Common aerosols will be used to challenge the test article to include: Arizona Road Dust (ARD), Aluminum Trihydroxide (Al(OH)<sub>3</sub>), Polyalphaolefin (PAO), and Acetylene Soot.

## II. Performance Objectives

The performance objectives are as follows:

1. The flow conditions at the inlet to the test article shall be:
  - a. Flow rate up to 20 actual cubic feet per minute (ACFM).
  - b. Temperature up to 250 °F (121.11 °C).
  - c. Relative humidity up to 90% (this capability will be installed later, after the initial construction and analysis of the SSTS).
2. To maintain a 20 ACFM flow rate when the pressure drop across the test article may be as high as 35 inches of water column (inch w.c.) and as low as 1 inch w.c..
3. To allow the introduction of various aerosols, initially anticipated as Arizona Road Dust (ARD), Aluminum Trihydroxide (Al(OH)<sub>3</sub>), Polyalphaolefin (PAO), and Acetylene Soot for the purpose of loading the filter and increasing the pressure drop across the filter.
4. To ensure (within reasonable expectation) the uniform distribution of the challenge aerosol within the cross-sectional area of the test duct.
5. To ensure the capture of relevant data related to the properties of the conditioned air in order to maintain proper control of the flow rates within the test stand. This includes air temperature, pressure, and relative humidity immediately upstream of the test article and the mass flow rate of air through the test stand and sampling instruments.

6. To allow for the expansion of the SSTS to include additional capability by incorporating a modular design in an effort to accommodate unplanned but probable tests in the future. These will likely include sintered metal and ceramic filtration media, pleated fibrous filter media, and other novel medias. Furthermore, the addition of planned and unplanned equipment, such as a humidifier and dehumidifier for control of the humidity the test article is subjected to.
7. To operate within the floor space profile determined by its designated laboratory space. Currently, Room 282 is assigned for the SSTS and future additions. Figure A.5 shows the proposed layout of Room 282 with the test stand.

### **III. Flow Path Description**

The test stand is to be assembled in a single-pass arrangement, with the air intake (test stand entrance) open to the lab environment and the air exhaust (test stand exit) venting through the available exhaust vents in the lab to the roof outside. Each section of the SSTS will be modular, consisting of flanged pipe sections that are bolted to one another. The SSTS can be divided into three sections: 1) Flow Conditioning, 2) Testing and Measurement, and 3) Flow Measurement and Control. The flow path begins with the air intake in the lab and passes immediately into the flow conditioning section. Following this, the air passes through the testing and measurement section, and then finally into the flow measurement and control section. After the flow measurement and control section, the air is exhausted. The flow conditioning section is comprised of equipment necessary to condition the flow to the desired testing point. Currently, the equipment in this section will be a pre-filter to remove any ambient dust or other particles from the air and a heating element to provide the necessary heat to reach the required temperature of the air. A humidifier will be added at a later time in order to control the relative humidity (RH) passing through the test article. The testing and measurement section will consist of a manifold style particle injector, an upstream isokinetic particle sampling system, a RH and T probe, a set of pressure transducers, the test article and holder, and a downstream isokinetic particle sampling system. The flow measurement and control section will consist of a downstream post-filter, temperature probe, mass flow meter, a blower fan to induce the flow, a

Variable-Frequency Drive (VFD) to control the power imparted to the fan, and an electrically actuated valve to control the flow of make-up air required for the fan. Figures A.1 and A.2 in Appendix A show the overall layout of the SSTS. A more detailed description of each section is given below:

## **1. Flow Conditioning**

The flow conditioning section is made of steel, with a square cross-section piece for the pre-filter housing, and a small diameter piece of pipe for the heating element. The nominal dimensions of the pre-filter housing will be 12x12-inches, and the piece of pipe will have a nominal inner diameter of 2-inches.

### **a. Air Inlet**

Fresh air from the ambient lab environment is drawn in through the test stand by the vacuum induced from the blower fan. This serves to facilitate a simple control of the mass flow rate through the test stand, as the added flow from the particle injection is accounted for automatically. However, the fraction of flow removed for particle sampling must still be accounted for in order to ensure an accurate sense of the volumetric flow of air through the test article. The flow rate of air will be controlled by balancing the effects of simultaneously utilizing the Variable-Frequency Drive (VFD) to decrease the power of the fan and utilizing the valve to control the amount of make-up air added downstream of the flow meter. A HEPA filter is recommended for use within the pre-filter housing in order to achieve low background counts for aerosol testing and to provide the ability to assert in any publication that the test article is solely challenged with a known variable.

### **b. Heating Element**

A small electric heating coil will be placed directly downstream from the pre-filter housing in a reduced diameter section of pipe (nominal 2-inch inner diameter) in order to condition the air flow to the desired testing condition. The

calculations to estimate the required size of this heating coil are available in Appendix B..

**c. Conditioning Section to Measurement Section transition**

A small transition from a 2-inch inner diameter to a 4-inch inner diameter connects the Flow Conditioning Section to the Testing and Measurement section.

**2. Testing and Measurement**

The testing and measurement section is made of stainless steel with a nominal circular cross-section of 4-inches. The testing and measurement section consists of, in order from upstream to downstream:

**a. Upstream section**

There is a roughly 74-inch long straight run of pipe to the inlet of the test article holder. This provides sufficient space to inject particles into the flow and to sample the particle concentration upstream of the test article. It is assumed that the flow will be fully developed by the time it has reached the test article. Calculations estimating the flow conditions may be found in Appendix B.

**i. Aerosol Injection**

There are four anticipated particle types that will be used for testing: 1) Arizona Road Dust (ARD), 2) Aluminum Trihydroxide ( $\text{Al}(\text{OH})_3$ ), 3) Polyalphaolefin (PAO), and 4) Acetylene Soot. The injection of bulk powders will be facilitated with a K-TRON SODER model KMOVKT20 powder feeder that feeds powdered material from a feed hopper using twin screw augers. Control of the feed rate is possible by controlling the rotational speed of these screw augers. A VACCON venturi vacuum pump will be installed between the particle feeder and the test stand and supplied with dried compressed air. This venturi will create a blast of air that subjects the particles to high turbulence levels and high shear rates, and thus serves to break up any large agglomerates that form. Furthermore, the



venturi will have the additional benefits of creating a suction at the outlet of the particle feeder, entraining the test particle in a steady flow of dry, clean air and smoothly conveying the particles into the particle injection manifold and ultimately the test stand. The particle injection manifold will be used to inject this flow of entrained particles into the test stand and facilitate in a uniform dispersion of the particles across the cross-sectional area of the pipe. Designs of the particle injection manifold are currently under development, but are likely to include several key concepts: 1) numerous small-diameter outlets that serve to deposit the particles at multiple locations distributed across the pipe cross-section, 2) outlets facing towards the oncoming flow of air, serving to briefly turbulate the air and assist in mixing the particles, and 3) streamlined construction in order to reduce the amount of drag and losses incurred by its presence within the flow. The design will be in accordance with the AG-1 Appendix HA-C Manifold Design Guidelines.

**b. Test Article Holder**

This is intended to hold the flat sheet media during tests. It is designed to hold a single piece of circular media backed with a very coarse wire mesh for added strength. An illustration of the initial design is given in Figure A.4.

**c. Downstream Section**

There is an 80.25-inch long straight run of pipe downstream of the test article running to the post-filter. This provides sufficient space to avoid flow disturbances for the downstream sampling, in the same way as the upstream particle sampling. It is assumed that the flow will be fully developed.

- i. There are no turns or elbows. This is intentionally done to reduce particle deposition to the walls of the pipe and to ensure and maintain a developed flow profile.
- ii. A post-filter is housed in a housing similar to the pre-filter in order to remove any remaining aerosol. This is important, as the mass flow meter

and blower fan both require clean air flows. Furthermore, it is necessary to remove any particles from the air before exhausting the flow, as the particles are potentially hazardous to breathe in.

### 3. Flow Measurement and Control Section

The flow measurement and control section is comprised of 0.75-inch stainless steel pipe connecting the mass flow controller to the post-filter housing, and then connecting the mass flow meter to a pipe tee. The tee will also connect the make-up air flow through its branch and will continue into a section comprised of 1.5-inch flexible hosing of sufficient length to reach the blower fan. The blower fan will also be connected to the ceiling vents with 1.5-inch flexible hosing.

- a. The mass flow meter will be incorporated into a feedback loop with the VFD, fan, and the actuated valve in order to provide automatic control of the flow through the test stand with no interaction from testing personnel.
- b. The electrically actuated valve is intended to be a ball-valve. Although a ball-valve does not provide the same control over the flow as a globe valve, for example, it should be sufficient for the proposed application given the electric actuation and the VFD controlling the speed of the fan. A simple filter and screen will be added to the inlet of the ball valve in order to keep out large particles and objects that may damage the valve or the fan.
- c. The blower fan is intended to be a Gast R4P115 60Hz blower fan. The specifications for this blower require that it be able to provide a flow of up to 20 ACFM of air with an inlet temperature up to 250 above 200 °F and an inlet pressure down to 12.72 psia (55 inch w.c. below atmospheric pressure), when discharging near atmospheric conditions to the exhaust vent. It is worth noting that the selected fan provides excess flow rate capacity of approximately 17.5 ACFM for a total volumetric flow rate of 37.5 ACFM at the estimated minimum inlet pressure condition (60 inch w.c. vacuum). This excess air will be added from the make-up air through the actuated valve and will serve to facilitate in keeping the fan at a reasonable temperature over long periods of testing time that require the fan to operate at maximum capacity.

#### IV. Instrumentation and Control

A Piping and Instrumentation Diagram (PID) for the SSTS is shown below in Figure 1 (a larger version is available in Figure A.3 in Appendix A). Relevant sections of the pipe will have ports used for aerosol injection, aerosol sampling, air property measurement, and air conditioning. Since the purpose of this test stand is to subject filtration media to specified testing conditions of flow rate, temperature, and pressure drop, the instrumentation of the SSTS is intended to provide these parameters at the inlet to the filter. Accordingly, the temperature and relative humidity of the air immediately upstream of the test article holder will be measured. Furthermore, the decrease in pressure across the test article holder will be measured to provide the relevant data associated with the loaded particle mass. The volumetric flow rate, and thus the filtration velocity, will be calculated from the data collected from the mass flow meter and the air properties immediately upstream of the test article. The temperature will be measured immediately upstream of the mass flow meter in order to ensure that the instrument is not subjected to temperature above its operating envelope. Since the capability to add water vapor to increase the humidity will not be installed initially, it is not necessary to measure the relative humidity downstream of the filter as the flow will remain non-condensing at the ambient conditions within the lab environment or at elevated conditions within the test stand.

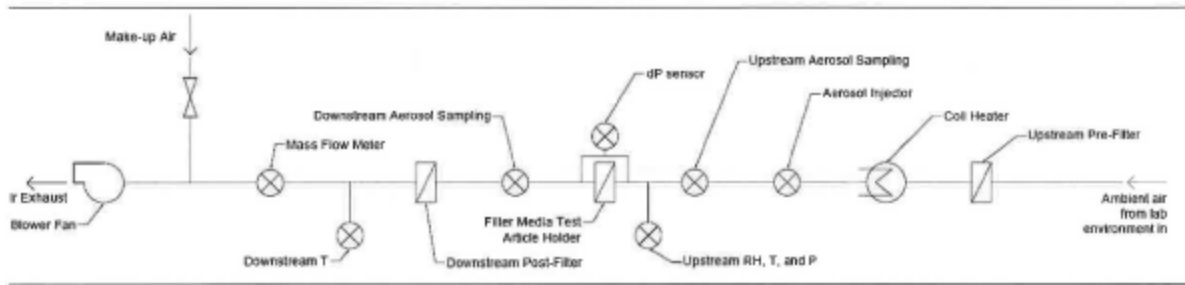


Figure 1. PID of the SSTS

The pressure drop across the test article will be measured by two differential pressure sensors. The reason for having two sensors is to provide a low-range sensor to accurately measure differential pressures from 0 to 10 inch w.c., and another to accurately measure 10 to 35

inch w.c.. This is consistent with the currently installed capability for the Axial Flow Large Scale Test Stand (ALSTS).

Particle sampling will utilize the same system as the ALSTS and RLSTS, with the exception of smaller sampling probes customized for isokinetic conditions at the selected flow rates. Both a Scanning Mobility Particle Sizer (SMPS) and a Laser Aerosol Spectrometer (LAS) will be utilized to provide the full-spectrum of particle sizes accurately.

LabVIEW will be used for data acquisition and test stand control. A Data Acquisition Unit (DAQ) will be used as an interface between the sensors and instruments in order to communicate with the LabVIEW program. This will serve to log the data on a computer, as well as provide feedback for test stand control. The control system for the SSTS will be capable of controlling three important parameters:

1. The air flow rate, maintained at the desired level by reading the mass flow rate through the mass flow meter and varying the blower rpm by means of the VFD connected to the blower motor and the amount of make-up air by opening and closing the valve incrementally until the desired rate is achieved.
2. The air temperature, maintained at the desired level by reading the temperature sensor immediately upstream of the filter. Adjusting the current to the electric heating coil will increase temperature if desired, and maintain it for the duration of the test. This should be a relatively easy task, as the lab environment is more-or-less stable and remains at a fixed temperature.
3. The humidity will not be maintained initially. The ability to control the humidity will require a humidifier at the inlet, and a dehumidifier downstream of the test article in order to provide non-condensing flow to the flow meter and fan at higher temperatures and humidities. Higher temperatures and humidities will also require removing the moisture from the air for the aerosol sampling systems as well. With the capability that will be initially installed, the relative humidity will have a maximum value equivalent to that of

the surrounding environment within the lab, and can only decrease with increasing temperature.

The control of the flow rate through the test stand and the temperature at the test article will be set by the operator, and maintained automatically through the controls programmed through LabVIEW. The data will also be logged through LabVIEW. Therefore, the test will not require constant input from the operators, which will facilitate in providing the highest quality of data possible. However, the operators will still be required to monitor the conditions of the test stand for the duration of the test, to ensure proper functionality.

## Appendix A. Concept Drawings



*Figure A.1. Preliminary model of the SSTS*

11

Uncontrolled Document If Printed

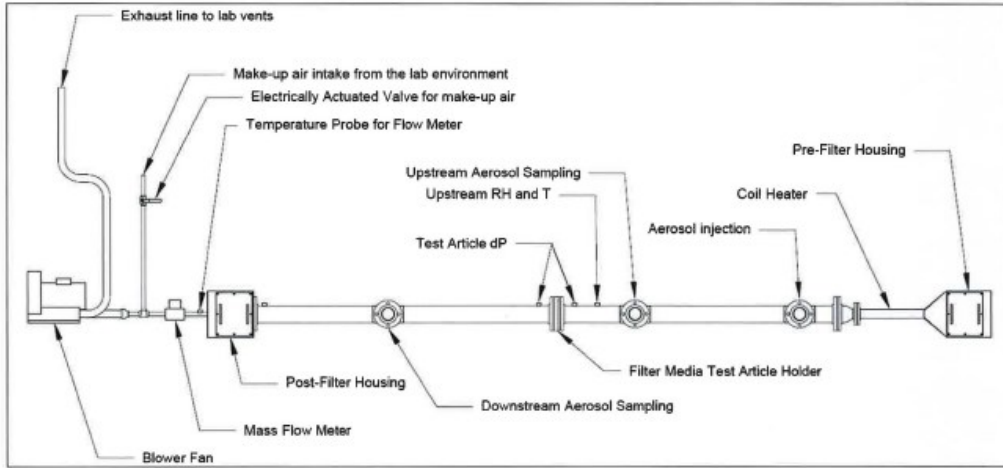


Figure A.2. Annotated drawing of the SSSYS model

Uncontrolled Document if Printed

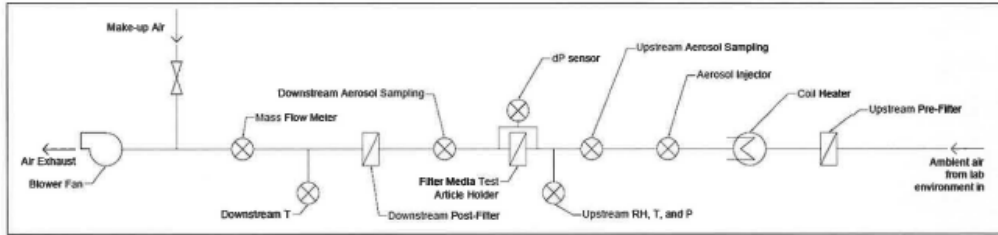
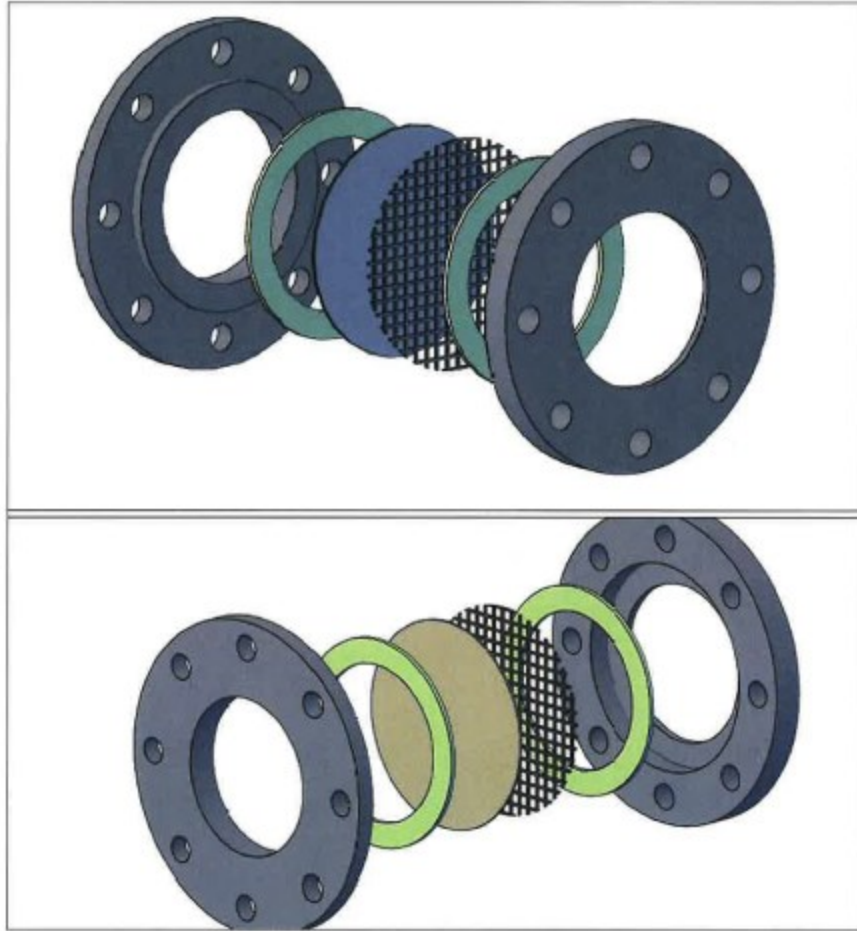


Figure 4.3. Preliminary PID of the SSTS





*Figure A.4. Test article holder*

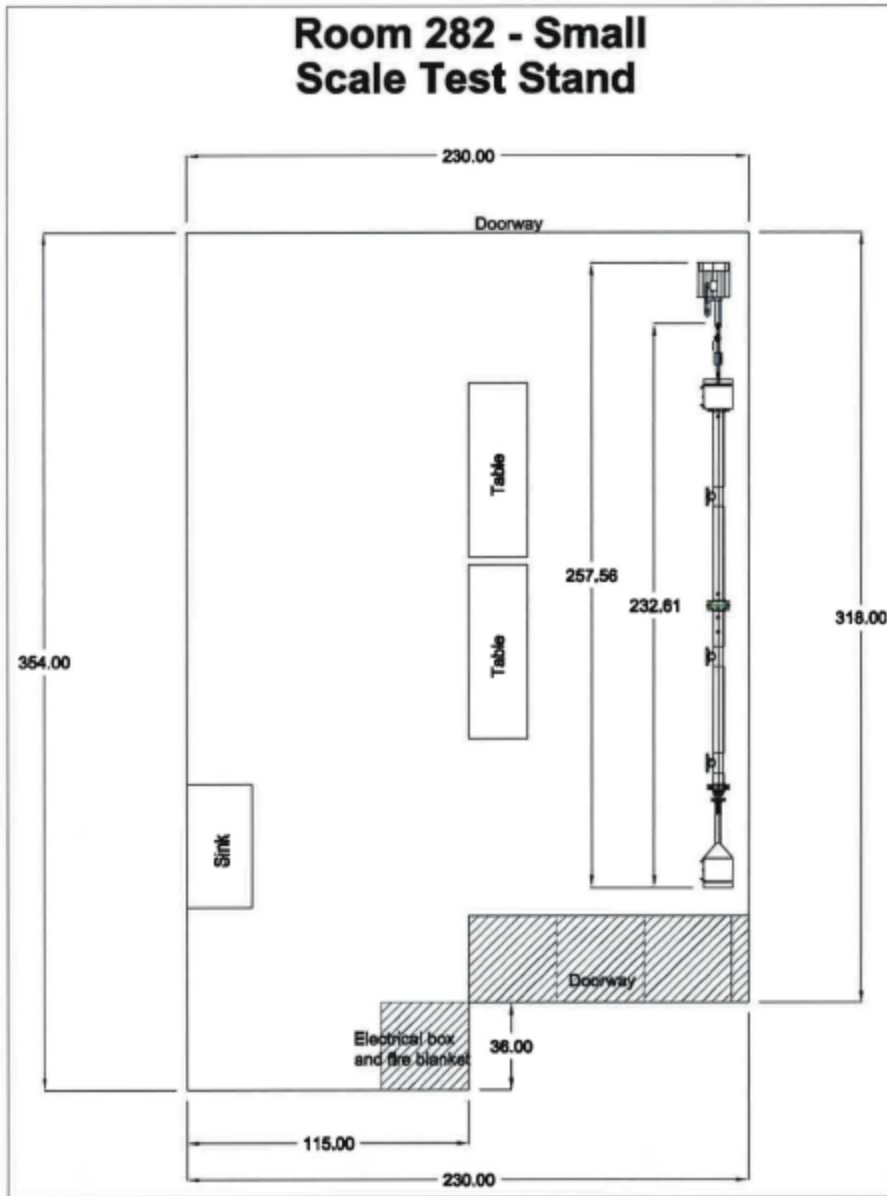


Figure A.5. Room 282 proposed layout

## Appendix B. Calculation and Estimates

### Small Scale Test Stand Heat Transfer Analysis.

The goal is to determine what the inlet temperature of the air must be in order for the temp to be 250F when the air reaches the filter. The temperature at each point of interest will be found for each cfm option.

#### Knowns/Constants

$$T_{\text{air}} := 250^{\circ}\text{F} = 121.111^{\circ}\text{C} \quad T_{\text{atm}} := 68^{\circ}\text{F} \quad D := 4.026\text{in} \quad L := 160\text{in of pipe from heater inlet to filter}$$

Assuming that the specific heat of air is constant at 1011 J/kg/K

$$\rho_{\text{air}350} := 0.0489 \frac{\text{lbm}}{\text{ft}^3} \quad c_{p\text{air}} := 1011 \frac{\text{J}}{\text{kg}\cdot\text{K}}$$

flow := 5cfm      **will be evaluating 5, 10, and 20 cfm**

$$\text{Area} := \frac{\pi}{4} \cdot D^2 = 12.73 \text{in}^2 \quad \text{Vel} := \frac{\text{flow}}{\text{Area}} = 0.943 \frac{\text{ft}}{\text{s}}$$

Assuming that the convective coefficient is equal to 2 W/m<sup>2</sup>/K.

$$h_{\text{air}} := 2 \frac{\text{W}}{\text{m}^2\text{K}}$$

Assuming for air outside for natural convection

$$h_{\text{out}} := 100 \frac{\text{W}}{\text{m}^2\text{K}}$$

#### Resistance Calculations for each wall layer:

$$\text{Area}_{\text{pipeIn}} := \pi \cdot D \cdot L = 1.306\text{m}^2$$

$$r_{\text{pipe}} := \frac{D}{2} = 2.013\text{in} \quad r_{\text{epo}} := 0.0625\text{in} + r_{\text{pipe}} \quad r_{\text{insul}} := 1\text{in} + r_{\text{epo}} \quad r_{\text{al}} := 0.0625\text{in} + r_{\text{insul}} = 3.138\text{in}$$

$$\text{Area}_{\text{pipeIn}} = 2.024 \times 10^3 \cdot \text{in}^2 \quad A_{\text{epo}} := \pi \cdot L \cdot r_{\text{epo}} \quad A_{\text{insul}} := \pi \cdot L \cdot r_{\text{insul}} \quad A_{\text{al}} := \pi \cdot L \cdot r_{\text{al}}$$

$$r_{\text{inner}} := r_{\text{pipe}} - 0.237\text{in}$$

**Where the radii correspond with the outer radius of the material section.**

**304SS at 400K**

Defining a conservative definition for the total length of 4in ID pipe as 160 inches.

$$\text{Area}_{\text{pipeIn}X(x)} := \pi \cdot D \cdot (x) \quad \text{Area}_{\text{outer}X(x)} := 2\pi \cdot (x) \cdot r_{\text{al}}$$

Uncontrolled Document if Printed

$$k_{\text{steel}} := 16.6 \frac{\text{W}}{\text{m}\cdot\text{K}} \quad k_{\text{epo}} := 2.00610^{-6} \frac{\text{Btu}}{\text{s}\cdot\text{in}\cdot\text{R}} \quad k_{\text{insul}} := 0.0385 \frac{\text{W}}{\text{m}\cdot\text{K}} \quad k_{\text{al}} := 200 \frac{\text{W}}{\text{m}\cdot\text{K}}$$

$$R_{\text{convair}} := \frac{1}{h_{\text{air}} \cdot \text{Area}_{\text{pipeIn}}} = 0.383 \frac{\text{K}}{\text{W}} \quad R_{\text{condsteel}} := \frac{\ln\left(\frac{r_{\text{pipe}}}{r_{\text{inner}}}\right)}{2\pi \cdot k_{\text{steel}} \cdot L} = 2.955 \times 10^{-4} \frac{\text{K}}{\text{W}}$$

$$R_{\text{condepo}} := \frac{\ln\left(\frac{r_{\text{epo}}}{r_{\text{pipe}}}\right)}{2\pi \cdot k_{\text{epo}} \cdot L} = 7.984 \times 10^{-3} \frac{\text{K}}{\text{W}} \quad R_{\text{condinsul}} := \frac{\ln\left(\frac{r_{\text{insul}}}{r_{\text{epo}}}\right)}{2\pi \cdot k_{\text{insul}} \cdot L} = 0.4 \frac{\text{K}}{\text{W}}$$

$$R_{\text{condal}} := \frac{\ln\left(\frac{r_{\text{al}}}{r_{\text{insul}}}\right)}{2\pi \cdot k_{\text{al}} \cdot L} = 3.939 \times 10^{-6} \frac{\text{K}}{\text{W}}$$

$$R_{\text{convairX}}(x) := \frac{1}{h_{\text{air}} \cdot \text{Area}_{\text{pipeInX}}(x)} \quad R_{\text{condsteelX}}(x) := \frac{\ln\left(\frac{r_{\text{pipe}}}{r_{\text{inner}}}\right)}{2\pi \cdot k_{\text{steel}} \cdot (x)}$$

$$R_{\text{condepoX}}(x) := \frac{\ln\left(\frac{r_{\text{epo}}}{r_{\text{pipe}}}\right)}{2\pi \cdot k_{\text{epo}} \cdot (x)} \quad R_{\text{condinsulX}}(x) := \frac{\ln\left(\frac{r_{\text{insul}}}{r_{\text{epo}}}\right)}{2\pi \cdot k_{\text{insul}} \cdot (x)}$$

$$R_{\text{condalX}}(x) := \frac{\ln\left(\frac{r_{\text{al}}}{r_{\text{insul}}}\right)}{2\pi \cdot k_{\text{al}} \cdot (x)} \quad R_{\text{convatmX}}(x) := \frac{1}{h_{\text{out}} \cdot \text{Area}_{\text{outerX}}(x)}$$

$$\text{Area}_{\text{outer}} := 2 \cdot \pi \cdot r_{\text{al}} = 0.501 \text{m}$$

$$R_{\text{convatm}} := \frac{1}{h_{\text{out}} \cdot \text{Area}_{\text{outer}} \cdot L}$$

17

Uncontrolled Document if Printed

**Defining the total resistance as a function of the distance X from the inlet of the test stand.**

$$R_{\text{totalX}(x)} := R_{\text{convairX}(x)} + R_{\text{condsteelX}(x)} + R_{\text{condepoX}(x)} + R_{\text{condalX}(x)} + R_{\text{condinsulX}(x)} + R_{\text{convatmX}(x)}$$

$$R_{\text{total}} := R_{\text{convair}} + R_{\text{condsteel}} + R_{\text{condepo}} + R_{\text{condal}} + R_{\text{condinsul}} + R_{\text{convatm}} = 0.796 \frac{\text{K}}{\text{W}}$$

$$R_{\text{totalX}(L)} = 0.796 \frac{\text{K}}{\text{W}} \quad \text{Thus, it may be seen that the Total Resistance as a function of X yields the same results as the total resistance over the whole length of the test stand, given above.}$$

Defining the density of air at 250°F in order to calculate the estimated mass flow rate through the test article

$$\rho_{\text{air250}} := 0.05591 \frac{\text{lbm}}{\text{ft}^3}$$

$$\dot{m}_{250} := 5 \text{ cfm} \rho_{\text{air250}}$$

Defining necessary variables and constants

$$c_p := 1.01 \frac{\text{kJ}}{\text{kg} \cdot \text{K}}$$

$$T_{\text{coupon}} := 250^\circ\text{F}$$

Using a simple LMTD method to determine the inlet temperature of the test stand (post heating coil) to obtain 250°F at the test article. It is worth noting that this does not account for cold air added by the particle injector.

$$T_{\text{in5cfm}} := T_{\text{atm}} - \frac{T_{\text{atm}} - T_{\text{coupon}}}{\exp\left(\frac{-1}{\dot{m}_{250} c_p \cdot R_{\text{totalX}}(80\text{in})}\right)} = 312.256^\circ\text{F} \quad \text{Temperature at the inlet of the testing and measurement section}$$

$$T_{\text{upstreamSampling5cfm}} := T_{\text{atm}} - \exp\left(\frac{-1}{\dot{m}_{250} c_p \cdot R_{\text{totalX}}(59\text{in})}\right) \cdot (T_{\text{atm}} - T_{\text{in5cfm}}) = 264.613^\circ\text{F} \quad \text{Temperature at the upstream sampling point}$$

$$T_{\text{couponTest5cfm}} := T_{\text{atm}} - \exp\left(\frac{-1}{\dot{m}_{250} c_p \cdot R_{\text{totalX}}(80\text{in})}\right) \cdot (T_{\text{atm}} - T_{\text{in5cfm}}) = 250^\circ\text{F} \quad \text{Temperature at the test article}$$

$$T_{\text{downstreamSampling5cfm}} := T_{\text{atm}} - \exp\left(\frac{-1}{\dot{m}_{250} c_p \cdot R_{\text{totalX}}(23\text{in})}\right) \cdot (T_{\text{atm}} - T_{\text{in5cfm}}) = 222.241^\circ\text{F} \quad \text{Temperature at the downstream sampling point}$$

$$T_{\text{out}5\text{cfm}} := T_{\text{atm}} - \exp\left(\frac{-1}{\dot{m}_{250} c_p R_{\text{total}} X(160\text{in})}\right) \cdot (T_{\text{atm}} - T_{\text{in}5\text{cfm}}) = 203.612^\circ\text{F}$$

Temperature at the exit of the test stand, upstream of the mass flow meter

$$T_{\text{atm}} - \exp\left(\frac{-1}{\dot{m}_{250} c_p R_{\text{total}}}\right) \cdot (T_{\text{atm}} - T_{\text{in}5\text{cfm}}) = 203.612^\circ\text{F}$$

**Using this value as a check to ensure that the resistance as a function of distance works as intended.**

Using the LMTD method to determine the heat transfer rate, along with a check using an energy balance.

$$\Delta T_{\text{lm}} := \frac{(T_{\text{atm}} - T_{\text{in}5\text{cfm}}) - (T_{\text{atm}} - T_{\text{out}5\text{cfm}})}{\ln\left(\frac{T_{\text{atm}} - T_{\text{out}5\text{cfm}}}{T_{\text{atm}} - T_{\text{in}5\text{cfm}}}\right)} = 102.576\text{K}$$

$$q_{\text{check}1} := \frac{\Delta T_{\text{lm}}}{R_{\text{total}}} = 128.834\text{W}$$

$$q_{\text{check}2} := \dot{m}_{250} c_p (T_{\text{in}5\text{cfm}} - T_{\text{out}5\text{cfm}}) = 128.834\text{W}$$

## Case for 10 CFM

Using the same method and assumptions as above, but with a volumetric flow rate of 20cfm.

$$\dot{m}_{10\text{cfm}} := 10\text{cfm} \rho_{\text{air}25\text{C}}$$

$$T_{\text{in}10\text{cfm}} := T_{\text{atm}} - \frac{T_{\text{atm}} - T_{\text{coupon}}}{\exp\left(\frac{-1}{\dot{m}_{10\text{cfm}} c_p R_{\text{total}} X(80\text{in})}\right)} = 278.843^\circ\text{F}$$

Temperature at the inlet of the testing and measurement section

$$T_{\text{upstreamSampling}10\text{cfm}} := T_{\text{atm}} - \exp\left(\frac{-1}{\dot{m}_{10\text{cfm}} c_p R_{\text{total}} X(59\text{in})}\right) \cdot (T_{\text{atm}} - T_{\text{in}10\text{cfm}}) = 257.165^\circ\text{F}$$

Temperature at the upstream sampling point

$$T_{\text{couponTest}10\text{cfm}} := T_{\text{atm}} - \exp\left(\frac{-1}{\dot{m}_{10\text{cfm}} c_p R_{\text{total}} X(80\text{in})}\right) \cdot (T_{\text{atm}} - T_{\text{in}10\text{cfm}}) = 250^\circ\text{F}$$

Temperature at the test article

$$T_{\text{downstreamSampling}10\text{cfm}} := T_{\text{atm}} - \exp\left(\frac{-1}{\dot{m}_{10\text{cfm}} c_p R_{\text{total}} X(125\text{in})}\right) \cdot (T_{\text{atm}} - T_{\text{in}10\text{cfm}}) = 235.546^\circ\text{F}$$

Temperature at the downstream sampling point

$$T_{\text{out}10\text{cfm}} := T_{\text{atm}} - \exp\left(\frac{-1}{\dot{m}_{10\text{cfm}} c_p R_{\text{total}} X(160\text{in})}\right) \cdot (T_{\text{atm}} - T_{\text{in}10\text{cfm}}) = 225.103^\circ\text{F}$$

Temperature at the exit of the test stand, upstream of the mass flow meter

$$T_{\text{atm}} - \exp\left(\frac{-1}{\dot{m}_{10\text{cfm}} c_p R_{\text{total}}}\right) \cdot (T_{\text{atm}} - T_{\text{in}10\text{cfm}}) = 225.103^\circ\text{F}$$

**Using this value as a check to ensure that the resistance as a function of distance works as intended.**

$$\Delta T_{\text{lm}10\text{cfm}} := \frac{(T_{\text{atm}} - T_{\text{in}10\text{cfm}}) - (T_{\text{atm}} - T_{\text{out}10\text{cfm}})}{\ln\left(\frac{T_{\text{atm}} - T_{\text{out}10\text{cfm}}}{T_{\text{atm}} - T_{\text{in}10\text{cfm}}}\right)} = 101.476\text{K}$$

19

$$q_{\text{check3}} := \frac{\Delta T_{\text{lm10cfm}}}{R_{\text{total}}} = 127.452\text{W}$$

$$q_{\text{check4}} := \dot{m}_{10\text{cfm}} c_p (T_{\text{in10cfm}} - T_{\text{out10cfm}}) = 127.452\text{W}$$

## Case for 20 CFM

Using the same method and assumptions as above, but with a volumetric flow rate of 20cfm.

$$\dot{m}_{20\text{cfm}} := 20\text{cfm} \rho_{\text{air}25\text{C}}$$

$$T_{\text{in20cfm}} := T_{\text{atm}} - \frac{T_{\text{atm}} - T_{\text{coupon}}}{\exp\left(\frac{-1}{\dot{m}_{20\text{cfm}} c_p R_{\text{total}} X(80\text{in})}\right)} = 263.891^\circ\text{F}$$

Temperature at the inlet of the testing and measurement section

$$T_{\text{upstreamSampling20cfm}} := T_{\text{atm}} - \exp\left(\frac{-1}{\dot{m}_{20\text{cfm}} c_p R_{\text{total}} X(59\text{in})}\right) \cdot (T_{\text{atm}} - T_{\text{in20cfm}}) = 253.548^\circ\text{F}$$

Temperature at the upstream sampling point

$$T_{\text{couponTest20cfm}} := T_{\text{atm}} - \exp\left(\frac{-1}{\dot{m}_{20\text{cfm}} c_p R_{\text{total}} X(80\text{in})}\right) \cdot (T_{\text{atm}} - T_{\text{in20cfm}}) = 250^\circ\text{F}$$

Temperature at the test article

$$T_{\text{downstreamSampling20cfm}} := T_{\text{atm}} - \exp\left(\frac{-1}{\dot{m}_{20\text{cfm}} c_p R_{\text{total}} X(125\text{in})}\right) \cdot (T_{\text{atm}} - T_{\text{in20cfm}}) = 242.624^\circ\text{F}$$

Temperature at the downstream sampling point

$$T_{\text{out20cfm}} := T_{\text{atm}} - \exp\left(\frac{-1}{\dot{m}_{20\text{cfm}} c_p R_{\text{total}} X(160\text{in})}\right) \cdot (T_{\text{atm}} - T_{\text{in20cfm}}) = 237.094^\circ\text{F}$$

Temperature at the exit of the test stand, upstream of the mass flow meter

$$T_{\text{atm}} - \exp\left[\frac{-1}{\dot{m}_{20\text{cfm}} c_p (R_{\text{total}})}\right] \cdot (T_{\text{atm}} - T_{\text{in20cfm}}) = 237.094^\circ\text{F}$$

**Using this value as a check to ensure that the resistance as a function of distance works as intended.**

$$\Delta T_{\text{lm20cfm}} := \frac{(T_{\text{atm}} - T_{\text{in20cfm}}) - (T_{\text{atm}} - T_{\text{out20cfm}})}{\ln\left(\frac{T_{\text{atm}} - T_{\text{out20cfm}}}{T_{\text{atm}} - T_{\text{in20cfm}}}\right)} = 101.20\text{K}$$

$$q_{\text{check5}} := \frac{\Delta T_{\text{lm20cfm}}}{R_{\text{total}}} = 127.108\text{W}$$

$$q_{\text{check6}} := \dot{m}_{20\text{cfm}} c_p (T_{\text{in20cfm}} - T_{\text{out20cfm}}) = 127.108\text{W}$$

20

Uncontrolled Document If Printed



## Small Scale Test Stand Heating Coil Size Estimate.

### Defining the air properties for the lab

$$T_{\text{lab}} := 68^{\circ}\text{F} \quad \phi_{\text{lab}} := 0.5 \quad P_{\text{lab}} := 1\text{atm}$$

Defining a dimensionless temperature, as the ASHRAE function does not take MathCAD units.

$$T_{\text{lab}} := \frac{T_{\text{lab}}}{\text{R}} - 459.67$$

Using the ASHRAE functions to calculate the properties of the moist air from the lab

$$W_{\text{lab}} := W_{\text{ptphi\_HAP\_IP}}\left(\frac{P_{\text{lab}}}{\text{psi}}, T_{\text{lab}}, \phi_{\text{lab}}\right) = 7.294 \times 10^{-3}$$

$$h_{\text{lab}} := h_{\text{ptW\_HAP\_IP}}\left(\frac{P_{\text{lab}}}{\text{psi}}, T_{\text{lab}}, W_{\text{lab}}\right) \cdot \frac{\text{BTU}}{\text{lbm}} = 24.29 \frac{\text{Btu}}{\text{lbm}}$$

$$\rho_{\text{lab}} := \frac{1}{v_{\text{ptW\_HAP\_IP}}\left(\frac{P_{\text{lab}}}{\text{psi}}, T_{\text{lab}}, W_{\text{lab}}\right) \cdot \frac{\text{ft}^3}{\text{lbm}}} = 0.074 \frac{\text{lbm}}{\text{ft}^3}$$

**Defining the anticipated air properties for the particle injector for air from the shop air supply. It is worth noting that these will likely not be constant in a realistic scenario.**

Defining the temperature from the compressed air supply as slightly lower than that of the lab air.

$$T_{\text{injector}} := 65^{\circ}\text{F} \quad \phi_{\text{injector}} := 0.5 \quad P_{\text{injector}} := 1\text{atm}$$

Defining a dimensionless temperature, as the ASHRAE function does not take MathCAD units.

$$T_{\text{injector}} := \frac{T_{\text{injector}}}{\text{R}} - 459.67$$

Using the ASHRAE functions to calculate the properties of the moist air from the compressed air supply.

$$W_{\text{injector}} := W_{\text{ptphi\_HAP\_IP}}\left(\frac{P_{\text{injector}}}{\text{psi}}, T_{\text{injector}}, \phi_{\text{injector}}\right) = 6.566 \times 10^{-3}$$

$$h_{\text{injector}} := h_{\text{ptW\_HAP\_IP}}\left(\frac{P_{\text{injector}}}{\text{psi}}, T_{\text{injector}}, W_{\text{injector}}\right) \cdot \frac{\text{BTU}}{\text{lbm}} = 22.767 \frac{\text{Btu}}{\text{lbm}}$$

$$\rho_{\text{injector}} := \frac{1}{v_{\text{ptW\_HAP\_IP}}\left(\frac{P_{\text{injector}}}{\text{psi}}, T_{\text{injector}}, W_{\text{injector}}\right) \cdot \frac{\text{ft}^3}{\text{lbm}}} = 0.075 \frac{\text{lbm}}{\text{ft}^3}$$

21

Uncontrolled Document if Printed



**Defining the outlet (from the heating coil) air properties as estimated from the preceding heat transfer analysis. This represents a "worst-case" scenario with maximum temperature at the maximum volumetric flow rate.**

$$T_{\text{total}} := 300^{\circ}\text{F} \quad \dot{V}_{\text{total}} := 20\text{cfm} \quad P_{\text{total}} := 1\text{atm}$$

Defining a dimensionless temperature, as the ASHRAE function does not take MathCAD units.

$$T_{\text{total}} := \frac{T_{\text{total}}}{R} - 459.67 = 300$$

Assuming that the humidity ratio is equal to that of the lab. This is a valid assumption, as long as the humidity level from the compressed air supply is approximately the same as it is in the lab environment.

$$W_{\text{total}} := W_{\text{lab}}$$

Using the ASHRAE functions to calculate the properties of the moist air from the exiting the heating coil section.

$$h_{\text{total}} := h_{\text{ptW\_HAP\_IP}}\left(\frac{P_{\text{total}}}{\text{psi}}, T_{\text{total}}, W_{\text{total}}\right) \cdot \frac{\text{BTU}}{\text{lbm}} = 81.043 \frac{\text{Btu}}{\text{lbm}}$$

$$\rho_{\text{total}} := \frac{1}{v_{\text{ptW\_HAP\_IP}}\left(\frac{P_{\text{total}}}{\text{psi}}, T_{\text{total}}, W_{\text{total}}\right) \cdot \frac{\text{ft}^3}{\text{lbm}}} = 0.052 \frac{\text{lbm}}{\text{ft}^3}$$

Thus, a total mass flow rate may be calculated by using the total volumetric flow rate exiting the heating coil section, and the density of the air at that point.

$$\dot{m}_{\text{total}} := \rho_{\text{total}} \cdot \dot{V}_{\text{total}} = 1.032 \frac{\text{lbm}}{\text{min}}$$

Creating a range of possible mass flow rates from the particle injector, in order to investigate the required heat transfer rate from the heating coil under different conditions.

$$\dot{m}_{\text{injector}} := \begin{cases} \text{percent} \leftarrow 1\% \\ \text{for } i \in 0..84 \\ \quad \left| \begin{array}{l} \text{output}_i \leftarrow \dot{m}_{\text{total}} \cdot \text{percent} \\ \text{percent} \leftarrow \text{percent} + 1\% \end{array} \right. \\ \text{output} \end{cases}$$

From conservation of mass

$$\dot{m}_{\text{lab}} := \dot{m}_{\text{total}} - \dot{m}_{\text{injector}}$$

$$\dot{Q}_{\text{heater}} := \begin{cases} \text{for } i \in 0.. \text{length}(\dot{m}_{\text{lab}}) - 1 \\ \quad \left| \begin{array}{l} \text{output}_i \leftarrow \dot{m}_{\text{lab}_i} \left( h_{\text{lab}} - \frac{\dot{m}_{\text{total}} \cdot h_{\text{total}} - \dot{m}_{\text{injector}_i} \cdot h_{\text{injector}_i}}{\dot{m}_{\text{lab}_i}} \right) \end{array} \right. \\ \text{output} \end{cases}$$

22

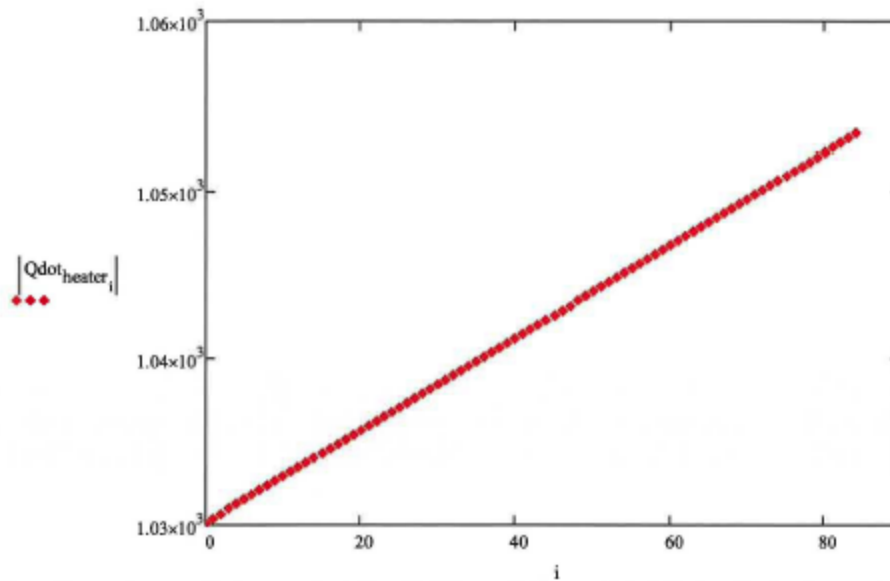
Uncontrolled Document if Printed

	0
0	-1.03013
1	-1.03041
2	-1.03069
3	-1.03096
4	-1.03124
5	-1.03151
6	-1.03179
7	-1.03207
8	-1.03234
9	-1.03262
10	-1.0329
11	-1.03317
12	-1.03345
13	-1.03373
14	-1.034
15	...

$\dot{Q}_{\text{heater}} =$  -kW This number is negative from the accepted sign convention that heat added to a system is considered negative.

$\max(-\dot{Q}_{\text{heater}}) = 1.053 \text{ kW}$

This represents the maximum heat transfer rate required from the heating coil under the conditions defined above, corresponding with the maximum amount of mass flow through the particle injector assuming a lower temperature from the compressed air supply than in the lab.



Thus, it may be seen that as more air is added through the particle injector, the heater must add more heat to the lab air in order to maintain the correct temperature at the outlet of the conditioning section once the air mixes.

### Small Scale Test Stand Head Loss Estimate

**Air Properties:**

inWC := 248.84Pa

**At 75 degF and 50% RH**

inHG := 0.491154psi

$$v_{50} := 13.65 \frac{\text{ft}^3}{\text{lbm}} \quad \rho_{50} := \frac{1}{v_{50}} = 0.073 \frac{\text{lbm}}{\text{ft}^3}$$

**At 75 degF and 30% RH**

$$v_{30} := 13.6 \frac{\text{ft}^3}{\text{lbm}} \quad \rho_{30} := \frac{1}{v_{30}} = 0.074 \frac{\text{lbm}}{\text{ft}^3}$$

**At 70 degF and 20% RH**

$$v_{20} := 13.41 \frac{\text{ft}^3}{\text{lbm}} \quad \rho_{20} := \frac{1}{v_{20}} = 0.075 \frac{\text{lbm}}{\text{ft}^3}$$

**Flow area of the pipe**

$$\text{Area} := \frac{\pi}{4} \cdot (4\text{in})^2 = 0.087 \text{ft}^2$$

**Stainless Steel Roughness**

$$\epsilon_w := 7 \cdot 10^{-6} \text{ft}$$

**Pipe Diameter (nominal inside diameter)**

$$D := 4 \text{in}$$

**Pipe Length, per AutoCAD**

$$L_a := 160 \text{in}$$

**Volumetric Flow Rate**

$$Q_{\text{max}} := 1 \text{cfm}$$

$$i := 1, 2, \dots, 20 =$$

1
2
3
4
5
6
7
8
9
10
11
12
13
14
15
...

**Pressure of the fluid**

$$\begin{pmatrix} P_a \\ P_b \end{pmatrix} := \begin{pmatrix} 0 \\ 0 \end{pmatrix} \text{psi}$$

$$Q_{\text{range}} := Q_{\text{max}} \cdot i \quad \text{cfm}$$

0	1
1	2
2	3
3	4
4	5
5	6
6	7
7	8
8	9
9	10
10	11
11	12
12	13
13	14
14	15
15	...

Uncontrolled Document If Printed

**Height Difference**

$$\begin{pmatrix} Z_a \\ Z_b \end{pmatrix} := \begin{pmatrix} 0 \\ 0 \end{pmatrix} \text{in}$$

$$\text{velocity}_{\text{range}} := \frac{Q_{\text{range}}}{\text{Area}} \quad \frac{\text{ft}}{\text{s}}$$

0	0.191
1	0.382
2	0.573
3	0.764
4	0.955
5	1.146
6	1.337
7	1.528
8	1.719
9	1.91
10	2.101
11	2.292
12	2.483
13	2.674
14	2.865
15	...

**Input density**

$$\rho := \rho_{SC}$$

**Kinematic Viscosity**

$$\mu := 1.9 \cdot 10^{-5} \frac{N \cdot s}{m^2} = 3.968 \times 10^{-7} \frac{lbf \cdot s}{ft^2}$$

**Constants and Functions**

$$g_c := 32.174 \frac{ft}{s^2}$$

$$g_c := 32.174 \frac{ft \cdot lb}{lbf \cdot s^2}$$

$$Re(q, d) := \frac{4 \cdot \rho \cdot q}{\pi \cdot d \cdot \mu} \quad f(q, d, \varepsilon) := \begin{cases} \frac{0.3086}{\log \left[ \frac{6.9}{Re(q, d)} + \left( \frac{\varepsilon}{3.7 \cdot d} \right)^{1.11} \right]^2} & \text{if } Re(q, d) > 2300 \\ \frac{64}{Re(q, d)} & \text{otherwise} \end{cases} \quad f_T(d, \varepsilon) := \frac{0.3086}{\log \left[ \left( \frac{\varepsilon}{3.7 \cdot d} \right)^{1.11} \right]^2}$$

**Estimated Loss Factors**

$$K_{ent} := 0.5 \quad K_{exit} := 1.0 \quad K_{elbow} := 30 \cdot f_T(D, \varepsilon) \quad K_{90} := \left[ \frac{12 - 20}{2 - 1} \cdot (1.5 - 2) + 12 \right] \cdot f_T(D, \varepsilon) = 0.146$$

$$K_{tees} := 20 \cdot f_T(D, \varepsilon)$$

$$K_{tot1} := 1 \cdot K_{exit} + 3 \cdot K_{ent} + 0 \cdot K_{90} + 3 \cdot K_{tees} = 3.046$$

**Specific work required**

$$Q_{max} := 20 \text{ cfm}$$

$$W_{s_{max}} := \frac{P_b - P_a}{\rho} + (Z_b - Z_a) \cdot \frac{g}{g_c} + \frac{8}{\pi^2} \cdot \frac{Q_{max}^2}{g_c \cdot (D)^4} \cdot \left( f(Q_{max}, D, \varepsilon) \cdot \frac{L}{D} + K_{tot1} \right) = 2.979 \frac{J}{kg}$$

$$W_{s_{range1}} := \begin{cases} \text{for } j \in 0.. \text{length}(i) - 1 \\ \text{SpecificWork}_j \leftarrow \frac{P_b - P_a}{\rho} + (Z_b - Z_a) \cdot \frac{g}{g_c} + \frac{8}{\pi^2} \cdot \frac{(Q_{range_j})^2}{g_c \cdot (D)^4} \cdot \left( f(Q_{range_j}, D, \varepsilon) \cdot \frac{L}{D} + K_{tot1} \right) \\ \text{SpecificWork} \end{cases}$$

**For the heater coil section.**

The head loss incurred by the heating coil is assumed later in the worksheet to be 2inWC.

$$L_2 := 6 \text{ in} \quad K_{tot2} := 0$$

$$W_{s_{range2}} := \begin{cases} \text{for } j \in 0.. \text{length}(i) - 1 \\ \text{SpecificWork}_j \leftarrow \frac{P_b - P_a}{\rho} + (Z_b - Z_a) \cdot \frac{g}{g_c} + \frac{8}{\pi^2} \cdot \frac{(Q_{range_j})^2}{g_c \cdot (D)^4} \cdot \left( f(Q_{range_j}, D, \varepsilon) \cdot \frac{L_2}{D} + K_{tot2} \right) \\ \text{SpecificWork} \end{cases}$$

**For the 2in to 4in transition section.**

$$L3 := 3\text{in}$$

$$\beta := \frac{2\text{in}}{4\text{in}}$$

$$K_{\text{tot}3} := \frac{(1 - \beta^2)^2}{\beta^4}$$

$$W_{s_{\text{range}3}} := \begin{cases} \text{for } j \in 0.. \text{length}(i) - 1 \\ \text{SpecificWork}_j \leftarrow \frac{P_b - P_a}{\rho} + (Z_b - Z_a) \cdot \frac{g}{g_c} + \frac{8}{\pi^2} \cdot \frac{(Q_{\text{range}j})^2}{g_c \cdot (D)^4} \cdot \left( f(Q_{\text{range}j}, D, \varepsilon) \cdot \frac{L3}{D} + K_{\text{tot}3} \right) \\ \text{SpecificWork} \end{cases}$$

**For the flex hosing between the flow meter and the blower fan.**

A length of 10ft of hosing is estimated, given the unknown total length of hosing that will be used between the make-up air tee and the fan.

$$L4 := 10\text{ft} \quad D4 := 1.5\text{in} \quad K_{\text{tot}4} := 1$$

$$W_{s_{\text{range}4}} := \begin{cases} \text{for } j \in 0.. \text{length}(i) - 1 \\ \text{SpecificWork}_j \leftarrow \frac{P_b - P_a}{\rho} + (Z_b - Z_a) \cdot \frac{g}{g_c} + \frac{8}{\pi^2} \cdot \frac{(Q_{\text{range}j})^2}{g_c \cdot (D4)^4} \cdot \left( f(Q_{\text{range}j}, D4, \varepsilon) \cdot \frac{L4}{D4} + K_{\text{tot}4} \right) \\ \text{SpecificWork} \end{cases}$$

**Summing the head loss from each section of the test stand to estimate the total head loss at the defined conditions above between the inlet of the test stand to the intake of the pump.**

$$\Delta P_{\text{losses}} := \rho \cdot (W_{s_{\text{range}1}} + W_{s_{\text{range}2}} + W_{s_{\text{range}3}} + W_{s_{\text{range}4}})$$

$$\Delta P_{\text{losses}}^T = \begin{array}{|c|c|c|c|c|c|} \hline & 0 & 1 & 2 & 3 & 4 \\ \hline 0 & 2.683 \cdot 10^{-3} & 6.367 \cdot 10^{-3} & 0.018 & 0.029 & \dots \\ \hline \end{array} \cdot \text{inWC}$$

$$(\rho \cdot W_{s_{\text{range}1}})^T = \begin{array}{|c|c|c|c|c|c|} \hline & 0 & 1 & 2 & 3 & 4 \\ \hline 0 & 8.034 \cdot 10^{-5} & 2.094 \cdot 10^{-4} & 3.87 \cdot 10^{-4} & 6.134 \cdot 10^{-4} & \dots \\ \hline \end{array} \cdot \text{inWC}$$

$$(\rho \cdot W_{s_{\text{range}2}})^T = \begin{array}{|c|c|c|c|c|c|} \hline & 0 & 1 & 2 & 3 & 4 \\ \hline 0 & 2.1 \cdot 10^{-6} & 4.2 \cdot 10^{-6} & 6.3 \cdot 10^{-6} & 8.4 \cdot 10^{-6} & \dots \\ \hline \end{array} \cdot \text{inWC} \quad 26$$

Uncontrolled Document if Printed

$$(\rho \cdot Ws_{range3})^T = \begin{array}{|c|c|c|c|c|c|} \hline & 0 & 1 & 2 & 3 & 4 \\ \hline 0 & 7.296 \cdot 10^{-5} & 2.898 \cdot 10^{-4} & 6.504 \cdot 10^{-4} & 1.155 \cdot 10^{-3} & \dots \\ \hline \end{array} \cdot \text{inWC}$$

$$\rho \cdot Ws_{range4}^T = \begin{array}{|c|c|c|c|c|c|} \hline & 0 & 1 & 2 & 3 & 4 \\ \hline 0 & 2.528 \cdot 10^{-3} & 5.864 \cdot 10^{-3} & 0.017 & 0.028 & \dots \\ \hline \end{array} \cdot \text{inWC}$$

$$\max(\Delta P_{losses}) = 0.541 \text{ inWC}$$

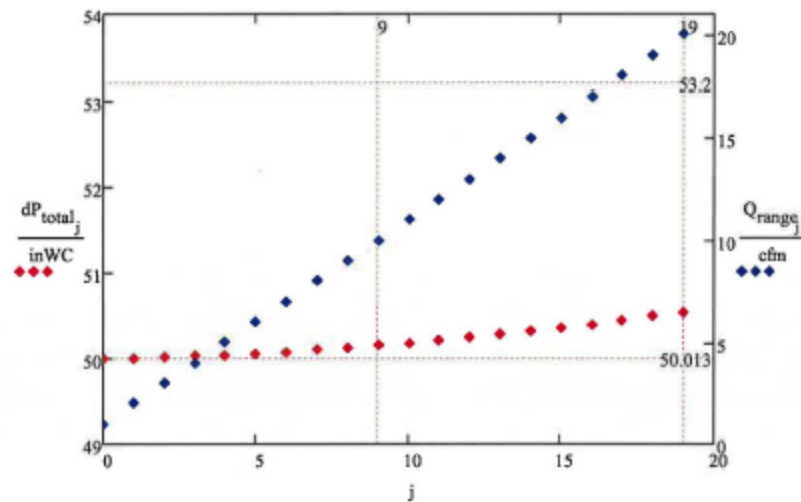
Defining a few expected losses from other components included in the SSTs.

$$dP_{media} := 35 \text{ inWC} \quad dP_{pre} := 1 \text{ inWC} \quad dP_{post} := 1 \text{ inWC} \quad dP_{coil} := 2 \text{ inWC} \quad dP_{flowmeter} := 1 \text{ inWC}$$

$$dP_{total} := \Delta P_{losses} + dP_{media} + dP_{pre} + dP_{post} + dP_{coil} + dP_{flowmeter}$$

$$dP_{total}^T = \begin{array}{|c|c|c|c|c|c|c|c|c|} \hline & 0 & 1 & 2 & 3 & 4 & 5 & 6 & 7 \\ \hline 0 & 50.003 & 50.006 & 50.018 & 50.029 & 50.044 & 50.06 & 50.08 & \dots \\ \hline \end{array} \cdot \text{inWC}$$

$$\max(dP_{total}) = 50.541 \text{ inWC}$$



27

The above plot illustrates the head loss (LHS y-axis) plotted with a variable flow rate between 1 and 20 cfm (RHS y-axis) plotted against the corresponding index number for each case.

### Small Scale Test Stand Reynolds Number Estimate

Estimated filtration area [ft <sup>2</sup> ]	0.082903139						
Temperature [°F]	75						
RH [%]	50						
Kinematic Viscosity [ft <sup>2</sup> /s]	0.000166						
Duct Diameter [in]	4						
Duct cross-section area [ft <sup>2</sup> ]	0.087266463						
Volumetric Flow Rate [CFM]	20	10	5	4	3	2	1
Filtration Velocity Range [ft/min]	241.245	120.623	60.311	48.249	36.187	24.125	12.062
Filtration Velocity Range [cm/s]	122.553	61.276	30.638	24.511	18.383	12.255	6.128
Duct Velocity [ft/min]	229.183	114.592	57.296	45.837	34.377	22.918	11.459
Duct Velocity [ft/s]	3.820	1.910	0.955	0.764	0.573	0.382	0.191
Duct Reynolds Number	7670.118	3835.059	1917.529	1534.024	1150.518	767.012	383.506
1/4 in probe diameter							
Sampling Velocity 1/4in probe [ft/s]	3.820	1.910	0.955	0.764	0.573	0.382	0.191
Probe Area [ft <sup>2</sup> ]	0.000						
Sampling volumetric flow rate [CFM]	0.078	0.039	0.020	0.016	0.012	0.008	0.004
Sampling volumetric flow rate [LPM]	2.212	1.106	0.553	0.442	0.332	0.221	0.111
1/8 in probe diameter							
Sampling Velocity 1/8in probe [ft/s]	3.820	1.910	0.955	0.764	0.573	0.382	0.191
Probe Area [ft <sup>2</sup> ]	0.000						
Sampling volumetric flow rate [CFM]	0.020	0.010	0.005	0.004	0.003	0.002	0.001
Sampling volumetric flow rate [LPM]	0.553	0.277	0.138	0.111	0.083	0.055	0.028



GAST MANUFACTURING, INC.  
A Unit of IDEX Corporation  
Post Office Box 97  
Benton Harbor, Michigan  
Ph. 269/928-6171  
Fax: 269/928-8384

PART NUMBER:  
LTD144

REV.  
E

Product Specifications

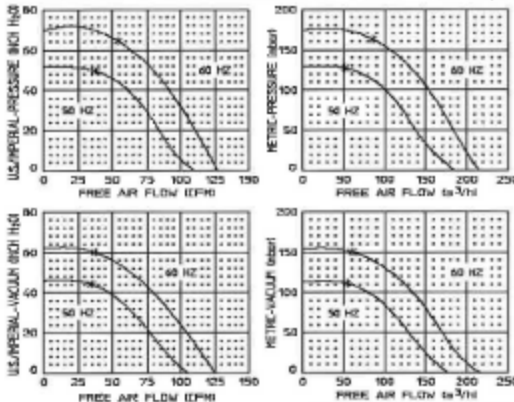
MODEL NUMBER	MOTOR SPECIFICATIONS	RPM	MAX VAC		MAX PRESS		HP	kW	NET WT.	
			"H <sub>2</sub> O	mbar	"H <sub>2</sub> O	mbar			lbs.	kg
R4P15	110/220-240-50-1	2850	45	112	50	125	1.0	0.75	62	28.2
	115/208-230-60-1	3450	60	149	65	162	1.5	1.1		

SOUND LEVEL 74/72 dB(A) MAX. @ 60/50 Hz  
 NORMAL AMBIENT -29°C TO 40°C  
 RELATIVE HUMIDITY 0% - 100% NON CONDENSING  
 ENVIRONMENT CLEAN DUST FREE

TECHNICAL DATA SUBJECT TO CHANGE WITHOUT NOTICE.

\* - RECOMMENDED MAXIMUM DUTY

Product Performance (Metric U.S. Imperial)



PERFORMANCE DATA  
 THE PERFORMANCE DATA SHOWN WAS DETERMINED UNDER THE FOLLOWING CONDITIONS:

LINE VOLTAGE @ 60 Hz, 230V OR 460V FOR 3 PHASE UNITS, 115V OR 230V FOR 1 PHASE UNITS.

LINE VOLTAGE @ 50 Hz, 220V FOR 3 PHASE OR 1 PHASE UNITS.

UNITS IN A TEMPERATURE STABLE CONDITION.

DELIVERY MEASUREMENTS MADE WITH OUTPUT PORT THROTTLED.

SUCTION MEASUREMENTS MADE WITH INPUT PORT THROTTLED.

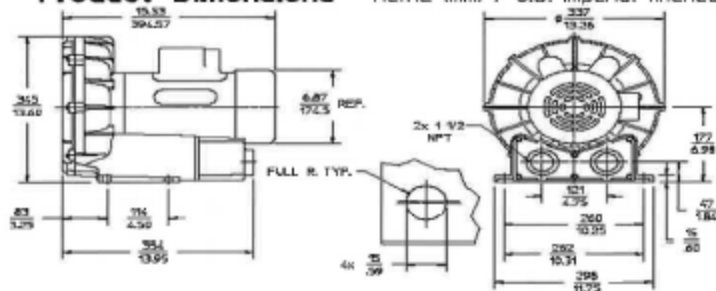
TEST CONDITIONS: INLET AIR DENSITY @ 0.075 lbs. per cu. ft. (20°C 168°F), 29.92" Hg (14.7 PSIA).

NORMAL PERFORMANCE VARIATIONS ON THE RESISTANCE CURVE WITHIN +10% OF SUPPLIED DATA CAN BE EXPECTED.

Product Dimensions

Metric (mm) / U.S. Imperial (inches)

- LOW VOLTAGE, SINGLE PHASE  
 P1 — LINE  
 P2 — TIE TOGETHER & INSULATE  
 T3 — LINE  
 T4 — LINE
- HIGH VOLTAGE, SINGLE PHASE  
 P1 — LINE  
 P2 — INSULATE  
 T3 — TIE TOGETHER & INSULATE  
 T4 — LINE



WIRING DIAGRAM

Figure B.1. Gast product specification



## APPENDIX B

### SMALL-SCALE TEST STAND FILTER EFFICIENCY TEST PROCEDURE





REVISION HISTORY

Revision Number	Reason for Revision	Revision By
0	Initial Issue	AWP

DRAFT



#### 1.0 PURPOSE

The purpose of this procedure is to ensure ICET personnel follow the steps necessary for safely starting up, testing, and shutting down the Small-Scale Test Stand (SSTS) and its control system.

#### 2.0 SCOPE

This procedure covers the steps involved in startup, operation, and shutdown of the SSTS.

#### 3.0 TERMS / DEFINITIONS

- 3.1 SSTS – Small-Scale Test Stand
- 3.2 M&TE – Measuring and Test Equipment
- 3.3 LAS – Laser Aerosol Spectrometer
- 3.4 SMPS – Scanning Mobility Particle Sizer
- 3.5 dP – differential pressure
- 3.6 RH – relative humidity
- 3.7 CFM – cubic feet per minute
- 3.8 rpm – rotations per minute
- 3.9 psi – pounds per square inch
- 3.10 in w.c. – inches of water column

#### 4.0 RESPONSIBILITIES

Staff with responsibilities for implementing this procedure are:

- 4.1 Test Stand Operator(s)/Test Personnel

#### 5.0 EQUIPMENT

**NOTE:**

Measuring and Test Equipment (M&TE) used to collect data during performance of this procedure is required to be within the current calibration cycle as evidenced by an affixed calibration label and be capable of the desired range specified in testing documentation.

- 5.1 SSTS control panel
- 5.2 Static pressure transmitter
- 5.3 RH/Temperature probe and transmitter (2)
- 5.4 dP gauge



- 5.5 Mass flow meter
- 5.6 Mass controller
- 5.7 Actuating Valve
- 5.8 SMPS
- 5.9 LAS

#### 6.0 SAFETY AND ENVIRONMENTAL CONCERNS

- 6.1 Gloves and eye protection when handling cleaning chemicals
- 6.2 Hearing protection is required during startup and operation of the SSTS
- 6.3 Dosimeter required when in Lab 282

#### 7.0 PREREQUISITES

- 1.1 7.1 All personnel operating the SSTS and instrumentation contained therein must be trained in accordance with ICET-QA-001.

#### 8.0 PROCEDURE

Note: Performance of procedures is recorded with supporting document check lists, test notebooks, and/or a test control document ().

The Test Stand Operator shall:

- 8.1 Ensure the sampling train is set to purge
- 8.2 Perform LAS and SMPS readiness and operation procedures if not previously performed the day of testing
- 8.3 Perform a Diluter Characterization to determine the dilution factor of the test
- 8.4 Ensure the following information is recorded:
  - 8.4.1 Time and Date
  - 8.4.2 Run ID
  - 8.4.3 Test Filter Media ID
  - 8.4.4 Challenge aerosol
  - 8.4.5 Duct flow rate to be set
  - 8.4.6 Aerosol generator settings
  - 8.4.7 Dilution factor from characterization
- 8.5 Install the filter coupon
  - 8.5.1 Unbolt the test filter coupon holder from the test stand.
  - 8.5.2 Disassemble the coupon holder on a table by removing the 8 set screws
  - 8.5.3 Ensure that the coupon holder is clean of any debris or dust.
    - 8.5.3.1 Use a chem whip and alcohol to remove any debris, dust, or residue.



- 8.5.4 Using tweezers, obtain a filter coupon from the storage bag and install in the coupon holder. Ensure that the coupon is not damaged or marked/creased in any way. Starting from the upstream face of the coupon holder, the components should be installed in the following order: 1) gasket, 2) test filter article, 3) gasket, 4) wire mesh backing.
- 8.5.5 Assemble the coupon holder and tighten the set screws in a star pattern to ensure even distribution of force.
- 8.5.6 Reinstall the holder on the test stand, ensuring that the wire mesh is on the downstream side of the test stand and that the flow direction arrows are pointing towards the blower. Tighten the bolts in a star pattern.
- 8.6 Ensure that the test stand control system (computer, software, and control panel) is powered on by checking the breaker switch on the control panel. (If the computer or control panel is turned off, contact Jay McCown or Mike Sullivan.)
- 8.7 Zero-out all the pressure gauges, dP sensors, and the mass flow meters if they do not output a value of zero.
- 8.8 Turn on the room exhaust fan.
- 8.9 Turn on the control computer.
  - 8.9.1 Set the desired flow rate for the filter face in CFM.
- 8.10 Record the following once the system reaches a steady state:
  - 8.10.1 Initial dP
  - 8.10.2 Initial Temperature and RH at the filter face
  - 8.10.3 Volumetric Flow Rate output from LabView program
- 8.11 Once the testing conditions are met, click the "Log to CSV" button in the LabView program to begin recording the data. The button will turn green when logging data.
- 8.12 Preparing the atomizer:
  - 8.12.1 Check that there is enough PAO in the atomizer.
    - 8.12.1.1 Do not fill more than 2/3 when refilling.
  - 8.12.2 Connect the compressed air line to the atomizer.
  - 8.12.3 Connect the exhaust line to the injection manifold on the test stand.
  - 8.12.4 Set the pressure on the wall regulator to a setting higher than the intended pressure to be used on the atomizer.
  - 8.12.5 Set the pressure on the atomizer to the value that correlates to the desired duct flow rate according to the Test Plan document.
  - 8.12.6 Ensure that the dilution flow rate valve is reading the expected value.



- 8.12.7 When ready to begin injecting the aerosol, flip the switch for the first jet on the atomizer (top switch). It is important that only the first jet is engaged, unless specifically noted otherwise.
- 8.13 Begin recording data on the aerosol measurement instruments. Record which sample sets are upstream, downstream, and purging.
- 8.13.1 Click “Downstream Sampling” on the LabVIEW Program
- 8.13.2 Record 5 samples downstream
- 8.13.3 Click “Downstream Sampling” once again to return the flowrate to the set flowrate.
- 8.13.4 Purge for 3 samples
- 8.13.5 Record 5 samples upstream.
- 8.14 End of test run (shutdown):
- 8.14.1 Once the filter has reached the desired dP of the test, the amount of samples have been recorded, or the filter has failed, power off the selected aerosol generator. **NOTE: The control program should automatically power off the test stand if a dP of 38 inWC is reached. However, do not allow the test to run until the dP is at 40 inWC to protect the dP sensor.**
- 8.14.2 Turn the blower off.
- 8.15 Remove the coupon holder and discard the used filter coupon.
- 8.16 Clean the coupon holder of any residue or dust acquired during testing or removal of the test article.

## 9.0 RECORDS

All records are considered quality records and shall be maintained and submitted to project records in accordance with ICET-QA-010, *Quality Assurance Records*:

- 9.1 The records included in this procedure include the following:
- 9.2 Test Control Document (HEPA-SSTS-000)

## 10.0 REFERENCES

- 10.1 ICET-QA-010, *Quality Assurance Records*
- 10.2 HEPA-ALSTS-000, *Test Control Documentation*

## 11.0 ATTACHMENTS

APPENDIX C

SMALL-SCALE TEST STAND LOADING TEST PROCEDURE





---

### Small-Scale Test Stand Loading Testing Procedure

---

**Implementation Date:**

**Effective Date is Immediate upon Approval Signature**

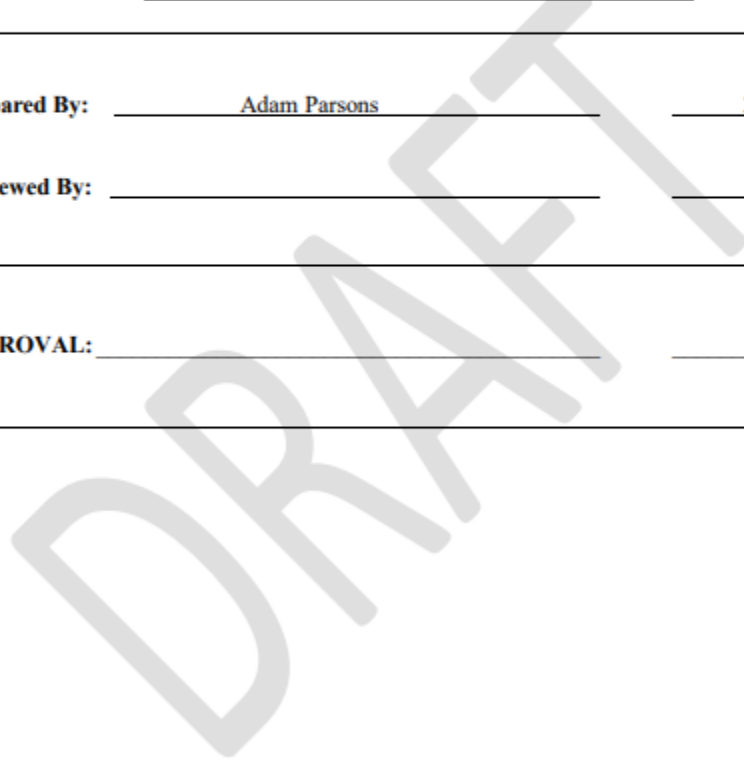
---

**Prepared By:** \_\_\_\_\_ *Adam Parsons* \_\_\_\_\_ *2/7/2022*  
**Date**

**Reviewed By:** \_\_\_\_\_ \_\_\_\_\_  
**Date**

**APPROVAL:** \_\_\_\_\_ \_\_\_\_\_  
**Date**

---





REVISION HISTORY

Revision Number	Reason for Revision	Revision By
0	Initial Issue	AWP

DRAFT



#### 1.0 PURPOSE

The purpose of this procedure is to ensure ICET personnel follow the steps necessary for safely starting up, testing, and shutting down the Small-Scale Test Stand (SSTS) and its control system.

#### 2.0 SCOPE

This procedure covers the steps involved in startup, operation, and shutdown of the SSTS.

#### 3.0 TERMS / DEFINITIONS

- 3.1 SSTS – Small-Scale Test Stand
- 3.2 M&TE – Measuring and Test Equipment
- 3.3 LAS – Laser Aerosol Spectrometer
- 3.4 SMPS – Scanning Mobility Particle Sizer
- 3.5 dP – differential pressure
- 3.6 RH – relative humidity
- 3.7 CFM – cubic feet per minute
- 3.8 rpm – rotations per minute
- 3.9 psi – pounds per square inch
- 3.10 in w.c. – inches of water column

#### 4.0 RESPONSIBILITIES

Staff with responsibilities for implementing this procedure are:

- 4.1 Test Stand Operator(s)/Test Personnel

#### 5.0 EQUIPMENT

**NOTE:**

Measuring and Test Equipment (M&TE) used to collect data during performance of this procedure is required to be within the current calibration cycle as evidenced by an affixed calibration label and be capable of the desired range specified in testing documentation.

- 5.1 SSTS control panel
- 5.2 Static pressure transmitter
- 5.3 RH/Temperature probe and transmitter (2)
- 5.4 dP gauge



- 5.5 Mass flow meter
- 5.6 Mass controller
- 5.7 Actuating Valve
- 5.8 SMPS
- 5.9 LAS

#### 6.0 SAFETY AND ENVIRONMENTAL CONCERNS

- 6.1 Gloves and eye protection when handling cleaning chemicals
- 6.2 Hearing protection is required during startup and operation of the SSTS
- 6.3 Dosimeter required when in Lab 282

#### 7.0 PREREQUISITES

- 1.1 7.1 All personnel operating the SSTS and instrumentation contained therein must be trained in accordance with ICET-QA-001.

#### 8.0 PROCEDURE

Note: Performance of procedures is recorded with supporting document check lists, test notebooks, and/or a test control document ().

The Test Stand Operator shall:

- 8.1 Ensure the sampling train is set to purge
- 8.2 Perform LAS and SMPS readiness and operation procedures if not previously performed the day of testing
- 8.3 Ensure the following information is recorded:
  - 8.3.1 Time and Date
  - 8.3.2 Run ID
  - 8.3.3 Test Filter Media ID
  - 8.3.4 Test type and challenge aerosol
  - 8.3.5 Duct flow rate to be set
  - 8.3.6 Aerosol generator settings
  - 8.3.7 Dilution factor from characterization
- 8.4 Install the filter coupon
  - 8.4.1 Unbolt the test filter coupon holder from the test stand.
  - 8.4.2 Disassemble the coupon holder on a table by removing the 8 set screws
  - 8.4.3 Ensure that the coupon holder is clean of any debris or dust.
    - 8.4.3.1 Use a chem whip and alcohol to remove any debris, dust, or residue.



- 8.4.4 Using tweezers, obtain a filter coupon from the storage bag and install in the coupon holder. Ensure that the coupon is not damaged or marked/creased in any way. Starting from the upstream face of the coupon holder, the components should be installed in the following order: 1) gasket, 2) test filter article, 3) gasket, 4) wire mesh backing.
- 8.4.5 Assemble the coupon holder and tighten the set screws in a star pattern to ensure even distribution of force.
- 8.4.6 Reinstall the holder on the test stand, ensuring that the wire mesh is on the downstream side of the test stand and that the flow direction arrows are pointing towards the blower. Tighten the bolts in a star pattern.
- 8.5 Ensure that the test stand control system (computer, software, and control panel) is powered on by checking the breaker switch on the control panel. (If the computer or control panel is turned off, contact Jay McCown or Mike Sullivan.)
- 8.6 Zero-out all the pressure gauges, dP sensors, and the mass flow meters if they do not output a value of zero.
- 8.7 Turn on the room exhaust fan.
- 8.8 Turn on the control computer.
  - 8.8.1 Set the desired flow rate for the filter face in CFM.
- 8.9 Record the following once the system reaches a steady state:
  - 8.9.1 Initial dP
  - 8.9.2 Initial Temperature and RH at the filter face
  - 8.9.3 Volumetric Flow Rate output from LabView program
- 8.10 Once the testing conditions are met, click the “Log to CSV” button in the LabView program to begin recording the data. The button will turn green when logging data.
- 8.11 Powder testing preparation:
  - 8.11.1 Check to make sure there is enough powder to perform the test.
  - 8.11.2 Connect the vacuum nozzle to the injection manifold in the test stand.
  - 8.11.3 Connect the compressed air line to the vacuum nozzle.
  - 8.11.4 Connect the powder feeder discharge line to the top of the vacuum nozzle.
  - 8.11.5 Set the pressure on the wall regulator to the value that correlates to the desired duct flow rate according to the Test Plan document.
  - 8.11.6 Set the feed rate to the value that correlates to the Test Plan document.
  - 8.11.7 Ensure that the lid remains on powder feeder while injecting aerosols to prevent the introduction of particles into the general lab environment.
- 8.12 Begin recording data on the aerosol measurement instruments.
  - 8.12.1 Set the valve train to sample upstream



8.12.2 Record the measured dP of the filter every 3 minutes. If there has been no increase in dP, ensure that the atomizer has enough PAO or that there is not a clog in the powder feeder.

8.12.2.1 If there is a clog in the powder feeder lines, sharply increase and then decrease the psi quickly to attempt to dislodge and break the clog. If this does not work, pause the test and clean the tubing, vacuum nozzle, and injection manifold. Use water and then alcohol/acetone to dry the components. Reassemble the system and continue testing. Make note of the pause in testing, and ensure that the dP across the test article is consistent to when the test was paused.

8.13 End of test run (shutdown):

8.13.1 Once the filter has reached the desired dP of the test, or the filter has failed, power off the selected aerosol generator. **NOTE: The control program should automatically power off the test stand if a dP of 38 inWC is reached. However, do not allow the test to run until the dP is at 40 inWC to protect the dP sensor.**

8.13.2 Turn the blower off.

8.14 Remove the coupon holder and discard the used filter coupon.

8.15 Clean the coupon holder of any residue or dust acquired during testing or removal of the test article.

## 9.0 RECORDS

All records are considered quality records and shall be maintained and submitted to project records in accordance with ICET-QA-010, *Quality Assurance Records*:

9.1 The records included in this procedure include the following:

9.2 Test Control Document (HEPA-SSTS-000)

## 10.0 REFERENCES

10.1 ICET-QA-010, *Quality Assurance Records*

10.2 HEPA-ALSTS-000, *Test Control Documentation*

## 11.0 ATTACHMENTS